

**Optimisation of HIV-1 enveloped
Virus-Like Particles as a personalised
vaccine platform for the delivery of
cancer neoantigens**

Ana Barajas Molina
Doctoral Thesis 2023

Universitat de Vic – Universitat Central de Catalunya
Programa de Doctorat en Medicina i Ciències Biomèdiques

Optimisation of HIV-1 enveloped Virus-Like Particles as a personalised vaccine platform for the delivery of cancer neoantigens

Ana Barajas Molina

Institut de Recerca de la SIDA – IrsiCaixa
Hospital Germans Tries i Pujol
Badalona, 2023

Thesis directors:

Julià Blanco Arbués, PhD
Carmen Aguilar Gurrieri, PhD



UNIVERSITAT DE VIC
UNIVERSITAT CENTRAL
DE CATALUNYA



Institut de Recerca de la Sida

*A mi familia
A Guillaume
Y, sobre todo, a Jorgito*

TABLE OF CONTENT

ABBREVIATIONS	9
SUMMARY	13
RESUM	15
INTRODUCTION	17
GENERAL BACKGROUND	19
THE CANCER IMMUNITY CYCLE	20
1. <i>Generation of antigen specific CD8+ T cells</i>	20
2. <i>Role of CD4+ in the anti-cancer immune response</i>	28
3. <i>Role of NKs in the anti-cancer immune response</i>	31
IMMUNE ESCAPE MECHANISMS.....	33
1. <i>Cancer immunoediting</i>	33
2. <i>Elements in the tumour microenvironment (TME)</i>	35
CANCER IMMUNOTHERAPIES	40
1. <i>Cytokines</i>	41
2. <i>Immuno-checkpoint inhibition</i>	44
3. <i>Cell therapies</i>	46
4. <i>Vaccines</i>	48
HYPOTHESIS	61
AIM AND OBJECTIVES	62
MATERIALS AND METHODS	63
RESULTS	79
SECTION 1: ANALYSIS AND COMPARISON OF LINKER SEQUENCES AND THEIR EFFECT IN ANTIGEN PROCESSING AND PRESENTATION IN A NEOANTIGEN POLYPEPTIDE VACCINE	81
1. <i>Development of an epitope presentation assay</i>	83
2. <i>Identification of the optimal spacer for MHC-I epitope presentation</i>	84
3. <i>Transfection efficiency controls</i>	86
4. <i>Activation and proliferation assay</i>	89
5. <i>Effect of neoantigen position on epitope presentation</i>	90
SECTION 2: OPTIMISATION OF HIV-1 GAG-BASED VIRUS-LIKE PARTICLES TO DISPLAY MELANOMA NEOANTIGENS	93
1. <i>Identification of nonsynonymous mutations and frameshifts in B16-F10 mouse melanoma cell line*</i>	96
2. <i>Production and purification of neoVLPs</i>	97
3. <i>Determination of the optimal vaccine regime</i>	100

4. <i>Immunogenicity of neoVLPs in C57BL/6 mice</i>	101
5. <i>Design, production, and purification of a new VLP containing 7 proven immunogenic neoantigens (Cippa7-GAG)</i>	105
6. <i>Prophylactic vaccination with neoVLPs delays tumour growth.</i>	108
7. <i>Optimisation of the neoVLP purification protocol</i>	112
SECTION 3: DEVELOPMENT OF SECOND GENERATION NEOVLPs DISPLAYING CANCER NEOANTIGENS.	
PROOF OF CONCEPT WITH THE PAN02 MURINE MODEL	115
1. <i>Identification of nonsynonymous mutations in Pan02, a murine pancreatic adenocarcinoma cell line*</i>	118
2. <i>Production and characterisation of C_neoVLPs</i>	119
3. <i>Preliminary immunogenicity assay of C_neoVLPs</i>	123
DISCUSSION	127
CONCLUSIONS	143
DISSEMINATION	147
REFERENCES	151
ACKNOWLEDGMENTS	177

ABBREVIATIONS

AA	Amino Acid
ACT	Adoptive Cell Transfer
ADCC	Antibody Dependent Cell Cytotoxicity
APC	Antigen Presenting Cells
β2M	β2 Microglobulin
BCA	Bicinchoninic Acid protein assay
CAFs	Cancer Associated Fibroblasts
CART	Chimeric Antigen Receptor T cells
CD3	Cluster of Differentiation 3 chains
cDC1	Conventional type 1 Dendritic Cells
CIT	Cancer Immunotherapies
Cryo-EM	Cryogenic Electron Microscopy
cTEC	Cortical Thymic Epithelial Cells
CTL	Cytotoxic T cells
CTLA-4	Cytotoxic T Lymphocyte 4
CTNNB-1	β-Catenin
DAMPs	Damage-associated Molecular Pattern
DCs	Dendritic Cells
DMEM	Dulbecco's Modified Eagle Medium
ECM	Extracellular Matrix Components
EMT	Epithelial Mesenchymal Transition
ER	Endoplasmic Reticulum
FBS	Fetal Bovine Serum
FelV	Feline Leukemia Virus
HBV	Hepatitis B Virus
HER2	Human Epidermal Growth Factor 2
HIV-1	Human Immunodeficiency Virus 1
HLA	Human Leucocyte Antigen
HPV	Human Papilloma Virus
Ib2	Inhibitor DNA Binding 2

Abbreviations

ICD	Immunogenic Cell Death
ICI	Immune Checkpoint Inhibition
ICB	Immune Checkpoint Blockade
IFNγ	Interferon gamma
ILC	Innate Lymphoid Cells
KIRs	Kill cell Immunoglobulin like Receptor
LN	Lymph Node
LSP	Long Synthetic Peptide
M1	Type 1 Macrophages
MDSCs	Myeloid Derived Suppressive Cells
MHC-I	Major Histocompatibility Complex I
MPLA	Monophosphoryl Lipid A
mTEC	Medullar Thymic Epithelial Cells
neoVLPs	Neoantigen Virus Like Particles
NGS	Next Generation Sequencing
NKs	Natural Killer Cells
NO	Nitric Oxide
NOAH	Neoantigen Optimisation Algorithm
PAMPs	Pathogen-associated Molecular Patterns
PAP	Prostate Recombinant fusion protein
PD-1	Programmed Cell Death 1
PD-L1	Programmed Cell Death ligand 1
PRRs	Pattern-Recognition Receptors
MHC-I/p	MHC-I Peptide complexes
SHP-2	Tyrosine Phosphatase 2
SMAC	Supramolecular Activation Complex
SNVs	Single Nucleotide Variants
Tregs	T Regulatory Cells
TAA s	Tumour Associated Antigens
TAM	Tumour Associated Macrophages
TAP	Transporter Associated with Antigen Presentation
TCD	Tolerogenic Cell Death

TCR	T-cell Receptor
TEM	Transmission Electron Microscopy
TESLA	Tumour Neoantigen Selection Alliance
TGF-β	Transforming Growth factor β
TILs	Tumour Infiltrating Lymphocytes
TMB	Mutational burden
TME	Tumour Microenvironment
TSA	Tumour Specific Antigens
UC	Ultracentrifugation
VLPs	Virus-Like Particles
WES	Whole Exome Sequencing
WT	Wild type

SUMMARY

Cancer immunotherapies (CIT) stand as novel and promising strategies for the treatment of cancer. Their aim is to enhance the individual's own immune system to recognise and eliminate cancer cells reducing side effects, with the ultimate goal of providing long-term tumour control. Among immunotherapy possible targets, neoantigens have arisen as suitable candidates as they are mostly patient- and tumour-specific. The possibility of identifying neoantigens has fostered the development of personalised vaccines with promising results. The prediction and prioritisation of immunogenic neoantigens is currently addressed mostly using *in silico* bioinformatic tools, but their formulation as vaccines needs to be improved. To maximize their therapeutic potential, optimal neoantigens-based vaccines should be manufactured in a superb delivery platform that enhances robust immune responses with potent antitumoral activity.

Here, we developed a highly immunogenic vaccine platform based on engineered HIV-derived Virus-Like Particles (VLPs) expressing a high density of selected neoantigens (neoVLPs). Predicted immunogenic peptides were presented as a concatenated long polypeptide spaced by specific designed sequences investigated to promote and enhance antigen processing and presentation. Then, polypeptides were either fused to the N-terminal or the C-terminal of the structural Gag protein. After self-assembling into VLPs, the peptides were exposed on the particle surface or at the particle core, respectively.

After successfully generating and purifying neoVLPs, their integrity and VLP morphology were confirmed by western blot and cryo-EM. The immunogenicity of selected vaccine candidates was evaluated in a mouse model (C57BL/6) and neoantigen-specific T-cell responses were detected by ELISpot. In total, 7 out of 44 neoantigens were able to elicit strong *de novo* CD8⁺ T-cell responses upon two vaccination doses. In addition, animals vaccinated with one of the selected candidates and challenged with the B16-F10 tumour showed delayed tumour growth compared to the control group, and an increased survival.

Taken together, our data show that neoVLPs promote the generation of new antitumor-specific immune responses against selected neoepitopes, suggesting that neoVLPs vaccination could be an alternative to current therapeutic vaccine approaches and a promising candidate for future personalised immunotherapy.

RESUM

Les immunoteràpies contra el càncer (CIT) s'han establert com estratègies prometedores en el tractament d'aquesta malaltia. El seu objectiu és estimular el sistema immunitari de l'individu per reconèixer i eliminar les cèl·lules canceroses reduint els possibles efectes secundaris, amb l'objectiu de proporcionar un control tumoral a llarg termini. Entre les possibles dianes de les immunoteràpies, els neoantígens han sorgit com a candidats rellevants, ja que són majoritàriament específics de cada pacient i de cada tumor. La possibilitat d'identificar neoantígens ha fomentat el desenvolupament de vacunes personalitzades amb resultats prometedors. No obstant això, mentre que la predicció i prioritització dels neoantígens més immunògens es pot abordar utilitzant eines bioinformàtiques, la seva formulació com a vacunes necessita especial atenció i optimització. Per maximitzar el seu potencial terapèutic, les vacunes basades en neoantígens haurien de ser formulades idealment fent ús d'una plataforma potent que busqui potenciar una resposta immune amb capacitat antitumoral.

En aquest treball hem desenvolupat una plataforma de vacuna altament immunògena basada en partícules similvíriques (VLPs) utilitzant la proteïna estructural del VIH, Gag. Aquestes partícules estan dissenyades per expressar una alta densitat de neoantígens a la seva superfície (neoVLPs). Els pèptids immunògens seleccionats es formulen com un polipèptid, format per un concatenat de neoepítops separats l'un de l'altre per seqüències específiques dissenyades per promoure i millorar el processament i la presentació d'antígens. Els polipèptids optimitzats estan fusionats a l'extrem N-terminal o C-terminal de la proteïna Gag que, un cop oligomeritzada, formarà VLPs exposant els pèptids a l'exterior; o a l'interior de la partícula, respectivament.

Després de generar i purificar amb èxit els diferents candidats de vacunes de neoVLPs, la integritat de les proteïnes i la seva morfologia van ser confirmades per western blot i cryo-EM. La immunogenicitat dels candidats seleccionats va ser avaluada en un model de ratolí (C57BL/6) i les respostes de cèl·lules T específiques de neoantigen van ser detectades per ELISpot. En total, 7 dels 44 neoantígens inclosos a les VLPs van generar una resposta de cèl·lules T després de dues dosis de vacunació. A més, els animals vacunats amb un dels candidats seleccionats i inoculats amb cèl·lules del model tumoral B16-F10 van ser capaços de retardar la progressió del tumor comparat amb el grup control, i van demostrar una major supervivència.

Resum

En resum, els nostres resultats demostren que les neoVLPs promouen la generació de noves respostes immunes antitumorals específiques contra els neoepítops seleccionats, suggerint que la vacunació amb neoVLPs podria ser una alternativa a les estratègies actuals de vacunes terapèutiques en el camp de les immunoteràpies personalitzades.

INTRODUCTION

General background

Cancer is probably one of the major public health concerns worldwide, with an estimated 19.3 million new cases and 10 million cancer-related deaths a year in 2020. The global cancer burden is expected to continue rising, estimating 28.4 million new cases by 2040¹.

Cancer is a complex and heterogeneous disease characterised by uncontrolled cell growth and proliferation. Malignant cells arise from normal cells through genetic mutations or epigenetic changes that alter their behaviour and physiology^{2,3}. These changes may include mutations in genes involved in cell cycle control, DNA repair and cell death regulation or alterations in the expression of key regulatory molecules, such as growth factors or transcription factors⁴. Once carcinogenesis is initiated, cancer cells undergo clonal expansion, giving rise to a heterogeneous population of cells with distinct phenotypic and functional characteristics⁵. Furthermore, these cells can acquire additional mutations or epigenetic changes that confer further advantages as proliferation, migration to other sites, invasion of tissues, resistance to therapy and immune evasion mechanisms³.

The main three approaches to reduce the cancer impact worldwide are prevention, early detection, and treatment⁶. Effective cancer prevention strategies include reducing exposure to tobacco and other carcinogens, promoting healthy lifestyles, and implementing vaccination programs for cancer-related viruses such as human papilloma virus (HPV) and hepatitis B virus (HBV)⁶⁻⁸. Early detection through screening programs and increased awareness improves outcomes and reduces mortality rates⁹.

The treatment of cancer typically involves a combination of strategies that aim to eliminate cancer cells or prevent them from growing and spreading¹⁰. Among these we find surgeries, chemotherapies, radiotherapies, and immunotherapies¹¹⁻¹⁴. The latter gathers all the cytokines-based, antibody-based, and cell-based therapies that intend to modulate and enhance the immune system. On one hand, to generate specific anti-tumour T cells responses capable of specifically eliminating neoplastic cells, and on the other hand, to overcome the immunosuppressive environment that characterises tumoral tissue and can difficult or inhibit the cytotoxic functions of the different immune components¹⁴.

Understanding the molecular and cellular mechanisms underlying cancer initiation and progression is critical for the development of more effective therapeutic strategies. The complexity and heterogeneity of tumours, and their relationship with the immune system

Introduction

pose a significant challenge for the development of effective therapies¹⁵. For that reason, there is a need for interdisciplinary approaches that combine basic and clinical research, as well as patient-based approaches that consider unique differences in tumour biology and response to therapy across patients¹⁵.

The cancer immunity cycle

1. Generation of antigen specific CD8+ T cells

The close relationship between cancer cells and the immune system has been extensively demonstrated. Research advances from the past 20 years have granted a deep understanding of the interactions between tumours and the immune system, revealing how complex and extremely regulated it is. These findings are notably important to learn how to enhance, modulate and manipulate the immune system to develop effective anti-cancer treatments. The interplay between tumours and the immune system was described by S. Chen *et al.* as the cancer immunity-cycle^{16,17}. This cycle collects all the steps that need to happen for the immune system to generate a specific and effective anti-cancer response (Figure 1).

First, tumour-specific antigens need to be released (Figure 1, step 1) from cancer cells and up taken by dendritic cells (DCs) for processing (Figure 1, step 2)¹⁶. This step must be bolstered by specific signals that trigger an immune response by promoting the release of pro inflammatory cytokines and factors¹⁶. Next, DCs present the capture antigens on MHC-I and II molecules to T cells, which results in priming and activation of tumour-specific T cells (Figure 1, step 3)¹⁶. Finally, the activated effector T cells travel to the tumour site and infiltrate it (Figure 1, step 4), to end up killing the target cells by the interaction between the TCR and the MHC-I bound to the specific peptide (Figure 1, step 5)¹⁶. Killing of cancer cells helps increase the breadth of response and positively feeds the cancer immunity cycle by releasing more antigens, ready to be uptaken by DCs¹⁶. In patients where the cycle does not work effectively, the tumour progresses and escapes the immune system. The aim of immunotherapies is to help start the cancer immunity cycle and propagate it to achieve tumour elimination.

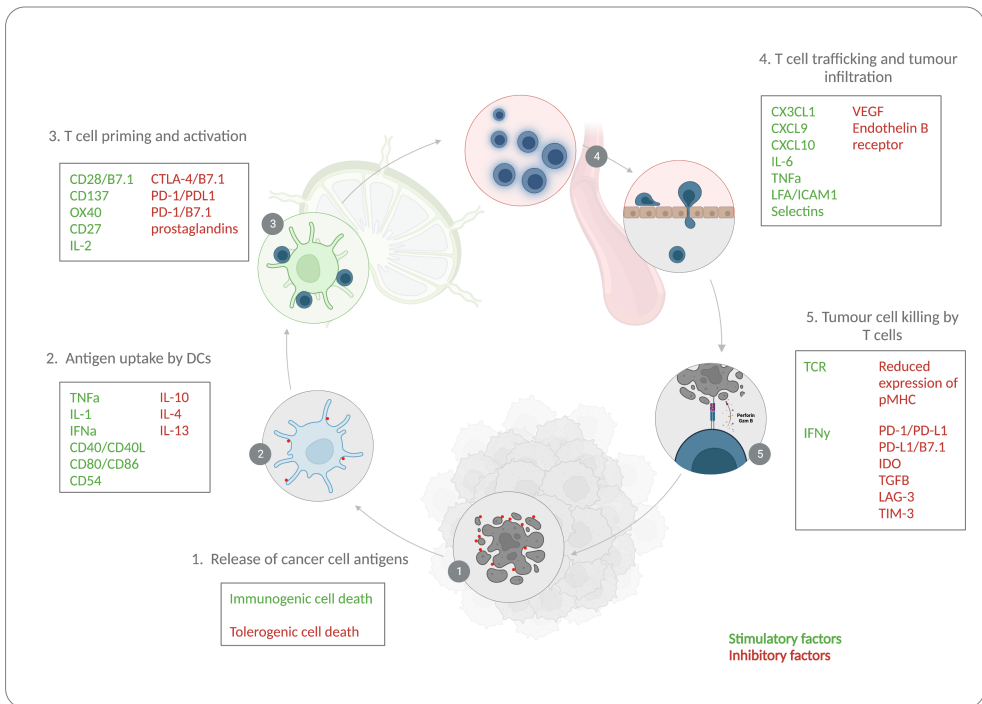


Figure 1. The cancer immunity cycle. The adaptive immune response generated against tumours functions as a continuous and accumulative cycle that can broaden the tumour-specific T-cell response. Each step of the cycle has stimulatory and inhibitory factors that work as negative or regulatory feedback mechanisms. Stimulatory factors, showed in green, contribute to generate and intensify the adaptive immune response, whereas inhibitory factors, in red, help regulate and halt the process, if necessary, to suppress immunity or autoimmunity. However, sometimes inhibitory factors can block the antitumour immune response as part of the immunoediting process. Created with Biorender. Adapted from Chen, D.S *et al.* (2013)¹⁶.

1.1 Antigen release (Step 1). Damage-associated molecular patterns (DAMPs) as sensors of immunogenicity

The first step of the cancer immunity cycle, the release of antigens, must be accompanied by the initiation of an immune response triggered by the expression of DAMPs (Figure 1, step 1). DAMPs are specific cell-derived signals, recognised by pattern-recognition receptors (PRRs), that can initiate an innate immune response¹⁸ operating as natural adjuvants^{19,20}. DAMPs function like the well-known pathogen-associated molecular patterns (PAMPs) that allow the recognition of pathogen infected cells¹⁸. However, DAMPs do not need to be expressed in an infectious context and can be released by necrotic cells or actively expressed by apoptotic ones^{19,21}. Despite this, the expression of these DAMPs does

Introduction

not guarantee the initiation of an immune response unless the dying cells express antigens that have overcome central tolerance, and thus can eventually prime high affinity T cells¹⁹. These strongly immunogenic antigens, or so-called neoantigens, can elicit specific T-cell responses²². Comprehensively, immunogenic cell death (ICD)²³ – a type of regulated cell death that triggers adaptive immunity – depends on two key aspects, adjuvanticity conferred by the expression and release of DAMPs from injured or apoptotic cells, and the immunogenicity associated with tumour-specific antigens²⁰. As opposed to ICD, there is another type of regulated cell death that does not contribute to the initiation of an immune response, the tolerogenic cell death (TCD; Figure 1, step1). TCD depends on several factors, including modification of DAMPs, absence of T-cell help during antigen-presentation, subtype and maturation state of the engulfing DCs and the release of immunosuppressive factors during apoptosis²⁴. Triggering an immune response against dying or apoptotic cells is a complex mechanism that can be key in generating a robust immune response against tumour cells (Figure 1, step 1)²⁴.

In a cancerous environment, processes like ICD are essential because they can promote cross-presentation through different mechanisms, such as the attraction of DCs to apoptotic tumour cells. The release of ATP, for example, can recruit myeloid cells into tumour sites and stimulate their differentiation into DC phenotypes^{25,26}. ICD can also increase the antigen uptake from dead cells by releasing factors that promote antigen processing and MHC-I presentation by DCs²⁷.

1.2 DCs antigenic uptake, processing, and presentation (Step 2). The major histocompatibility complex I

DCs, professional antigen presenting cells (APCs), are a diverse group of different sensing and presenting cell subtypes that play a key role in mediating innate and adaptive immune responses²⁸. To fully activate CD8+ T cells into effector cytotoxic lymphocytes, these need to be activated by DCs that present exogenous peptides in the Major Histocompatibility Complex I (MHC-I) molecules, by a mechanism known as cross-presentation (Figure 1, step 2)²⁹.

MHC-I molecules play a critical role in the adaptive immune system as they are responsible of presenting protein-derived peptides to CD8+ T cells³⁰. MHC-I molecules are expressed in all nucleated cells and the peptides presented by them contribute to define the

specificity of the response. The MHC-I molecule is a heterodimer formed by two domains, a polymorphic heavy α -chain and an invariant light chain known as β 2-microglobulin (β 2M) that binds the heavy chain non-covalently supporting the peptide-binding unit³¹. The space in between the α -helices that form the α -chain is the peptide binding groove (Figure 2)³¹.

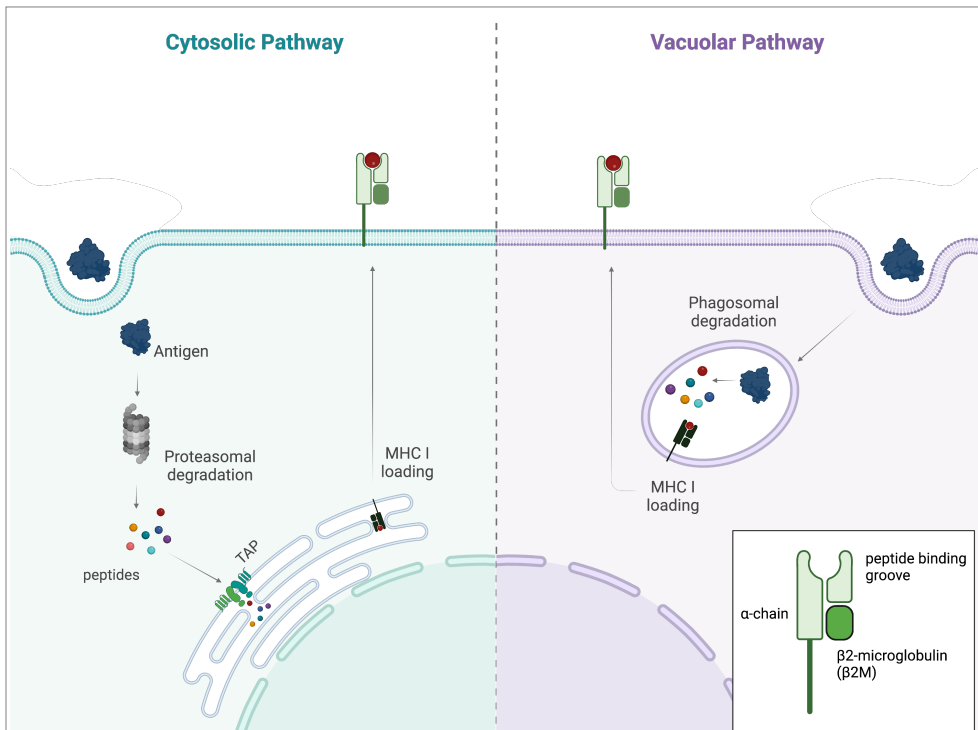


Figure 2. Intracellular pathways of cross-presentation in dendritic cells. During cross-presentation, exogenous antigens are engulfed by DCs. Once in the cytosol (cytosolic pathway), antigens are degraded by the proteasome into peptides, that are transported into the ER by TAP proteins. In the ER, MHC-I molecules assemble, and peptides insert themselves in the peptide-binding groove. Eventually the MHC-I/peptide (MHC-I/p) complex translocates to the membrane and peptides are presented extracellularly. Alternatively, antigens can be degraded in phagosomes, independently from proteasomal degradation (vacuolar pathway), and loaded onto the MHC-I to be presented at the cell membrane. Created with Biorender. Adapted from Pishesha, N *et al.* (2022)²⁹.

The composition and features of the peptide binding groove are primarily defined by the three highly polymorphic regions that code for the MHC-I molecules, these are the HLA-A, HLA-B and HLA-C³⁰. This high allelic variation of the different human leucocyte antigen (HLAs) contributes to the immense repertoire of peptides that can be presented on MHC-I molecules and recognised by T-cell receptors^{31,32}. In the cancer context, predicting the

Introduction

affinity of peptides to different MHC-I allotypes has been one of the biggest challenges. Several immunotherapeutic strategies are based on identifying pre-existing tumour-specific T-cell responses or generating them via vaccination³¹. For both approaches, the need to predict what tumour peptides will be presented on MHC-I molecules and therefore may potentially mediate a CTL response is indispensable, and currently the prediction efficiency is still low^{33–36}.

Generally, MHC-I molecules present endogenous peptides that come from cytosolic or nuclear degraded proteins³². Proteins are degraded by the proteasome, and peptides are translocated to the endoplasmic reticulum (ER) by the TAP protein (transporter associated with antigen presentation)³⁷. In the ER, the heavy and light chains of the MHC-I heterodimer assemble, together with stabilising proteins like chaperones^{29,32,38}. These stabilising proteins secure the complex until high affinity peptides insert themselves into the binding-groove^{29,32,38}. In opposition, and as aforementioned, during cross-presentation the peptides presented in the MHC-I molecules are exogenous (Figure 2). The processing and presentation of peptides from an exogenous origin can differ from the endogenous processing. Two main pathways have been described, the cytosolic and the vacuolar²⁹ (Figure 2). The cytosolic pathway, similar to the endogenous peptide presentation, is proteasome dependent³⁹. Proteins that enter the cell through endocytic routes are degraded by proteasomes into peptides. These are transported to the ER by the TAP protein and loaded onto MHC-I through classical mechanisms (Figure 2)³⁹. Contrarily, the vacuolar pathway is proteasome and TAP independent, but it is sensitive to lysosomal inhibitors⁴⁰. Hence, the processing and loading onto MHC-I molecules is most certainly occurring in endocytic vesicles, avoiding the ER (Figure 2)²⁹.

DCs are also sensing cells, and upon specific signals from PRR recognition, they undergo maturation. This promotes the upregulation of the expression of MHC-I and II molecules, alongside with chemokine receptors (CCR2, CCR6, CXCR3)⁴¹, costimulatory molecules (CD80, CD86, CD40 and CD54) and the release of pro-inflammatory cytokines (Figure 1, step 2)⁴². This maturation process enables DCs to migrate to lymph nodes and be in close contact with naïve T cells, leading to T-cell activation⁴³.

1.3 T cell priming and activation (Step 3). The T-cell receptor (TCR).

The activation of T cells in an antigen-dependent manner requires the recognition of MHC-I/peptide (MHC-I/p) complexes by T-cell receptors (TCRs). The TCR consists of two TCR chains and clusters of differentiation 3 chains (CD3). TCR α and TCR β , the two most common isoforms, form a heterodimer that interacts with CD3 chains forming a multiprotein complex on the cell surface⁴⁴. TCR chains are formed by a cytoplasmic tail, a transmembrane domain, and an extracellular region. This outer region contains a constant domain (C) and a variable domain (V), arranged in an immunoglobulin-like structure⁴⁴. The immunoglobulin-like variable domain constitutes the antigen-binding site of the TCR and defines its specificity, and it is assembled from segments coded by the V, D and J genes, by genomic recombination^{44–46}. DNA rearrangement of these genes generates a high number of random TCRs with potential to bind to the extensive MHC-I repertoire, broadening the capacity of the immune system to react against a large number of unpredictable peptides. But this random rearrangement inevitably generates TCRs that can recognise self-antigens, which can lead to autoimmunity^{32,37,45}. For this reason, TCRs undergo positive and negative selection upon formation⁴⁷. First, immature double positive CD8+CD4+ T cells encounter cortical thymic epithelial cells (cTEC) in the thymus, expressing MHC-I and MHC-II/self-peptide (MHC/sp) complexes⁴⁷. T cells bind these complexes and commit to either CD8+ or CD4+ cell lineage, through a process known as positive selection⁴⁷. CD8+ T cell lineage constitutes the major killer cell group, targeting and eliminating neoplastic cells, whereas CD4+ T cells play an indispensable role maintaining the CD8+ T-cell response and preventing exhaustion⁴⁸. Next, MHC-restricted T cells migrate to the medulla, where single positive T cells interact with medullar thymic epithelial cells (mTEC) and undergo negative selection⁴⁷. Most T cells that strongly recognise MHC/self-peptide complexes do not progress and become apoptotic, while a small number of clones get survival signals and become T regulatory cells (Tregs). T regs are key players in balancing the cytotoxic function of CD8+ T cells, and the general immune homeostasis⁴⁹. This negative selection in the thymus operates as the main mechanism of central immune tolerance⁴⁹. Mature naïve T cells, expressing a functional TCR without affinity for self-antigens, migrate to secondary lymphoid organs to be activated^{45,47}.

Interaction between DCs and T cells results in T-cell activation upon cross-priming (Figure 1, step 3). The main cell-to-cell contact between APCs and naïve T cells is known as

Introduction

the immunological synapse⁵⁰. In the cancer context it has two main objectives, inducing the activation and clonal expansion of T cells, and triggering their effector functions in tumour sites⁵¹. During the synapse, three main cues occur: the adhesion of the two cells in contact through adhesion molecules, the recognition of MHC-I/p complex by the TCR, and the co-stimulation/checkpoint signalling, fundamental for the killing machinery to fully activate⁵⁰. This extracellular signalling is translated into intracellular pathways within the cell that promote the expression of key genes for T-cell activation⁴⁴.

During the immunological synapse, T cells and APCs interact in a receptor-ligand manner and adhere to each other (Figure 1, step 3)⁵⁰. CD8+ T cells migrate through the interactions of chemokine receptors expressed on both cell types (CXC3, CXC10 and CXC9) and adhere through the receptors (CD27 and CD2) for ligands expressed on DCs⁵². This contact is the first step of the T cell priming⁴⁸. When the TCR recognises the MHC-I/p complex expressed on the cell surface, a multi protein complex is formed in the interaction spot between the two cells. Not only the TCR:MHC-I/p, but also co-receptors and co-stimulatory molecules take part of this supramolecular activation complex (SMAC)⁴⁸.

Co-stimulatory molecules do not have a strong signalling or adhesive capacity on their own, but they have the potential to enhance signalling or adhesion when they are combined with other stimuli⁴⁸. Thus, to enhance signalling, their incorporation in cancer vaccines has been explored⁵³. Two-step activation in T cells, which requires not only recognition but also co-stimulation, constitutes one of the pathways to regulate the cytotoxic activity of CD8+ T cells. Having single-step activated T cells could specially risk the generation of specific T-cell responses against self-antigens that could not have been present in the thymus⁵⁰. Despite this, bystander activation of T cells exists and can be detrimental in the development of cancer vaccines, entirely based on eliciting a tumour-antigen specific T-cell response^{54,55}. Although generally bystander activation of T cells in infectious processes refers to activation of T cells independently of TCR recognition, in the cancer context it is typically used as an umbrella term that clusters all the T cells that recognise cancer unrelated antigens and are found in the tumour microenvironment (TME) regardless⁵⁴. The role of these non-specific T cell subsets within tumours is not still completely understood, but despite not being tumour specific they can present an activated phenotype and, in some cases, could be exploited in immunotherapeutic strategies⁵⁴.

1.4 Trafficking of T cells and tumour infiltration (Step 4). The TME.

A successful anti-tumour immune response does not only consist in the proper activation of tumour-specific CD8+ T cells, but also in the ability of these to traffic to the tumour site and penetrate the tumour microenvironment (TME)⁵⁶, becoming tumour infiltrating lymphocytes (TILs; Figure 1, step 4). Subsequently, the success of cancer immunotherapies is exactly this, being able to elicit an anti-tumour response targeted and effective on tumour site. Tumours that present an inflamed phenotype with high T cell presence are known as “hot” tumours. Resistance to T-cell infiltration, which leads to immune-excluded or “cold” tumours, translates into poor immunotherapy outcomes in patients^{57–60}.

Mature activated CD8+T cells must be able to traffic to the tumour core and infiltrate it, along with surviving by trying to maintain an effector cytotoxic phenotype, and finally differentiating into memory phenotypes for long-lasting responses⁵⁶. Primed T cells undergo a shift in the expression of extracellular receptors and release of pro-inflammatory cytokines^{61,62}. They gain the expression of molecules that target them to the tumour site and facilitate their extravasation⁶¹. Upon activation, effector T cells reach the blood flow and travel to the site of extravasation (Figure 1, step 4)^{61,63}. Then, they upregulate the expression of homing molecules such as E- and P-selectins which enable T cells to roll on the endothelium of the vasculature⁵⁶. T cells also gain expression of chemokine receptors, such as CXCR3, which ligand binding triggers the activation of adhesion molecules (LFA-1, VLA-4), that in turn bind to ICAM1 facilitating T-cell adhesion^{62,64}. Cytokine expression like IL-6 and TNF α also enhance this adhesion process by stimulating expression of adhesion molecules on the tumour vasculature⁶⁵. As well as activating factors, we can also find the expression of blocking molecules (VEGF or Endothelin B receptor) and signalling pathways that prevent or difficult the adhesion and extravasation of T cells into the tumour site, discussed further.

1.5 Recognition and killing of tumour cells by cytotoxic CD8+ T cells (Step 5)

Activated cytotoxic T cells (CTLs) that successfully extravasate the tumour vasculature and reach the tumour microenvironment recognise specifically target cells that present antigens on MHC-I molecules. This recognition leads to the effector function of CTLs, cell killing (Figure 1, step 5). CTLs can mediate target-cell death via the intrinsic or the extrinsic apoptotic pathway⁴⁸. The intrinsic pathway, or so-called granule exocytosis pathway, is

Introduction

facilitated by the release of granzymes A and B, that enter the cell cytoplasm through membrane pores^{66,67}. Granzymes A is a tryptase that mediates a caspase-independent death, that first interferes with the mitochondrial transmembrane potential and the ATP generation, and later damages the DNA by accessing the nucleus^{68,69}. Granzyme B, a serine protease, cleaves initiator pro-caspases, such as pro-caspase-3, that results in proteolysis of several apoptosis phenotype substrates⁷⁰. The extrinsic apoptotic pathway, or FasL pathway, is also caspase-dependent⁷¹. FasL activation results in the release of cytochrome c by caspases, which leads to apoptosis⁴⁸. Killing of cancer cells increases the breadth and depth of the response, by releasing tumour-specific antigens and hence, re-activating the immunity cycle again¹⁶.

In an ideal context, this cycle would start and propagate until activated CD8+T cells would be capable of eliminating specifically all neoplastic cells. However, the cancer nature, and its relationship with the immune system, is a complex matrix of extremely regulated elements that can often fall off balance. The regulatory arm of the immune system, which primary function is to maintain the systemic homeostasis, can become effectively suppressive and prevent or hamper the cytotoxic function of CD8+ T cells. The intricacy of the tumour microenvironment and the negative feedback mechanisms executed by the regulatory and suppressive immune players (T-regulatory cells or check point inhibitors) will be discussed in depth further on.

2. Role of CD4+ in the anti-cancer immune response

Cancer immunotherapies have predominantly focused on the cytotoxic anti-tumour activity of CD8+ T cells, mainly because of its direct cancer-cell killing function, but also because most tumour cells lack MHC-II expression⁷². For that reason, the study of CD4+ T cells and their role in the systemic immune response against cancer has been long overlooked.

As aforementioned, the cancer immune-cycle initiates and boosts a specific cytolytic anti-tumour T-cell response, that propagates due to the release of more antigens in the TME and the priming of new T cells on secondary lymphoid organs¹⁶. Enhancing the immune system through immunotherapy focusing only on harnessing antigen-specific CD8+ T cell activity may not be the best approach, as there are other cell types that can contribute greatly to the comprehensive immune response towards tumour rejection⁷³.

CD4+ T cells constitute the other major T cell family of the adaptive immune response, alongside the already mentioned CD8+ T cells. CD4+ T cells are extremely versatile and present high phenotypic plasticity⁷⁴. Contrarily to CD8+ T cells, that mainly mediate cell contact-dependent killing, CD4+ T cells exhibit great polyfunctionality, and can become very different effector subsets depending on the environment and context (Figure 3)^{74,75}. CD4+

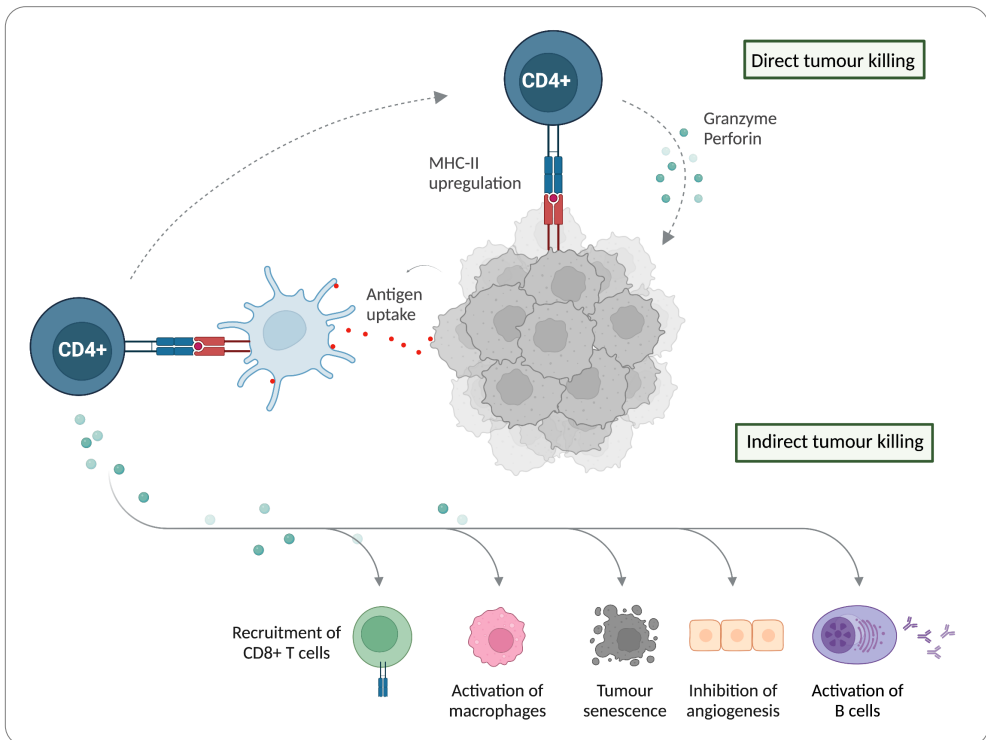


Figure 3. CD4+ T helper tasks in antitumour immunity. CD4+T cells can kill MHC-II expressing tumours directly after priming and activation, by releasing perforin and granzyme B. Furthermore, CD4+ T cells contribute to tumour killing by the release of IFN γ and TNF that recruit T cells and macrophages. In turn, macrophages participate in tumour cell killing by helping release antigens and propagate the cancer immunity cycle. Cytokines and stimulatory factors released by CD4+ T cells also inhibit angiogenesis and drive tumour senescence. Created with Biorender. Adapted from Richardson *et al.* (2021)⁷³.

T cells express TCRs, also generated by DNA recombination, that recognise peptides in the context of MHC-II molecules⁷⁶. Exactly like CD8+ T cells, CD4+ T cells undergo positive and negative selection in the thymus, and their survival is subjected to their affinity for MHC-II/sp complexes⁷⁷. Only CD4+ T cells with moderately affinity for MHC-II/sp progress by receiving surviving signals via TCR/MHC-II contact and continue their thymic maturation

Introduction

until becoming naïve conventional CD4+ T cells⁷⁸. The majority of CD4+ T cells with high affinity for MHC-II/sp do not survive, but a small percentage is redirected into T regulatory cells, that acquire modulatory and suppressive functions to maintain the overall tissue homeostasis^{77,78}.

The key role of CD4+ T cells is 'helping' modulate the state and function of other immune cells, and hence orchestrating a common systemic response^{79,80}. The three main mechanisms of action of CD4+ T cells against a tumour are: (i) help activating CD8+ T cells through dendritic cell licensing; (ii) help activation of B cells and establishment of germinal centres; and (iii) acquiring a cytolytic phenotype and executing their own contact-dependent killing function as cytotoxic CD4+ T cells (Figure 3)⁷⁹.

The contribution of CD4+ T helper cells in the CD8+ T cell cross-priming mechanism by DCs has been extensively examined⁸¹⁻⁸⁴. A recent study of intravital microscopy in mice resolved that CTL priming occurs in two different steps separate in time and location⁸⁵. First, both naïve CD8+ and CD4+ T cells encounter conventional DCs and are primed independently in separate areas of the lymph node (LN)⁸⁵⁻⁸⁷. Next, in a second priming step, both T cells interact with the same lymph-node resident conventional type 1 DC (cDC1s), and the help signalling by CD4+ T cells is delivered^{86,88}. For the second priming to occur, the two cells must interact with the same cDC1 cell, thus DCs need to have an optimal cross-presentation capacity, which allows them to process exogenous proteins and present antigens on both MHC-I and MHC-II. The 'help' signalling offered by CD4+ T cells is mediated primarily by the CD40-CD40L axis⁸⁹. CD4+ T cells upregulate CD40 molecules, which engage with the CD40 receptor on DCs inducing and maintaining a type I phenotype on APCs⁸⁰.

CD4+ T cells also play a major role in providing the appropriate signals to B cells to derive their differentiation into class-switched plasma cells, with affinity maturation (Figure 3). The presence of antibodies specific against tumour antigens can mediate antibody-dependent cell cytotoxicity (ADCC), a killing mechanism carried out by NK cells⁷⁵ or macrophages⁹⁰.

As mentioned, CD4+ T cells can also differentiate into an effector cytotoxic phenotype and contribute to the anti-tumour immunity through cell contact-dependent killing^{91,92}. The differentiation mechanisms that lead to the acquisition of this cytotoxic phenotype remain unknown, but evidence of the direct killing of CD4+ T cells have been found⁹³. Dr. Allison's group demonstrated that CTL CD4+ can directly kill cancer cells in an MHC-II restricted manner⁹².

The importance of CD4+ T cells in the development of therapeutic strategies has been eclipsed by the successful outcomes in eliciting effective cytotoxic CD8+ T-cell responses⁷⁵. However, in the past years CD4+ T cells have grown especial attention, and their critical role in the comprehensive response against cancer has been highlighted.

3. Role of NKs in the anti-cancer immune response

Natural killer cells (NKs) are effector cells from the innate immune response that belong to the innate lymphoid cell (ILC) group and thus, lack antigen specificity⁹⁴. All ILCs come from the same lymphoid common progenitor as T and B cells, but the expression of the transcription factor Inhibitor DNA binding 2 (Ib2) represses the development of T and B cell lineages, making it indispensable for the maturation of ILCs⁹⁵. NKs are professional killer cells that rapidly identify targets that can be a threat to the host, such as infected, stressed or transformed cells, and thereby contribute greatly to the tumour immunosurveillance⁹⁴. If the main feature of the adaptive immune response is the antigen recognition and acquired precision in the T and B-cell responses, NKs effector function does not rely on antigenic specificity (Figure 4)⁹⁶. Thus, because of their low specificity, NKs breadth of response can be higher compared to T cells, making them a suitable strategy of cancer immunotherapy⁹⁶.

NKs are a heterogeneous cell population that can express different cell surface receptors depending on the function acquired and the tissue where they reside. Briefly, all NKs express CD56 on the surface, but lack expression of CD3⁹⁷. Often divided into circulating and tissue resident, NKs found in the blood are highly cytotoxic and express CD56^{dim}CD16^{hi}, whereas NKs found in secondary lymphoid organs are mainly modulatory and cytokine producers, and their phenotype is CD56^{bright}CD16^{lo}^{98–100}.

The first step of the NK orchestrated response against tumours is the recruitment of such cells on tumour sites. NKs, as most immune cells, travel and migrate by the expression of chemoattractant receptors for chemokines expressed in inflammation sites. Peripheral and resident NKs express varying receptors, resulting in differential location of NKs subsets in tissues. Despite these differences, CD56^{bright}CD16^{lo} NK cells have been found to be the predominant phenotype in the TME of several different cancers^{101,102}. An increased NK recruitment in tumour sites correlates with better overall outcome for several various cancers^{103–106}, including melanoma^{107–109}. Furthermore, in metastatic melanoma, the

Introduction

presence of immuno-modulatory NKs in the tumour microenvironment has been linked to a better anti-Programmed cell death 1 (PD-1) immunotherapy response in patients¹¹⁰.

Once NKs have travelled to the tumour site, they must be activated upon recognition of damaged or transformed cells. Unlike T cells, NKs do not have a clonotypic receptor generated by random DNA recombination, but rather a combination of germ-line encoded activating and inhibitory receptors¹¹¹. The nature of NK's effector function always relies on the balance between stimulatory or suppressive signals (Figure 4), and their outcome will determine the response to or the tolerance of target cells¹¹². One of the main mechanisms

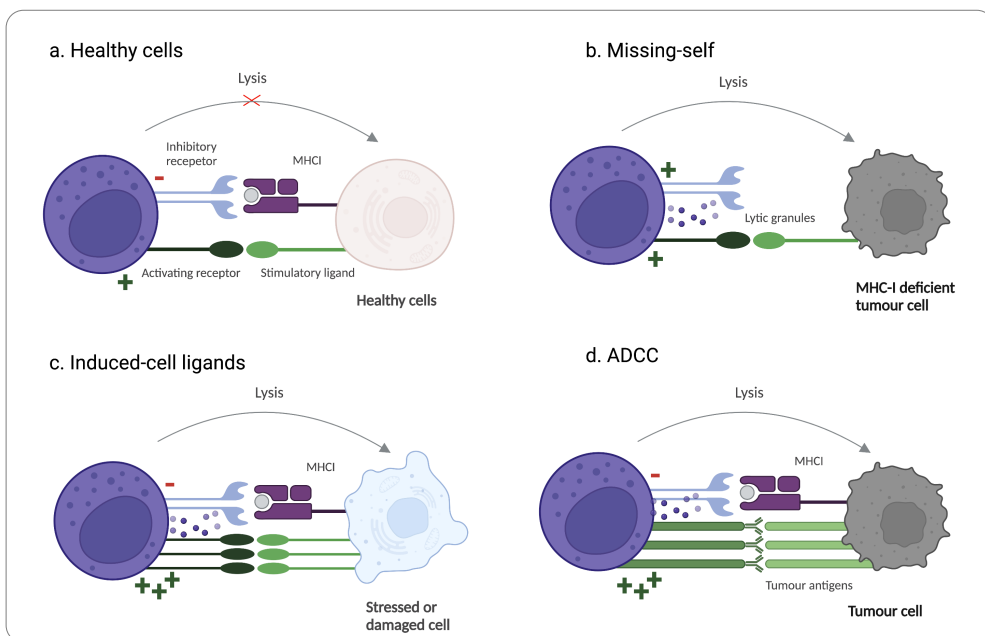


Figure 4. Functionality of NK cells. **a)** The recognition of healthy cells by NK cells is regulated by the signaling balance between stimulatory and inhibitory receptors. **b)** Cells that do not express MHC-I are detected as “missing self” and killed by NKs. Tumour cells often downregulate MHC-I to limit antigenic presentation, and thus can become targets of NKs. **c)** Damaged cells can upregulate the expression of induced stress ligands recognised by activating NK cell receptors. **d)** Antitumour-specific antibodies bind CD16 and elicit ADCC. Created with Biorender. Adapted from Morvan, M.G *et al.* (2015)¹¹⁴.

by which NKs can kill target cells is the recognition of “missing-self” (Figure 4)^{94,111,113,114}. NK cells have Kill cell Immunoglobulin-like Receptors (KIRs) that can bind MHC-I molecules in an unrestricted manner. While healthy cells are spared of NKs’ killing function because of normal MHC-I surface expression, tumour cells become targets as they often downregulated the expression of MHC-I to escape from the adaptive immune response. This missing of self-

molecules on the cell surface automatically triggers a killing signalling, along with the upregulation of activating ligands induced by stress or damage^{112,115–118}.

The cytotoxic activity of NKs is very similar as the cytotoxic activity of CD8+T cells. NKs can kill either through the release of granules and perforin, inducing pore formation and the access of the granules into the cells, or by activation of the FasL pathway. Furthermore, NK cells can mediate an antibody dependent cell killing or ADCC, through the crosslinking between antibody coated cells and the NK surface receptor CD16 (Figure 4)^{113,119}.

All these mechanisms contribute to the direct tumour cell killing, but also to increase antigen availability in the TME, which helps modulate and propagate the adaptive immune response⁹⁴.

Immune escape mechanisms

1. *Cancer immunoediting*

The cancer immunoediting hypothesis contemplates the complex interplay between the tumour-promoting vs the tumour-suppressive functions exerted by the immune system that co-exist in a cancer context¹²⁰. This concept emphasises the dual actions that the immune system can have towards tumour development. The immune response not only contributes to the immunosurveillance and elimination of neoplastic cells, but it can also shape tumour immunogenicity, consequently favouring loss of immune control and tumour growth¹²¹. This immunoediting process is composed of three phases: elimination, equilibrium, and escape (Figure 5)^{120,121}.

During the elimination phase (Figure 5), the innate and adaptive arms of the immune system generate a coordinated response to recognise and kill transformed cells^{120,121}. The elimination phase becomes the endpoint of the immunoediting process only when all transformed cells are eliminated, if there are surviving subclones that can avoid killing, the tumour progresses into an equilibrium state¹²². During equilibrium (Figure 5), the tumour enters a dormancy functional state where its growth is specifically controlled by the immune system. This phase can be a stable period where latent tumour cells can survive in the patient for a long period of time until resuming growth¹²¹. The balance between an immunosuppressive environment and the immune cells with anti-tumour effector functionality contributes greatly to maintaining this state of immune-mediated dormancy. A shift in this balance towards elimination or escape will decide the tumour fate (Figure 5)¹²².

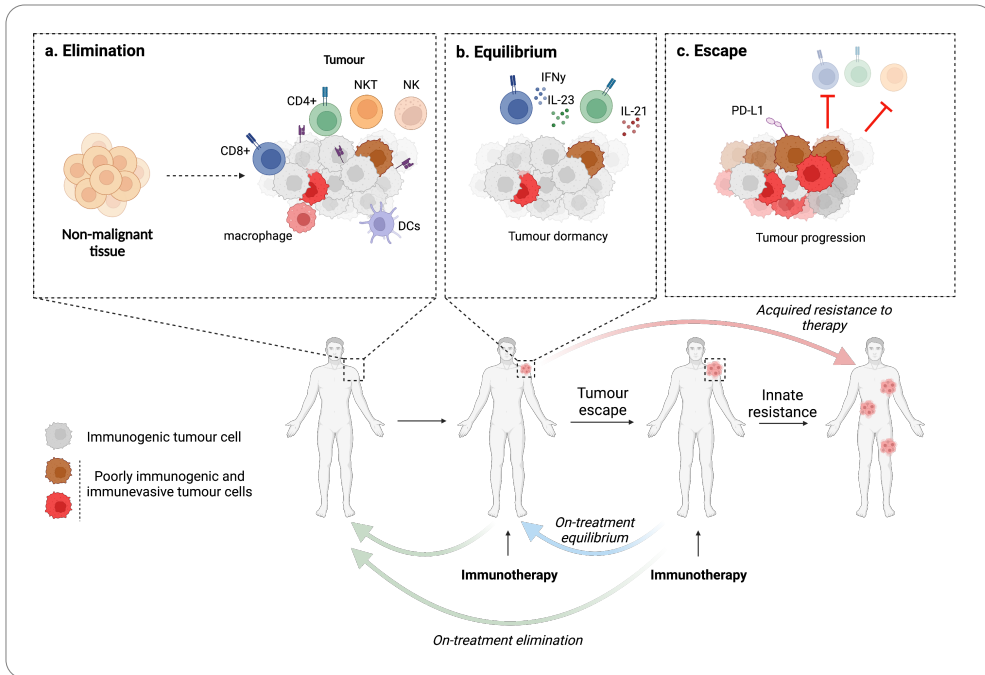


Figure 5. Cancer immunoediting and response to cancer immunotherapy. The cancer immunoediting process consists of three phases. **a)** Elimination: during the elimination phase innate and adaptive immune cells orchestrate a response to kill neoplastic cells. **b)** Equilibrium: if tumours are not eliminated, they progress into an equilibrium phase, in which growth is limited and tumour immunogenicity is altered by the immune response generated. **c)** Escape: edited tumours that escape equilibrium progress uncontrollably, acquiring a suppressive phenotype that halts the effector function of the cytotoxic response. If immunotherapy cannot elicit an effective cytotoxic response or overcome the immunosuppressive environment, the tumour will continue growing and the patient will have acquired an innate resistance. Alternatively, immunotherapy can lead tumours into an elimination phase again, that would result in a complete response, or into an on-treatment equilibrium, hence a partial response to treatment. Created with Biorender. Adapted from O’Donnell, J.S *et al.* (2019)¹²².

Some mechanisms happening during the equilibrium phase help edit the antigenicity of tumours and participate in disrupting the balance¹²². For cytotoxic T cell to execute their effector functions, these need to recognise tumour-specific antigens (TSA) on neoplastic cells presented in the context of MHC-I molecules. The availability of TSA, including neoantigens, depends, among other aspects, on the mutational burden of tumours¹²³. A higher rate of mutations within a tumour increases the probability of generating non-synonymous mutations that are expressed and correctly presented by APCs to cross-prime T cells^{123,124}. Therefore, the tumour mutational burden (TMB) has become a predictive biomarker of response to some immunotherapeutic strategies, and patients with high mutational burden generally correlate with better therapeutic outcomes^{125–127}. However,

the association between a high mutational rate and the level of tumour immunogenicity is not entirely accurate, as only clonal neoantigens promote immune surveillance and effective killing of tumours^{128,129}. The chance of neoantigen clonality does not only depend on the mutational burden, which makes tumour heterogeneity a critical aspect of their immunogenicity¹³⁰. Patients that respond well to checkpoint blockade immunotherapies appear to have a high clonal neoantigen burden and a low subclonal heterogeneity, probably resulting in more effective cytotoxic activity from TILs¹²⁸. Despite this, the immune pressure exerted over tumours during immunoediting processes can result in loss of neoantigen expression overtime, promoting immune escape and tumour resistance^{130–132}.

Other mechanisms that can drive the tumour towards escaping the immune response are an increased survival through an upregulation of STAT-3 and anti-apoptotic molecules, and the establishment of an immunosuppressive microenvironment¹³³.

2. *Elements in the tumour microenvironment (TME)*

The TME is a matrix of different cell types whose overall phenotype can guide tumour progression (Figure 6)¹³⁴. Beyond fibroblasts, endothelial cells and stromal cells, tumours are infiltrated by many different innate and adaptive immune cells that represent the complexity of the cancer nature¹³⁴. In the past, adaptive immune cells, specifically T cells, have drawn the attention for their cytotoxic capacity and their success in different treatment strategies^{135,136}. However, recent studies have demonstrated that the presence of innate and other adaptive immune cells in the TME is critical in controlling T-cell fate and shaping the overall TME phenotype. During the immunoediting process, tumoral cells, resisting the effector immune response generated, can alter the TME into a suppressive state (“cold” tumours) that impairs the effector function of the anti-tumour immune mediators¹³⁴. The balance between pro and anti-tumour inflammatory players determines the progression of the tumour and the capacity to sustain the cancer immunity-cycle¹³⁷. Hence, the aim of immunotherapies is to restore a stimulatory microenvironment that promotes anti-tumour killing, turning “cold” tumours into “hot” ones^{134,138,139}.

Immune cells found in tumours can be categorised into two main groups: anti-tumour cells, that generally have a cytotoxic phenotype polarisation and promote tumour killing, and pro-tumour cells, which maintain a suppressive environment that sustains tumour growth and development (Figure 6)^{134,140}.

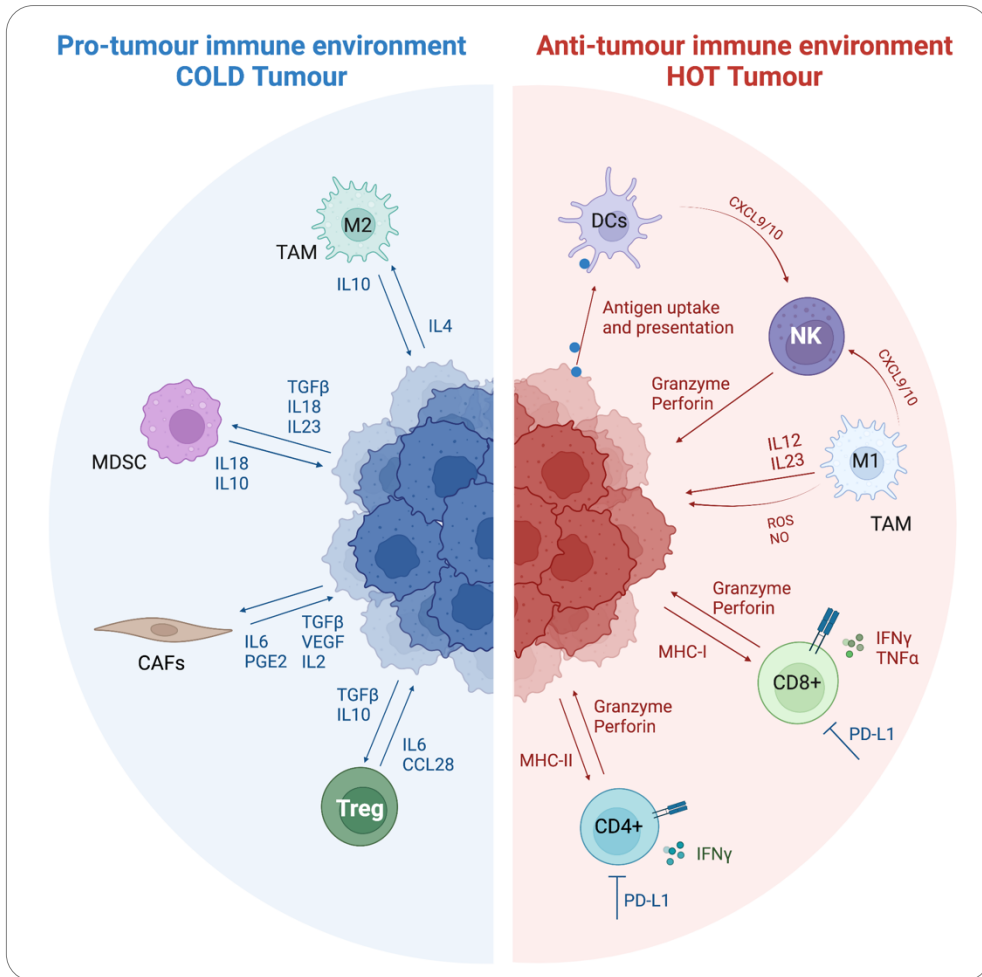


Figure 6. “Cold” vs. “Hot” tumours. A cold or pro-tumoral environment is characterised by low immunogenicity due to lack of neoantigens and impaired MHC-I presentation. Moreover, the lack of chemokine secretion and the fibroblast-rich stroma results in a low T-cell infiltration. The presence of immunosuppressive cell subsets (Tregs, MDSCs, CAFs or TAMs) and the release of inhibitory cytokines leads to T cell dysfunction. Contrarily, hot tumours are highly immunogenic and promote an anti-tumour environment that results in tumour cell elimination. These tumours are infiltrated by CD8+ T cells, that recognise and kill transformed cells via HLA-peptide complex interaction, and NKs that kill non-specifically through “missing self”. The inflamed tumour phenotype releases cytokines that recruit more immune cells like DCs and M1, which in turn contribute to maintaining the cancer immunity cycle. Created with Biorender. Adapted from Zhang, J *et al.* (2022)¹³⁷.

a. Anti-tumour immune environment

Cell subtypes that promote tumour elimination in the TME are T cells, DC1, type 1 macrophages (M1) and NKs. Cytotoxic T cells are the main executors of the anti-tumour responses, and their activation and priming are mediated by DCs. High infiltration of T cells

in tumours correlates with immune checkpoint blockade (ICB) responsiveness and better prognosis in patients^{141,142}. Furthermore, a stimulatory immune environment is also characterised by a high infiltration of NK cells, a killing subset that play a key role in the context of cancer. Immunoedited tumours can impair MHC-I expression to avoid T-cell recognition, which in turn makes tumour cells a direct target of NK killing. NK abundance in tumour has been associated with increased overall survival in different cancers^{94,143}.

Tumour-associated macrophages (TAMs) represent one of the main cell subtypes within the tumour microenvironment¹³⁴. TAMs can be polarised into the classically activated M1, which exert anti-tumour functions, or the alternative activated M2, that promote tumour progression and invasion¹⁴⁴. TAMs present high plasticity and their phenotypes can be modulated through changes in the environment or by therapeutic interventions^{134,145,146}.

M1 macrophages

M1-like polarised macrophages have an intrinsic pro-inflammatory nature and a strong capacity to present antigens in MHC-II context. M1 macrophages are also characterised by a high production and release of pro-inflammatory cytokines (IL-12 and IL-23; Figure 6), that lead to the recruitment of NKs and T cells, and eventually to the activation of Th1 immune profiles¹⁴⁷. M1 macrophages can also mediate cell killing through the release of molecules like ROS or nitric oxide (NO; Figure 6), which have direct cytotoxic effects on cells, and ADCC that requires participation of specific antibodies¹⁴⁸.

b. Pro-tumour immune environment

Immune Checkpoints

Immune checkpoints are stimulatory and inhibitory pathways that modulate the activation and functionality of T cells (Figure 6). They are important immune regulators to maintain the balance between stimulatory and suppressive activity, therefore controlling immune homeostasis and preventing possible autoimmune responses¹⁴⁹. These pathways, besides contributing to maintain self-tolerance, also regulate the type of adaptive immune response, its magnitude and duration¹⁴⁹. In the cancer context, the expression of these immune checkpoint molecules by neoplastic cells in the TME can dysregulate completely the anti-tumour T-cell response, preventing T cells to exert their effector function, thus enhancing tumour growth and development¹⁵⁰. Blocking these regulatory pathways through

Introduction

therapeutic antibodies has been the biggest contribution to cancer immunotherapy strategies in the past 30 years, and it has provided a shift in the cancer therapy paradigm¹⁵¹. Two different groups, Dr James Allison's^{151,152} and Dr Jeffery Blueston's¹⁵³, described the activity of cytotoxic T-lymphocyte associated protein 4 (CTLA-4) and the immune enhancement after blockade. CTLA-4 is an intracellular molecule which upon T-cell activation translocates to the cell surface and competes with CD28 for CD80/CD86 binding, a co-stimulatory signal indispensable for proper T-cell activation by APCs. CTLA-4 binding to CD28 results in arrest of T-cell activation and proliferation^{150,154}.

The other major immune checkpoint that has been extensively analysed in the cancer context is the PD-1/PD-L1 axis¹⁵⁴. PD-1 receptor has become the main inhibitory modulator in the TME to negatively regulate T cell activity and prevent its antitumoral function. PD-1, expressed by T cells, starts an inhibitory pathway mediated by phosphatase SHP-2 (tyrosine phosphatase-2), which dephosphorylates signalling molecules downstream of the TCR synapse¹⁵⁰. In turn, signalling in the subsequent cascade is attenuated and T-cell activation and cytokine production decrease¹⁵⁵. PD-1 has two ligands, the most common being PD-L1¹⁵⁰. Broadly expressed by many different somatic cells upon pro-inflammatory cytokine exposition¹⁵⁵, PD-L1 is also expressed by tumour cells in the TME and its binding results in T cell exhaustion, inhibiting the cytotoxic antitumour T cell function¹⁵⁴.

Beyond CTLA-4 and PD-1/PD-L1 molecules, there are other emerging inhibitory checkpoints identified that are involved in inhibiting immune cells that contribute to the anti-tumour response in the cancer immunity-cycle. Some examples of newly identified immune checkpoints are TIGIT, a receptor expressed on lymphocytes that impairs T cell priming, preventing tumour cell killing by NKs and tumour specific T cells¹⁵⁶; Lag3, an immunoglobulin-like receptor expressed on activated T cells that negatively regulates their function in the TME¹⁵⁷; and TIM3, highly expressed on TILs, it can engage with Gal9 and suppress antitumour immunity by both adaptive and innate immune cells¹⁵⁷.

T regulatory cells

CD4+ T regulatory cells (Tregs) are a subset of highly immunosuppressive CD4+ T lymphocytes that serve to maintain self-tolerance and prevent autoimmunity¹⁵⁸. Phenotypically expressing FoxP3, these CD4+ T cell subset express high levels of cytokine IL-10 and transforming growth factor β (TGF- β), two immunosuppressive molecules⁷⁵ (Figure

6). In normal conditions, Tregs work as immune modulators, and maintain a homeostatic environment promoting peripheral tolerance through the regulation of effector T cells^{158,159}. In the context of cancer and as part of immune escape mechanisms, tumours promote the recruitment of Treg cells in the TME, which suppresses the activity of T effector (Teff) cells and prevent anti-tumour rejection¹⁵⁸. The balanced interplay between Teff cells and Tregs determines the immunological outcome of tumours¹⁵⁸. These two populations of cells have a complex dynamic characterised by an opposition in functionality. The immunosuppressive capacity of Tregs can be compromised by the effector function of activated T cells in an acute infectious or inflammatory state, to guarantee a clearance of infection. In a tumour context, while a typical response represents the suppression of Teff cells by a functional Treg population, under specific conditions such as immune modulatory therapy, this dynamic can be reversed, and Teff cells can antagonise a Treg population to regain functionality¹⁵⁸.

Myeloid-derived suppressive cells (MDSCs)

MDSCs are neutrophils and monocytes with a high immunosuppressive capacity and represent the main suppressive cell subset in the TME, sustaining cancer progression¹⁶⁰ (Figure 6). MDSCs are usually divided in two main groups: polymorphonuclear MDSCs and monocytic MDSCs, which phenotypically coincide with neutrophils and monocytes respectively¹⁶¹. MDSCs participate actively in different immune escape mechanisms that favour tumour progression, such as angiogenesis, pre-metastatic niche formation and epithelial-mesenchymal transition (EMT), but the most defining feature among these pro-tumoral functionalities is the suppression of immune cells, being T cells the main target¹⁶¹.

MDSCs can interfere with T-cell trafficking into the tumour site. MDSCs express a disintegrin enzyme that cleaves the extracellular domain of L-selectin on CD4+ and CD8+ surface, which limits their homing into target sites¹⁶². Furthermore, MDSCs can negatively regulate T cell function by producing NO, which prevents T-cell proliferation by inhibiting the Jak/STAT5 pathway in T cells, or indirectly by hindering antigen presentation by DCs^{163,164}. Another mechanism that MDSC use to inhibit T-cell functionality is to deplete amino acids required for proper T-cell activation and proliferation. MDSCs produce high levels of arginase 1 which leads to the depletion of L-arginine in the TME, resulting in a down regulation of CD3 chains and hence, T-cell proliferation arrest¹⁶⁵.

Introduction

MDSCs are also high producers of suppressive cytokines, mainly IL-10 and TGF- β ¹⁶⁶ (Figure 6). IL-10 has been proven as a non-redundant immunosuppressive mechanism and its blockade results in an improved therapeutic outcome in patients, correlating with a release in T cell suppression and delayed tumour progression^{167,168}. TGF- β is another well-known cytokine that negatively regulates the immunological environment in the tumour¹⁶⁹. TGF- β can polarise macrophages into a pro-tumoral M2-like phenotype and its essential in Treg induction^{170,171}. In mice models it can directly inhibit the activity of NK cells and NKT cells in a cell-dependent manner^{172,173}.

Overall, MDSCs play a critical role in maintaining a pro-tumoral context and in animal models where MDSC have been depleted, the TME breaks down allowing access and activation of immune effector cells^{166,174,175}.

Cancer associated fibroblasts (CAFs)

CAFs are a type of stromal cells that constitutes one of the key components of the tumour microenvironment. As established, the TME is a complex multi-cellular system, and the interactions between cancer cells and stromal cells are critical for the tumour evolution¹⁷⁶. CAF is usually an umbrella term that clusters a variety of mesenchymal cells from different origins that present an activated phenotype in the TME and differ in function from regular fibroblasts¹⁷⁷. CAFs represent a highly heterogeneous cell population with great plasticity. Such heterogeneity can be attributed to the wide spectrum of origins these cells can have depending on the cancer type¹⁷⁷⁻¹⁸¹. CAFs are known to produce extracellular matrix components (ECM) such as collagen, fibronectin and hyaluronan that provide a physical scaffold for tumour cells to evolve¹⁸². They also play a critical role in angiogenesis by the secretion of pro-angiogenic factors such as VEGF¹⁸³. Along with the immunoediting process and the establishment of an immunosuppressive environment, CAFs also participate in immune evasion mechanisms that help sustain this environment through the release of factors such as IL-6, TGF- β and PGE2 that inhibit activation and function of adaptive immune cells^{169,184,185}.

Cancer immunotherapies

Conventional cancer therapies are based on three main approaches: surgical excision, irradiation, and chemotherapy. The major approach for either localised or metastasised

tumours is chemotherapy, which often can be used in combination with others¹⁸⁶. However, chemotherapy treatment has several limitations, the most important being the high toxicity levels. Chemotherapeutic agents have low aqueous solubility and require solvents for the final formulation, which increases their toxicity^{186,187}. Furthermore, these cytotoxic agents have non-specific targets, acting on the DNA itself or on enzymes required for DNA synthesis and repair¹⁸⁸. Cancer cells have high proliferative rates and limited repair capacity which makes them vulnerable for these kinds of agents, but the lack of specificity of this treatment leads to off-target damage to other tissues, such as the endothelium or hair follicles¹⁸⁸. Moreover, cancer cells generate resistance to chemotherapeutic agents overtime, mainly through the increased expression of membrane transport proteins which are responsible for pumping the drugs out of the cells¹⁸⁹. Limitations of conventional therapies, mostly the lack of treatment specificity, have created a necessity of developing new treatment approaches.

Cancer immunotherapies (CIT) have completely revolutionised cancer treatment¹⁹⁰. Their aim is to enhance and modulate the patient's own immune system to generate a specific immune response that can target tumour cells, exactly how it would work with a foreign viral infection^{138,190,191}. Since the onset of cancer, an intertwined relationship is generated between the tumoral cells and the immune system. As the cancer evolves, and the immunoediting process starts, the complex interplay between the tumour and the immune system unfolds. The tumour progresses from the elimination phase to an equilibrium, to finally fall towards escape in a context-dependent manner¹³⁹. The goal of immunotherapies is to alter and modify these outcomes to obtain a complete cancer eradication¹⁹⁰.

1. Cytokines

Cytokines are one of the most important immune molecules, and they act as major regulators of the immune system, enabling immune cells to communicate over short distances¹⁹². As one of the main immune molecular messengers, cytokines have drawn considerable interest in recent years (Figure 7). Their capacity to modulate the innate and adaptive immune responses, to enhance cell mobility and to potentiate cytotoxic activity have made cytokine therapies one of the first immune therapy approaches developed¹⁹². Cytokines can regulate and signal very different immune functions, such as promote growth, stimulate differentiation, or participate in inflammatory or anti-inflammatory signalling

Introduction

processes¹⁹³. Their half-life in circulation is limited, which reduces their action span to a defined period triggered by specific stimulus resulting in cytokines exerting either autocrine or paracrine functions¹⁹³.

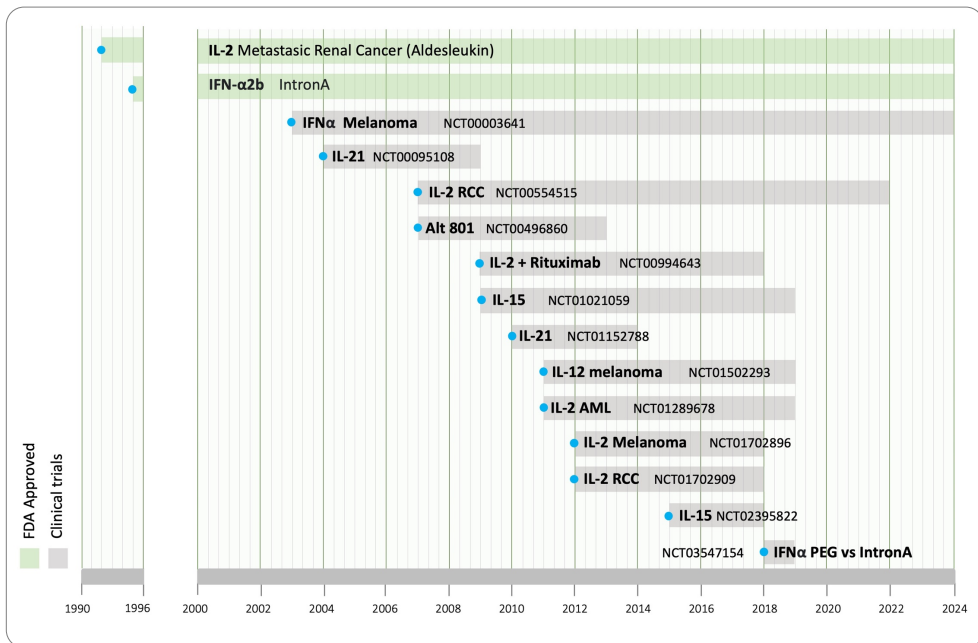


Figure 7. Timeline of cytokine therapies. Relevant cytokine therapies either FDA approved (in green) or in at least phase I of a clinical trial (in grey) (clinicaltrials.gov)^{192,194–196}.

Up to 2021, there were 2630 clinical trials registered on *clinicaltrials.gov* using cytokines, alone or in combination, as part of the cancer treatment¹⁹⁴. Among these, IL-2 and IFN α are two of the most studied, and the only two approved by the FDA (1992 and 1995, respectively) for immunotherapeutic applications in different malignancies (Figure 7)^{195,196}. The approval of cytokines for cancer therapies was probably the biggest milestone in CITs until immune checkpoint inhibitors, as it was the first time that therapeutic interventions were able to modulate the response and alter the balance between the immune system and the tumour, leading to durable effective outcomes¹⁹³.

IFN α belongs to the type I Interferon family, and it plays a critical role in the presentation of cancer derived antigens as it promotes MHC-I presentation on tumour cells and induces DC activation^{197,198}. It is also characterised by a potent apoptotic inducing activity on tumour cells. IFN α administration in high doses can also have antiangiogenic effects, as this cytokine can influence the tumour vasculature¹⁹⁹. Other variants of this molecule, which aim to

increase its solubility and short half-life, have also been tested to study the effects of longer exposure time of tumour cells to IFN α ²⁰⁰.

IL-2 is mostly produced by activated CD4+ T cell with a Th1 polarisation, followed by CD8+ T cells, NK and NKT cells¹⁹². It acts mainly as a lymphocyte growth factor in the initiation of the immune response and promotes antigen activated CD8+ T cells¹⁹². Moreover, the IL-2 cytokine has also a key role in regulating the magnitude of the T cell response and it is involved in its termination, helping maintain self-tolerance²⁰¹. On its immunosuppressive side, IL-2 can act as a potent negative immune regulator stimulating the Treg subset of CD4+ T cells²⁰². IL-2 alone has been tested for several types of malignancies but despite being a potent lymphocyte stimulator (Figure 7)^{196,203,204}, IL-2 administration in high-doses can have severe systemic side effects due to its toxicity, and its clinical application has been hampered in the past years¹⁹³. Second generation IL-2 formulations are being developed to improve its pharmacodynamic properties¹⁹³. Furthermore, IL-2 administration has also been tested in combination with other treatments, which results in enhanced efficacy. The transfer of autologous TILs expanded *in vitro* is almost universally used with a combined administration of an IL-2 regime^{205,206}. IL-2 has also been tested in combination with chemotherapies showing partial or total remission in <50% of patients (Clinical trial ID: NCT00994643; Figure 7)¹⁹⁴.

Due to the therapeutic effects of IL-2, other cytokines from the IL-2 family (IL-15, IL-21) have also been studied in clinical applications with different malignancies. Interleukin-15 shares some functionalities with IL-2, such as the stimulation of activated T cells and production of CTLs, as well as inducing the proliferation of NK cells¹⁹². Whereas IL-2 has a critical role in terminating the T-cell response and modulating its magnitude, IL-15 does not contribute to this process and does not take part in maintaining the fitness of the Treg subset¹⁹². Recombinant IL-15 has been tested in a clinical context showing a rapid redistribution and activation of NKs and memory CD8+ T cells upon its administration (Figure 7)²⁰⁷.

Interleukin-21, another cytokine from the IL-2 family, has also been studied in clinical applications. IL-21 is involved in different immune processes, but mainly in helping induce the activation and survival of anti-tumoral CD8+ T cells and in the development of CD4+ follicular helper cells^{208,209}. In a phase I study of recombinant IL-21 (rIL-21) administration to

Introduction

two different cohorts (Clinical trial ID: NCT00095108; Figure 7), a 50% and 89% of overall disease control rate was observed upon cytokine administration²¹⁰.

2. Immuno-checkpoint inhibition

As described in a previous section, immune checkpoint inhibition (ICI) is the biggest milestone achieved in the past years among cancer immunotherapy strategies. During the escape phase, tumour cells evade immune surveillance and elimination by activating checkpoint pathways that suppress the cytotoxic activity of immune cells²¹¹. ICI blocks the immunosuppressive pathways interrupting the inhibition signalling, which results in a restoration of the antitumour immune response²¹¹.

Ipilimumab, an anti-CTLA-4 antibody, was the first IC blockade approved by the FDA in 2011 (Figure 8)²¹². Dr Allison and colleagues demonstrated that CTLA-4 blockade could lead to complete tumour regression in syngeneic animal models with partially immunogenic tumours^{151,152}. Animals challenged with poorly immunogenic tumours did not respond upon administration of anti-CTLA-4 as a single agent but did generate partial responses when the antibody administration was combined with a vaccination against GM-CSF, indicating that CTLA-4 blocking enhanced a pre-existing endogenous response against the tumour²¹³. With these preclinical results, Ipilimumab entered clinical trials in patients with advanced melanoma in the early 2000s²¹⁴. After demonstrating for the first time that patients had a 3.5-month survival benefit compared to the standard treatments, Ipilimumab was approved for use in advanced melanoma patients²¹⁵. Furthermore, in long-term analysis of survival after Ipilimumab administration, patients that received the IC blocker showed an 18% increased survival over 2 years²¹⁵. Long-term responses after therapy supported the hypothesis that ICI could be modulating the overall immune response generated, with prolonged results long after administration²¹⁶. Since then, anti-CTLA-4 antibodies have been studied in hundreds of trials, as single agents or in combination, for many diverse types of malignancies²¹¹.

PD-1 has emerged as a dominant negative immune regulator of T cell activity within tumours and peripheral tissue, and it is the target of the other main class of ICI. PD-1 is expressed when T cells become activated, and it can engage with its primary ligand (PD-L1) expressed on the surface of tumour cells¹⁵⁰. This mechanism results in a critical immune

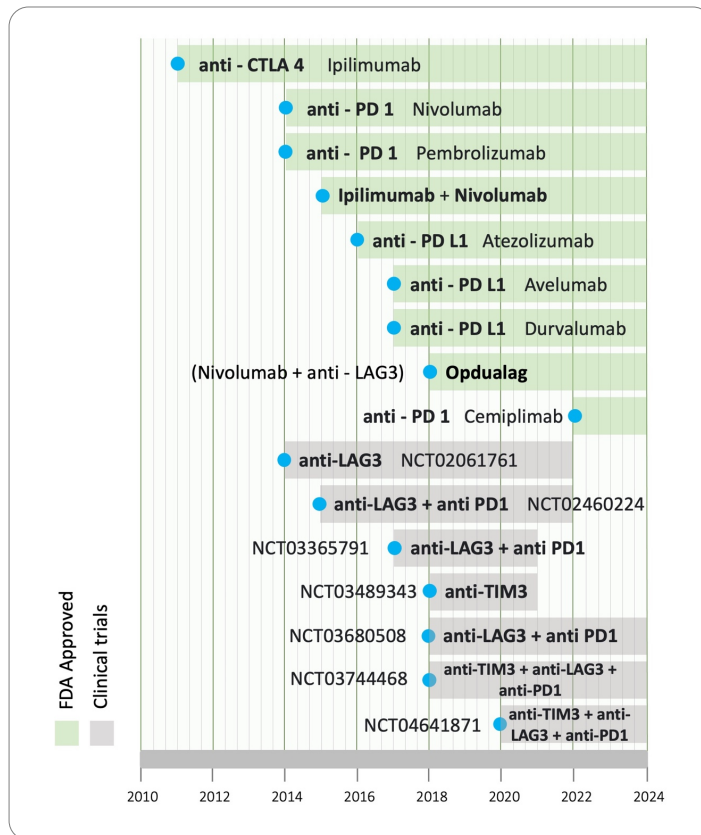


Figure 8. Immuno-checkpoint inhibition (ICI). In green therapies approved by the FDA, in grey therapies that have reached at least phase I in clinical trials (clinicaltrials.gov) ^{150,212}.

evasion strategy in the tumour microenvironment^{217,218}. The PD-1/PD-L1 axis, first discovered^{219,220} and extensively investigated by Dr Honjo and colleagues, has become the main immunosuppressive regulator of T cell effector functionality within tumours, and it contributes to maintaining a pro-tumoral immune microenvironment²²¹. The first preclinical results supporting the hypothesis that interaction with PD1/PD-L1 pathways could affect anti-tumour responses were obtained with a mouse mastocytoma cell line. In this setting, the overexpression of PD-L1 inhibited activity of CD8+ T cells via PD-1 ligation inducing increased tumour growth and invasiveness²²². The first anti-PD-1 antibody, which entered phase I of a clinical study with advance melanoma patients, showed durable remission in 32% of patients²²³. Since its first approval in 2014, the safety and efficacy of anti-PD-1 antibodies have been tested in a variety of solid tumours and haematological malignancies, either as monotherapy or in combination²²⁴. After the approval of Nivolumab, there have

Introduction

been two more anti-PD-1 (Pembrolizumab and Cemiplimab; Figure 8) approved antibodies, and three anti-PD-L1 (Atezolizumab, Durvalumab and Avelumab; Figure 8). Currently, after the major success of anti-PD1/PD-L1 antibodies, other IC blockade therapies are being investigated including anti-LAG3 and anti-TIM3 antibodies.

3. Cell therapies

Adoptive cell transfer (ACT) is the other major class of cancer immunotherapy. Whereas ICI is an antibody-based therapy, ACT is based on the transfer of allogenic or autologous immune cells to enhance the function of the immune system and potentiate tumour elimination²²⁵. Cells are modified or expanded *ex vivo* before being transferred back to the patient²²⁶. This strategy has been applied in naturally generated autologous TILs, lymphocytes with engineered TCRs, adoptive transfer of NKs, and chimeric antigen receptor T cells (CAR-T cells)¹³⁹. CAR-T cells are currently the most successful cell-based therapy in the cancer context, with 6 CAR-T cells approved by the FDA, all for haematological malignancies and non for solid tumours (Figure 9). These lymphocytes have engineered chimeric receptors that recognise specific antigens on target cells, mediating their killing^{227,228}. First generation CAR-T cells consisted of minimal structures expressed on T cells formed by an activation domain, usually a CD3 chain, and an extracellular immunoglobulin-like domain that directs specificity^{229,230}. These T cells can recognise antigens independently of HLA but are unable to sustain T-cell responses, due to lack of costimulatory molecules. Second and third generation CAR-T cells have been developed to overcome this challenge and promote proliferation of engineered T cells and their sustained cytotoxic function upon adoptive transfer in patients²³¹. CAR-T cells represent the most successful cell-based immunotherapy to date, especially for haematological malignancies.

The development of CAR-T cells for solid tumours has been extremely challenging despite the promising results in hematologic malignancies²³². Targeting solid tumours does not only rely on the antigenicity of tumour cells, but also on the capacity of engineered T cells to traffic to the tumour site, infiltrate the tumour microenvironment and maintain an effector phenotype to achieve durable and sustainable responses overtime^{233,234}. The barriers and hostile environment of solid tumours represent the biggest limitation in the development of these cell-based immunotherapies²³². Despite this, a significant number of

trials have studied the efficacy of these therapies in different cancer types targeting tumour associated antigens (TAAs) such as: HER2, IL-13Ra2 or CEA^{235–238}.

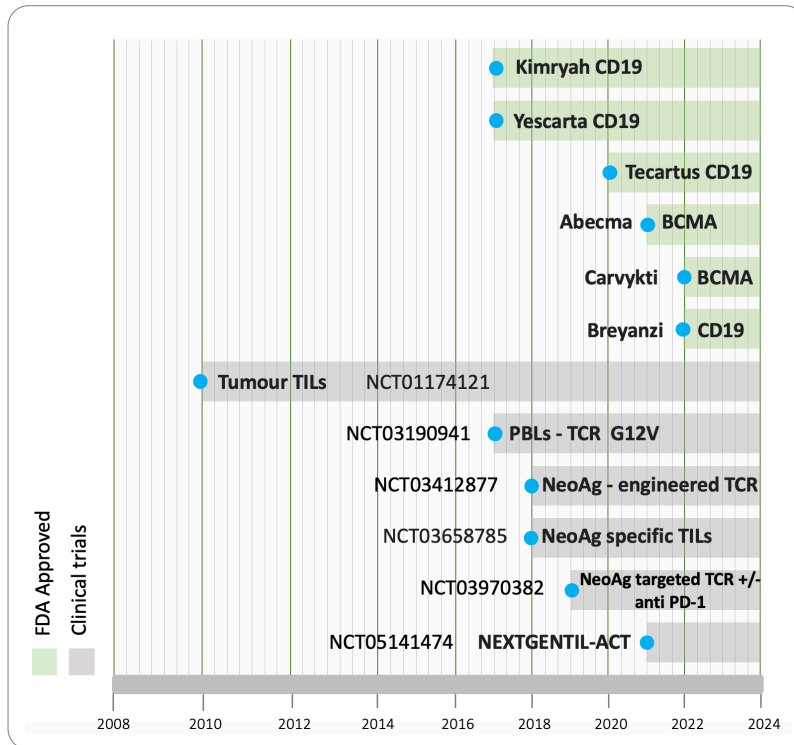


Figure 9. Development of cell-based therapies overtime. In green therapies approved by the FDA, in grey therapies that have reached at least phase I in clinical trials (clinicaltrials.gov)^{226,239}.

Another interesting approach of ACT is the use of autologous TILs²³⁹. Rosenberg and colleagues hypothesised that the use of TILs would be more effective compared to IL-2-expanded lymphocytes from peripheral blood, as TILs would be enriched with tumour-specific T cells²⁴⁰. Certainly, TILs were 50 to 100 times more effective than peripheral expanded T cells in rejection of lung and pancreatic solid tumours in mice²⁴⁰. In patients with metastatic melanoma, transfer of autologous TILs plus high-doses of IL-2 resulted in 34% of overall response rate (complete and partial responses)²⁴¹. A key aspect that plays an important role in determining the clinical outcome of patients undergoing ACT of TILs is the phenotype and tumour reactivity of the autologous TILs. Tumour-reactive enriched TILs are associated with higher overall response²⁴². Within this population, neoantigen-specific T cells have gained special interest in the past years. Expanding T cells with TCR specific for tumour neoantigens probably constitutes the most advanced and personalised strategy

Introduction

among cell-based immunotherapies. Successful tumour regression in patients that have received TILs is likely mediated by these neoantigen specific T cells, as they target neo-epitopes generated by *de novo* somatic mutations that are not expressed in healthy tissue^{243–245}. This technique has been successfully used in several trials of different cancer types and has shown promising results, obtaining complete and partial responses durable in time (Figure 9)^{246–248}. However, the ACT of neoantigen-specific TILs still has important limitations, such as the complex process of neoantigen identification and specific TIL isolation, the homing and infiltration of the tumour by transferred T cells and the effect of the immunosuppressive microenvironment²²⁶. An alternative strategy to autologous neoantigen-specific TILs is the use of T cells with engineered TCRs. These can be genetically altered to express TCRs specific for TAAs or for neoantigens (Figure 9)²⁴⁹.

Finally, other cell-based therapies being currently investigated are the ones involving the use of NK cells. NKs are professional killer cells that do not have antigen specific receptors; therefore, they can recognise and kill target cells independently of HLA. Besides their role as killers, NKs also modulate the innate and adaptive immune response via cellular crosstalk and cytokine production²⁵⁰. Adoptive transfer of NKs constitutes a promising strategy because they do not require antigen exposure to elicit their cytotoxic response. Moreover, NKs have limited persistence *in vivo* which results in a decrease of systemic toxicities associated with some lymphocyte cell transfer therapies²⁵¹. Finally, NKs with a CAR receptor that mediates recognition of antigen-expressing cells are also being explored²⁵².

4. Vaccines

Vaccines developed to prevent infectious diseases constitute the biggest public health success in the modern era²⁵³. Vaccines against viral or bacterial pathogens have demonstrated high efficacy, and a recent excellent example of this are the vaccines developed for the COVID19 pandemic^{254–258}. Approaching cancer as a malignancy that can be treated through vaccination has a clear rationale based on extensive knowledge of the intricate relationship between the immune system and cancer growth, and it is an obvious extension of vaccine functionality. However, despite preclinical and clinical data^{259,260} supporting the promising approach of therapeutic cancer vaccines and their benefits, this journey has been a frustrating one. The increased interest in other immunotherapeutic strategies such as ICI and CAR-T cells have drawn focus away from vaccine development.

Only one cancer vaccine (Sipuleucel-T) has been approved by the FDA since 2010, more than 10 years ago. Sipuleucel-T is a type of vaccine that consists in the activation of autologous PBMCs *ex vivo* with a prostate recombinant fusion protein with GM-CSF (PAP-GM-CSF)^{261,262} for castration-resistant prostate cancer patients. Upon vaccination with Sipuleucel-T, patients showed a 22% reduced risk of death over the placebo group²⁶².

Lin *et al.* reviewed thoroughly the field of cancer vaccines and classified all the current approaches based on: (i) characteristics of the tumour antigen selected, (ii) frequency of expression of the antigens in each patient's tumour, and (iii) strategy used for antigen uptake from APCs (Figure 10)²⁶³.

Antigens used for vaccine development can be known or unknown (Figure 10). Known or predefined antigens are identified ahead using antigen identification pipelines²⁶⁴, and their expression by tumour cells is confirmed. Then, these antigens are formulated as

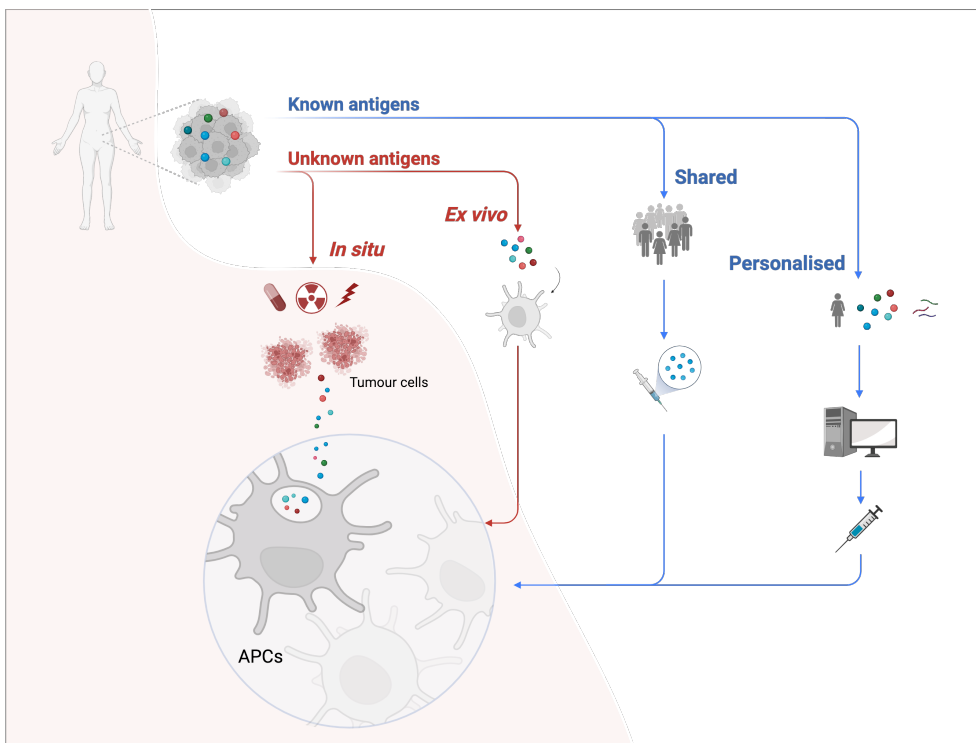


Figure 10. Types of cancer vaccines. Classification of cancer vaccines according to antigen type, antigens can be known (predefined) or unknown (anonymous). Among predefined antigens, these can be individual for each patient or shared among several different tumours that express the same antigens. Regarding anonymous antigens, these cannot be identified before, therefore antigens need to be colocalised with DCs, which can be done *ex vivo* or *in situ*. Created with Biorender. Adapted from Lin, M.J *et al.* (2022)²⁶³.

Introduction

peptides, DNA/RNA or nanoparticles and administered following a classical vaccination strategy²⁶³. On the other hand, unknown antigens cannot be formulated into molecules for administration, and thus need to be loaded onto APCs, which can be made either *ex vivo* or *in situ* (Figure 10)²⁶⁵. A proper activation of loaded cDCs with tumour antigens is critical to ensure cross-presentation and efficient T cell priming²⁹. Whereas *ex vivo* APC loading involves excision of tumour cells, followed by their lysis and delivery to autologous APCs²⁶⁵; *in situ* vaccines promote APC uptake in the tumour site by induction of immunogenic-cell death (Figure 10)²⁶⁶. Vaccines using anonymous or unknown antigens can promote T-cell reactivity against a larger number of antigens, most of them difficult to identify and not included as filters in the predefined antigen identification pipelines.

Vaccines using known or predefined antigens can be further differentiated according to the level of expression of the chosen antigen among different patients and tumours. Antigens expressed in a sufficient number of patients, so-called shared antigens, might be suitable candidates to develop “off-the-shelf” cancer vaccines (Figure 10)²⁶³. “Off-the-shelf” therapies aim to target a group of patients probably expressing a specific tumour type subset²⁶⁷. These strategies are less time consuming and require less resources than personalised approaches. Known shared antigens can include: TAAs, which can be tissue specific or development specific, and TSAs that can originate from non-synonymous somatic mutations or viral antigens²⁶⁷. Tissue specific TAAs are antigens overexpressed in the tissue where the cancer is developing, and one of the most important examples of this is the breast cancer associated human epidermal growth factor 2 (HER2)²⁶⁸. HER2 is overexpressed in 30% of breast cancer tumours and has been the target of anti-HER2 monoclonal antibody therapy^{269–271}. Several peptide-based vaccines using HER2 HLA-I or HLA-2 restricted epitopes failed to elicit relevant responses with clinical benefit^{272,273}, but a multiepitope combination of both types of peptides, targeting the generation of CD4+ and CD8+ T-cell responses, showed durable responses for more than one year in vaccinated patients²⁷⁴. Another type of TAAs are the development-specific antigens²⁷⁵, such as WT1 and NY-ESO-1, expressed in several types of cancer (melanoma, breast cancer, cervical cancer, etc)^{276,277}. A WT1 peptide-based vaccine with high HLA-I affinity (Galipepimut-S) was able to elicit immune responses associated with 5-year survival, and the study progressed to a phase III²⁷³.

In contrast, TSAs or neoantigens are exclusively found in tumour cells and are often drivers of oncogenesis²⁷⁸. Cancer gene drivers, localised in mutational “hot spots”, are

common among several patients²⁷⁹. Therefore, altered peptides originating from these mutations can be presented in common HLA alleles, giving neoantigens that are shared among patients expressing the same tumours and the same HLA allele²⁷⁵. However, these so-called public neoantigens, do not constitute the vast majority of neoantigens yield by driver mutations, which most often are private and patient specific²⁷⁸. Public neoantigens can also be the target of “off-the-shelf” vaccines, and developing resources for the identification of these patients with a relevant expression of public neoantigens is a major challenge²⁷⁸. Some examples of well-known public neoantigens have derived from mutation in these genes: EGFRvIII, KRAS, Tp53 and BRAF^{V600E 280–284}.

Vaccines using known shared antigens have been the main focus in cancer vaccine development since the early 90s. They have drawn the attention from personalised neoantigens as possible therapeutic targets, as the complexity of analysing T cell-reactivity on a patient-basis was too resource consuming²². Now, with the development of high-throughput techniques such as Next Generation Sequencing (NGS) and T-cell based assays, the use of neoantigens is gaining interest and has probably become the most novel and advance strategy among cancer vaccines.

i. Neoantigens

Personalised neoantigens, unlike public shared neopeptides, are unique for each patient and are the most common type of TSAs, most often originating from non-synonymous somatic mutations²⁶³. The clinical relevance linked to the use of neoantigens in a therapeutic context is associated with their intrinsic characteristics. Neoantigens arise from DNA alterations that can lead to completely new DNA stretches non-existing in normal tissue²². These alterations include single-nucleotide variants (SNVs), indels and structural variants^{285,286}. For viral associated tumours, open reading frames in the viral genome can also lead to neoantigen expression. From an immunological perspective, these antigens being truly foreign brings crucial benefits, as the repertoire of T cells that can recognise them is not subjected to central tolerance, and thus will not be eliminated in the thymus during positive selection²². Furthermore, the absence of these neoantigens in healthy tissue guarantees that the T-cell response generated upon vaccination will not be associated with off-target damage²².

Introduction

a. Neoantigen-based therapeutic cancer vaccines

Altogether, cancer vaccine strategies are moving towards the development of therapies that harness the heterogeneity of tumours by trying to overcome challenges such as clonal evolution and immune escape mechanisms, which can eventually edit the expression of specific antigens²⁸⁷. This involves targeting multiple neoantigens that are personalised to each individuals' tumour²². However, only a minor fraction of mutations is presented by MHC molecules and generates relevant immune responses. For that reason, an accurate prediction or identification of mutations that lead to immunogenic neoantigens is a key step in the cancer vaccine developmental process²² (Figure 11). There are three main approaches to identify genetic variations in a tumour: (i) *In silico* computational pipelines, (ii) mass-spectrometry, and (iii) T-cell based assays, which can also be used to validate *in silico* predictions²².

The current process usually starts with the detection of aberrant tumour-specific mutations using whole-exome sequencing (WES)²⁸⁸. Briefly, DNA libraries from tumour cells and normal cells are generated and compared to detect mutations (Figure 11). In addition, RNA-sequencing data is also included to detect possible alternative splicing events and determine the actual level of expression of the mutation²⁸⁸. Then, *in silico* computational pipelines will take all the data obtained from the variant calling and the RNA expression and apply sequential filters to further select these mutations as possible immunogenic peptides²⁶⁴. Two main filters need to be applied to resolve if a mutation will lead to a T-cell recognised-neoantigen. First, knowing if the peptide generated will be loaded onto an MHC molecule, and second, if the MHC/p complex will be recognised by a TCR. NetMHC²⁸⁹ and NetMHCPan^{290–292} are examples of algorithms that allow prediction of epitope binding to MHC molecules. Furthermore, other pipelines incorporate extra steps, such as algorithms that predict peptide processing through correct proteasomal degradation and transport to the ER (NetChop, NetCTL or NetCleave)^{293,294}. However, ensuring the correct presentation of the peptide candidates in the MHC molecules does not guarantee they will elicit a T-cell response^{295,296}. Thus, adding a second main filter that can determine the interactions between MHC/p complexes and TCR is crucial in the peptide identification pipelines²⁶⁴.

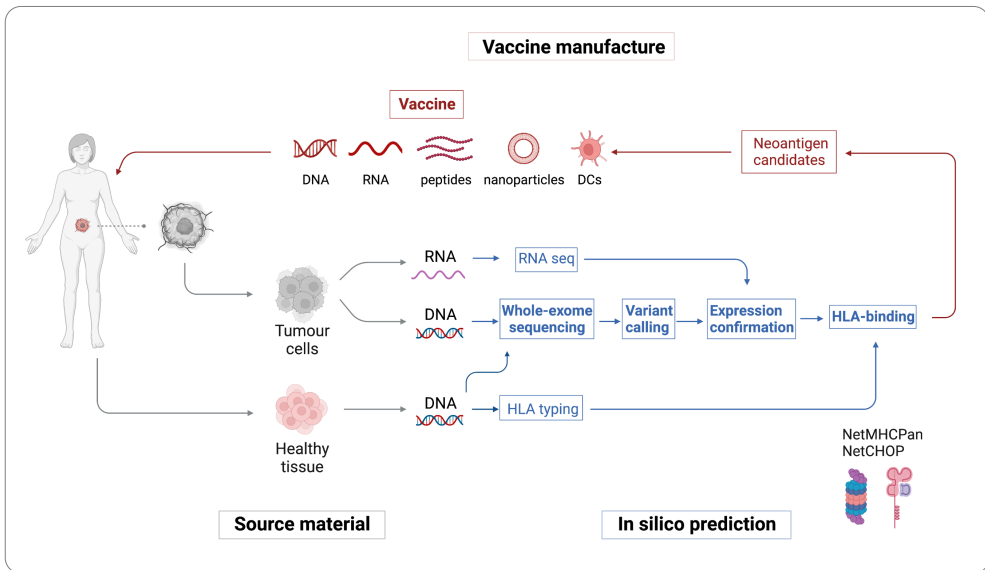


Figure 11. Neoantigen vaccine pipeline. Classical workflow of the development of neopeptide vaccines. First, mutations are identified from WES of tumour cells and healthy tissue. Then, several filters are applied in the *in silico* pipelines to predict if these peptides generated from mutations will be immunogenic, and thus will be correctly presented by MHC-I molecules. After the *in silico* prediction, the selected candidates are formulated as vaccines through different delivery platforms. Created with Biorender. Adapted from Hu, Z *et al.* (2018)²⁹⁷.

An in depth understanding of epitope presentation and immunogenicity is still yet to come, and the fact that the different pipelines developed until now give very different outputs of immunogenic peptide prediction is an example of that. To improve our ability to predict relevant neoantigens, which is indispensable for developing personalised vaccines, the Tumour Neoantigen Selection Alliance (TESLA) has been formed to keep exploring the different *in silico* pipelines developed in different research groups.

b. Types of neoantigen vaccines

Besides the importance of immunogenic neoantigen prediction, vaccine design and formulation are also critical for proper peptide presentation to DCs and optimal T-cell activation. At present, the vaccine platforms tested in ongoing clinical trials include long synthetic peptides (LSP), nucleic acid-based vaccines (DNA or RNA), DCs vaccines and nanoparticles (Figure 11)²⁹⁷.

LSP vaccines are currently the most common studied platform to date in preclinical and clinical studies (Figure 12)^{298,299}. This platform has several advantages regarding safety and

Introduction

feasibility. The manufacturing processes are standardised and well characterised, peptides have high stability and, additionally, are easy to administer in human clinical trials²⁹⁷. LSP are usually 20-30 amino acids long and peptides of this length are preferentially processed and presented by DCs and thereby enhance CD8+ T-cell activation³⁰⁰. Moreover, processed long peptides can bind both MHC-I and MHC-II molecules, eliciting also CD4+ T-cell responses as well as CD8s. This has been observed in different trials, where preferential presentation of MHC-II restricted peptides occurred^{301–303}. Gubin *et al.* conducted notable work in a preclinical setting where they tried to identify targets of T-cell reactivity upon IC blockade therapy in mice, followed by the formulation of a LSP vaccine incorporating these mutants identified after ICI. After vaccination, the tumour rejection induced was comparable to the one obtained post-ICI therapy³⁰⁴. In a clinical application, NeoVax is a long peptide-based vaccine evaluated in a phase I trial with stage III and IV melanoma patients (Figure 12)³⁰¹. The vaccine comprised around 20 peptides and it was formulated along with a PolyI:CLC adjuvant, a TLR3 agonist³⁰¹. The four patients with stage III melanoma remained cancer free for up to 32 months, and specific CD4+ T and CD8+ T cells were detected after vaccination³⁰¹.

Among nucleic acid-based vaccines, both DNA and mRNA vaccines have been developed as means to encode the antigens of interest to be transcribed or translated upon delivery, respectively²⁹⁷. DNA vaccines can provide adjuvant functionality, as double-stranded DNA or unmethylated-GC-rich plasmid DNA can work as build-in adjuvants and stimulate the innate immune system directly (Figure 12)³⁰⁵. Nevertheless, these vaccines have shown poor immunogenic results *in vivo* and very few candidates have progressed into phase II trials³⁰⁶. On the contrary, mRNA vaccines have gained increased interest in the past years, more so since the COVID19 pandemic and the successful formulation of SARS-CoV2 mRNA-based vaccines distributed worldwide (Figure 12)²⁵⁸. The technological advances made during this time have accelerated exponentially the development of cancer mRNA vaccines and their interest in clinical application³⁰⁷. These vaccines have become attractive and robust delivery platforms because of their versatility, feasibility, and large-scale development potential³⁰⁷. A personalised mRNA poly-neoantigen vaccine for patients with melanoma reported robust T-cell responses and strong anti-tumour immunity, with one patient (out of 5) showing a complete response when the vaccine was combined with anti-PD-1 antibody³⁰³. In pancreatic cancer, Balachandran and colleagues published results of a personalised mRNA

neoantigen vaccine phase I trial³⁰⁸. 16 pancreatic ductal adenocarcinoma patients were treated with anti-PD-L1, followed with recurrent mRNA immunisations with up to 20 neoantigens per patient³⁰⁸. In 8 out of 18 patients vaccination induced *de novo* strong T-cell responses against at least 1 neoantigen included in the formulation³⁰⁸.

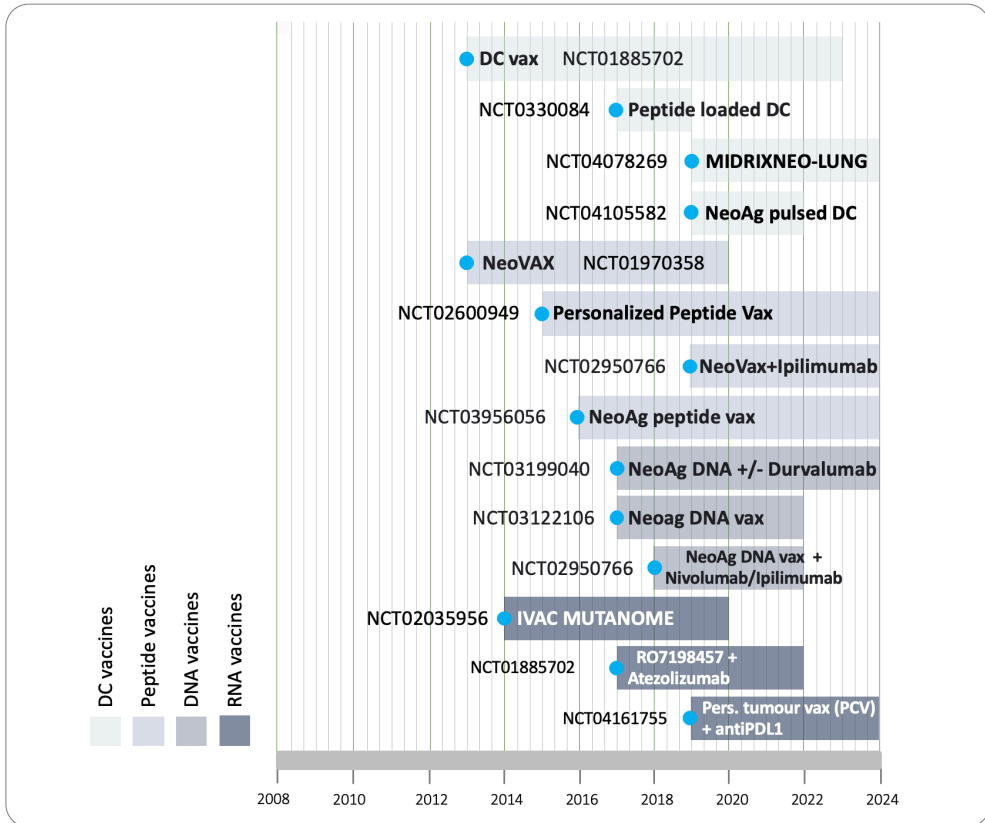


Figure 12. Neoantigen cancer vaccines. Among types of neoantigen vaccines that have reached at least phase I in clinical trials there are DC based vaccines, peptide vaccines, DNA based vaccines and RNA based vaccines (clinicaltrials.gov)^{261,301}.

ii. Nanoparticles. Virus Like particles

Besides all the other types of vaccines formulations available, virus-like particles (VLPs) are an attractive alternative that has gain interest in the past years, and research efforts have been made towards their development and application in several fields³⁰⁹. VLPs are self-assembled viral protein particles that mimic the conformation and structure of native viruses but are not replicative, and hence they lack infectivity³⁰⁹. VLPs represent an efficient and safe strategy for the delivery of antigens, as they can serve as a scaffold or carrier for

Introduction

the presentation of epitopes to DCs^{310,311}. VLPs can present conformationally advantages compared to individual proteins or peptides, as they expose epitopes in a similar way as native viruses, and thus, the antibody and cellular response are expected to be enhanced³⁰⁹. Generally, VLPs have been developed as a vaccine platform against viral infections, but their application in cancer therapeutic strategies has had some relevance in recent years³¹¹. As aforementioned, an efficient antigen uptake from DCs is critical for an optimal T cell priming, which is indispensable for the correct elimination of tumour cells. VLPs have the appropriate size to drain freely to LN and thus encounter DCs for antigen presentation³¹².

Structurally, VLPs are classified as non-enveloped or enveloped particles, depending on the presence or absence of an external lipid bilayer³¹³. Non-enveloped VLPs are simpler in structure as they are composed of a single or multiple capsid protein that assembles³¹³. On the contrary, enveloped VLPs contain a lipid bilayer derived from the producing host cells during the assembly and budding process³¹³. Depending on the structural protein of the virus used and the nature of the host cell, the characteristics of this lipid bilayer and its protein content will differ³¹⁴. The formation of enveloped VLPs is a two-step process that requires the formation of the nucleocapsid and/or matrix first, and then the acquisition of the lipidic bilayer³¹⁵.

In the cancer context, VLP-based vaccines have been tested in preclinical and clinical studies in different malignancies³¹¹. A relevant preclinical study tested a VLP coated with a melanoma associated antigen, the human glycoprotein 100 (gp100)³¹⁶. The protein was incorporated in a RHDvirus based VLP, and vaccination in mice generated a robust CD8+ T cell proliferation and IFN γ production. Immunisation with gp100-VLP also showed a therapeutic effect against tumour development in mice, and vaccinated animals remained tumour free for over 60 days³¹⁶.

a. HIV-based Virus Like Particles

VLPs can be produced from many different viruses, one being the human immunodeficiency virus-1 (HIV-1). During the virus life cycle, the assembly of new HIV-1 virions depends on the viral structural protein Gag^{317,318}. HIV-1 Gag-based VLPs are formed similarly, upon Gag synthesis, the protein migrates to the host cell membrane where it oligomerises, which results in budding of enveloped VLPs mimicking HIV-1 virion's size and morphology (Figure 13a)³¹⁷.

HIV-1 Gag-based VLPs have been used as vaccine immunogens to elicit immune responses against Gag or Gag-pol proteins³¹⁹. However, these versatile VLPs can also be used as carriers since they can incorporate immunogens on the surface of their lipid membrane³¹⁷. Despite this, one of their major limitations is the low-density incorporation that can occur because of the structural mimicry to HIV-1. HIV-1 has evolved to evade the immune system by incorporating Env molecules poorly, reducing antibody avidity³²⁰. This poses a significant challenge in strategies that rely on high-density incorporation to elicit potent responses³²⁰. In our case, the first Gag-VLPs our group developed expressing antigens on their surface were produced by the co-transfection of an antigen of interest and the Gag protein. This resulted in low density Gag-VLPs, incorporating a reduced number of antigens (Figure 13b). To overcome this limitation, our group has been working on a new VLP design based on the fusion of the immunogen of interest and the Gag structural protein through a transmembrane domain and a linker sequence^{321,322}. This allows for an equivalent incorporation of the immunogen for every Gag molecule expressed. (Figure 13c).

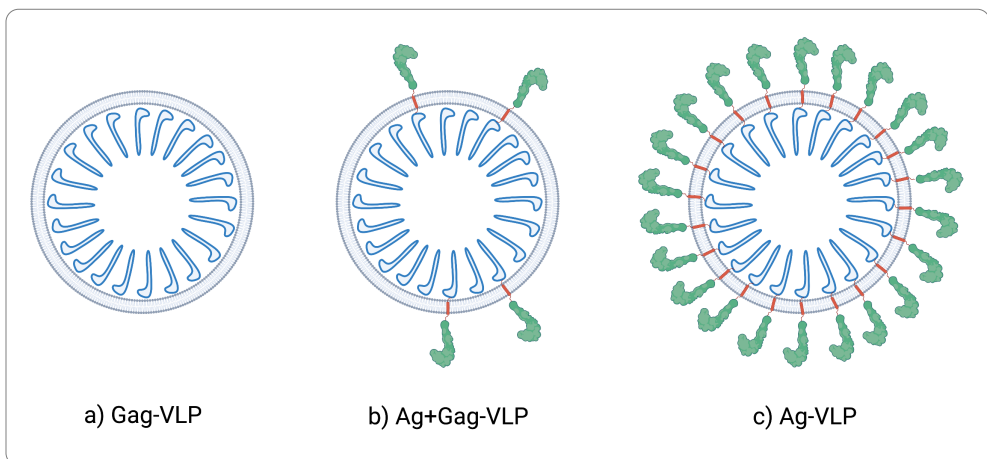


Figure 13. HIV-1 based Virus-Like Particle development. a) HIV-1 Gag-based VLP generated from the oligomerisation of the Gag protein. b) Low density VLP incorporating an antigen of interest on the surface. c) High-density fusion protein VLP generated by the fusion of the antigen of interest to the Gag protein through a transmembrane domain.

HYPOTHESIS AND OBJECTIVES

HYPOTHESIS

Cancer immunotherapies are currently the most novel approach in the treatment of cancer. These therapies have dramatically reshaped the cancer treatment field by reducing associated side effects and increasing their specificity. Among these different strategies, cancer vaccines aim to generate robust tumour-specific T-cell responses able to eliminate tumour cells and control tumour progression. However, the complexity and heterogeneity of tumours have raised the necessity of developing more personalised vaccines that target tumour specific neoantigens.

Our group has developed a novel HIV-1 Gag-based VLP platform that expresses a high density of antigens on its surface by the fusion of an antigen of interest to the Gag protein through a transmembrane domain³²¹. Here, we hypothesised that this platform could be adapted in a cancer context and used to display cancer neoantigens, which would be expressed as a polypeptide of concatenated neoepitopes.

Delivering neoantigens as single polypeptide molecules is a common strategy^{301,308,323}, but the proteasome trimming process can hamper the presentation of the selected neoepitopes, potentially affecting the CTL response generated. We hypothesised that adding designed linker sequences flanking the epitopes can enhance the peptide processing and MHC-I presentation.

Taking advantage of the HIV-1 Gag-VLP design, we expect that neoantigen VLPs will generate a strong T-cell response in a mouse model with relevant antitumour activity.

AIM AND OBJECTIVES

The main aim of this project is to optimise, characterise and purify HIV-1 Gag-based VLPs as a personalised neoantigen vaccine platform and test its immunogenicity in an animal model.

Thus, the specific objectives to fulfil this aim are:

1. To design neoantigen concatenated polypeptide sequences that enhance antigen processing and MHC-I presentation.
2. To adapt the HIV-1 Gag-based VLP platform to display concatenated neoantigens by optimising the design and production of Gag-neoantigen fusion proteins (neoVLPs).
3. To test the immunogenicity of neoVLPs in a mouse model, assessing their capacity to generate detectable neoantigen-specific T-cell responses.
4. To study the antitumoral efficacy of neoVLP vaccination in a tumour challenge *in vivo* experiment in a mouse model.

MATERIALS AND METHODS

SECTION 1: Analysis and comparison of linker sequences and their effect in antigen processing and presentation in a neoantigen polypeptide vaccine.

Cell lines

B16-F10 cells (ATCC CRL-6475) were grown and maintained in Dulbecco's Modified Eagle Medium (DMEM) containing 4.5 g/L D-/L-Glucose and 110 mg/L Sodium Pyruvate (Gibco) supplemented with 10% heat-inactivated fetal bovine serum (FBS; Gibco). Cells were cultured at 37 °C in a humidified 5% CO₂ atmosphere.

Design and molecular cloning of multi-epitope genes

Thirteen B16-F10-derived neoantigens (nine amino acids long) were selected based on their putative binding to MHC-I. We designed a single chimeric gene containing (from N-terminal to C-terminal ends): a signal peptide (MDWTWRFLFVVAATGVQS), a FLAG tag (DYKDDDDK), all selected peptides, the OVA peptide (SIINFEKL) positioned as indicated in the text, and the CD44 transmembrane domain. The cytosolic domain of CD44 was not included. Thus, the recombinant proteins were designed to be detected on the surface of the transfected B16-F10 cells by flow cytometry. All regions and peptides were spaced by specific short linkers: 1) AAA (5'-GCTGCTGCC-3'), 2) AAL (5'-GCTGCCCTG-3'), 3) ADL (5'-GCTGACCTG-3'), 4) A (5'-GCC-3') and 5) GGGs (5'-GGAGGCGGCTCT-3'). One individual construction was prepared for each linker used. In addition, an intracellularly expressed version of each polypeptide described above was designed lacking the signal peptide and the CD44 transmembrane domain. These artificial genes were synthesised by GeneArt (Invitrogen) and cloned in a pcDNA3.4 vector (Invitrogen).

Expression and western blot analysis

B16-F10 cells were seeded in a 12 well-plate at a rate of 1x10⁵ cells/well. Cells were transfected 24 hours post-seeding using the Lipofectamine 3000 Reagent (Thermo Fisher Scientific) following manufacturer's instructions. Six hours post-transfection, cells were stimulated with mouse IFN γ (Biolegend) at a final concentration of 20 ng/mL and incubated for 48 hours. After that, cells were treated with 10 μ M of MG132 (Sigma) for 4 hours. Only stimulated and only treated cells, as well as untreated and unstimulated cells, were also included in the experiment as controls. Cells were washed twice with 1xPBS pH 7.4 (Gibco), detached using Versene (Gibco), transferred to a clean tube and centrifuged for 5 min at

Materials and methods

420xg. Cell pellet was resuspended in lysis buffer containing 1x RIPA buffer (Cell Signaling) and protease inhibitors HALT (Thermo Scientific) and PMSF (Cell Signaling) and centrifuged for 10 min at 10,000 rpm at 4°C. The supernatant containing the cell lysate was recovered. Proteins were discriminated by SDS-PAGE using 4-12% Bis-Tris Nu-PAGE under reducing conditions (Thermo Fisher Scientific) and electro-transferred to a PVDF membrane using the Trans-Blot Turbo Transfer Pack (BioRad). Nonspecific binding sites were blocked using 1xPBS pH 7.4, 0.05% of Tween20, and 5% of non-fat skim milk (blocking buffer) at room temperature (RT) for one hour. Subsequently, the membrane was washed 3 times with wash buffer (1x PBS, 0.05% Tween20), and incubated with diluted mouse anti-DYKDDDDK monoclonal antibody (MA1-91878; Thermo Fisher Scientific; dilution 1:1,000) with gentle shaking overnight at 4°C. Alternatively, the membrane was incubated with diluted anti- α -actin monoclonal antibody-HRP conjugated (clone BA3R, Thermo Fisher Scientific; dilution 1:3,000) with gentle shaking for 1h at RT. The washed membrane was incubated with diluted Peroxidase AffiniPure Donkey anti-mouse IgG (H+L) antibody (Jackson ImmunoResearch; dilution 1:10,000) with gentle shaking for 1 hour at RT. Finally, the membrane was developed using the SuperSignal West Pico PLUS Chemiluminescence Substrate (Thermo Fisher Scientific), and images were obtained using a ChemidocTMMP Imaging System (BioRad).

Expression and flow cytometry analysis

B16-F10 cells were transfected as indicated above. Six hours post-transfection, cells were stimulated with mouse IFN γ (Biolegend) at a final concentration of 20 ng/mL and incubated for 48 hours. After that, cells were treated with 10 μ M of MG132 for 4 hours. Untreated and unstimulated cells were used as controls. To detach cells, they were washed twice with 1xPBS pH7.4 (Gibco) and incubated with Versene (Gibco). Detached cells were stained extracellularly using APC anti-DYKDDDDK antibody (clone L5, Biolegend; dilution 1:400). After staining, cells were washed three times and fixed in a formaldehyde 1% solution. For some experiments, cells were fixed and permeabilised using the Fix&Perm Kit (Invitrogen) and the antibody staining was performed intracellularly. Cells were incubated in Medium A for 15 mins in the absence of light. After that, cells were incubated for 20 mins in the antibody dilution in Medium B with 5% FBS. After staining cells were washed three times and resuspended in staining buffer. All samples were acquired with a BD

FACSCelesta™ Cell Analyser. All data collected was analysed using the FlowJo v10.6.2 Software (Tree Star Inc.).

Epitope presentation assay

B16-F10 cells were transfected and IFN γ stimulated as indicated above. As positive control, non-transfected but IFN γ stimulated cells were incubated with the OVA peptide (SIINFEKL; InvivoGen) at a final concentration of 10 μ M for 2 hours prior to cell harvest as indicated before. Cells were centrifuged at 420xg for 5 min, resuspended in staining buffer (1xPBS + 1% FBS) and stained using an APC-conjugated anti-mouse H-2K^b_{D^b} (clone 28-8-6, Biolegend; dilution 1:1000) and a PE-or APC-conjugated anti-mouse H-2K^b/SIINFEKL (clone 25-D1.16, Biolegend; both dilutions 1:500). Cells were washed and fixed in formaldehyde 1%.

When transfection controls were added to the experiment, the transfection of B16-F10 cells was done using a mix of two plasmids in a 1:4 ratio: 1) pMAX GFP vector (Amara), a GFP expressing plasmid, and 2) pcDNA3.4 coding for the polypeptide. Six hours post-transfection, cells were stimulated with mouse IFN γ as previously explained. Cells were washed twice with 1xPBS and detached with Versene (Gibco). Cells were centrifuged at 420xg for 5 mins and resuspended in staining buffer. Then, cells were stained with the antibody APC-conjugated anti-mouse H-2K^b/SIINFEKL (clone 25-D1.16, Biolegend; dilution 1:500) for 20 mins at RT. Consequently, cells were washed and fixed with formaldehyde 1%. All samples were acquired with a FACSCelesta flow cytometer (BD Biosciences) and the acquired data was analysed using the Flow-Jo software (Tree Star Inc.).

Splenocyte activation and proliferation assay

B16-F10 cells were transfected as indicated above and stimulated with IFN γ for 48h. On day 2 post-transfection, cells were washed twice with 1xPBS and detached with Versene (Gibco). Cells were then seeded at two different densities: 10,000 or 20,000 cells per well in flat bottom 96-well plates, to test two different ratios with the splenocytes (1:20 and 1:10 respectively). Splens from OT-I mice (Charles River) were collected in 1xPBS pH7.4 (Gibco) after sacrifice. A single cell suspension was obtained through mechanical disruption of the spleen using 70 μ m cell strainers (542070, DDBiolab). Cells were washed with R10 (RPMI (Gibco) supplemented with 10% FBS (Gibco)). Red blood cells were depleted by incubating

Materials and methods

the cell suspension with an ACK (Lonza) buffer for 2 min at RT. After centrifuging, cells were washed twice, resuspended in R10 medium, and counted. Cell concentration was adjusted to 2-10M/mL for CFSE (C34554, Life Technologies) staining. Cell suspension was incubated with a CFSE 0,25 μ M dilution for 5min at RT. R10 was added after 5min and cells were thoroughly washed with 1xPBS pH7.4 (Gibco) at least three times to remove any remaining traces. Cells were counted again, and concentration was adjusted to 2M/mL. 2×10^5 splenocytes/well were added to the previously seeded plate with the transfected B16-F10. As positive controls, the OVA peptide (InvivoGen; 1 ng/mL) and Concanavalin A (L7647-25MG, Merck; 2 μ g/mL) were used. Finally, CD28 (16-0281-82, Thermo Fisher) was added as a costimulatory antibody at 1 μ g/mL. Activation and proliferation of CD8⁺ OT-I cells were analysed at 24 and 72 hours, respectively, by Flow cytometry. In brief, cells were harvested and stained with viability stain solution (565388, BD) at a 1:4000 dilution and were incubated for 15 min at RT. After washing three times, cells were stained with the following antibodies: anti-CD19 (560245, BD), anti-CD3e (551163, BD), anti-CD4 (56-0042-82, Thermo Fisher), anti-CD8 (560778, BD), anti-CD25 (566228, BD) and anti-CD44 (561862, BD). Finally, cells were washed, fixed with a formaldehyde 1% solution, and acquired in a FACSCelesta flow cytometer (BD Biosciences). Acquired data was analysed using the Flow-Jo software (Tree Star Inc.).

Statistical analysis

Levels of MHC-I/SIINFEKL on the surface of B16-F10 cells were expressed as geometric mean (GeoMean) and percentage of positive cells. Data was analysed using a Kruskal-Wallis test corrected for multiple comparisons using the Dunn's test or by False Discovery Rate (FDR) method of Benjamin and Hochberg in the GraphPad Prism 7.0e software. The exact test used in each experiment is indicated at the corresponding figure caption.

SECTIONS 2 and 3: Optimisation of HIV-1 Gag-based VLPs for a functional display of cancer neoantigens.

Cell lines

B16-F10 (ATCC, CRL-6475) and Pan02 (DCTD Tumour Repository, 0507795) cell lines were cultured in DMEM (Gibco) supplemented with 10% FBS (Gibco; D10). Cell cultures were maintained in a humidified incubator at 37 °C with 5% CO₂. Cell line was mycoplasma-free, assessed by PCR.

Expi293F cell line (ThermoFisher Scientific) were used for protein production. Cells were cultured in Expi293 Expression medium (Gibco) at 37°C, 8% CO₂ and under agitation at 125rpm.

Whole exome and RNA sequencing

DNA whole exome libraries of B16-F10 and Pan02 cell lines and C57BL/6J0laHsd germline sample were prepared with Agilent Mouse All Exon kit (Agilent) following manufacturer's instructions. For RNA sequencing, a total of 1 µg of RNA from the B16-F10 or Pan02 cell line (RIN > 7 and rRNA ratio > 1) was used. RNA library was prepared using the TruSeq Stranded Total RNA Library Prep Gold (Ribozero) kit (Illumina) following manufacturer's instructions. Quality control of DNA libraries was assessed with Bioanalyzer 2100 (Agilent) and further quantified by qPCR, normalised, and multiplexed into a balanced pool. DNA- and RNA-derived libraries were sequenced on an Illumina NovaSeq6000 platform (2x150 paired-end chemistry). Sequencing output of WES and RNA-seq per library yielded 18 Gb (>500X) and 200M reads, respectively.

*In silico neoantigen selection**

B16-F10

To identify and select candidate neoantigens, first the reads from WES were matched to identify somatic mutations. Then, to predict the likelihood of the peptides generated from these mutations to bind to MHC-I molecules, and thus forecast their immunogenicity, the BSC developed the Neoantigen Optimisation Algorithm (NOAH). NOAH is a pan-allele method based on a position-specific weight matrix (PSWM) approach. It works under the assumption that binding strength relies on: (i) each position of the peptide; and (ii) the

*Work carried out by the BSC

Materials and methods

residues of the allele that are in contact with each peptide's amino acid. The final score produced by NOAH is the addition of all local contributions, one per amino acid (aa) in the peptide. With this approach they have reported a correlation between binding score and immunogenicity, not observed in the current state-of-the-art neural network methods.

The neoantigen selection using NOAH was then based on different criteria: i) being classified as binders by NOAH in consensus with two additional widely used prediction methods, NetMHCpan4³²⁴ and MHCflurry³²⁵; ii) having an expression filter of more than 5 RNA reads; iii) having a clonality value > 0.2.

Pan02

After performing WES of the tumour cell line and healthy tissue, the read alignment was performed with BWA-MEM and the variant calling of somatic mutations with Mutect2. Neoepitopes derived from tumour mutations were then evaluated with PredIG (which includes NOAH for HLA binding affinity, and NetCleave for proteasomal processing) to assess their immunogenicity.

Plasmids

HIV-1 Gag-based VLPs were designed to generate enveloped particles capable of expressing antigens of interest on their surface. The fusion-protein VLP contains the structural Gag protein fused to the antigen of interest by a transmembrane domain and a linker. In the case of the neoVLPs presented here, two types of constructs were designed. The classical neoVLPs where the neoantigen polypeptide was fused to Gag at the N-terminal of the protein, and the C_neoVLPs where neoantigens were expressed at the C-terminal, and thus expressed at the core of the particle. Classical N-term neoVLPs, containing neoantigens from the B16-F10 cell line, were generated by concatenating the selected neoantigens or frame shifts by an AAA spacer, followed by the transmembrane domain of mouse CD44 and fused to HIV-1 subtype B GAG_{HXB2}. At the N-terminus we could also find a signal peptide and the FLAG tag (DYKDDDDK).

C_neoVLPs had the concatenated neoantigens from the Pan02 cell line cloned at the C-terminus of the HIV-1 Gag protein. These new C_neoVLPs had a GGGS spacer between the Gag protein and the neoantigens, and these were separated by AAA linker sequences. At the C-terminus there was also a 6xHis tag.

As controls, two separate VLPs working as empty carriers were generated for the two types of constructs designed. For the N-terminal approach, a NakedVLP was designed where the FLAG tag was directly fused to the murine CD44 transmembrane domain and HIV-1 subtype B GAG_{HXB2}. For the C_neoVLPs, the control VLP included the Gag protein alone and a 6xhis tag (C_Gag).

All coding sequences were codon optimised and synthesised by GeneArt (Invitrogen) and cloned into pcDNA3.4 (Thermo Fisher). All plasmids were transformed in One Shot TOP10 Chemically Competent E. Coli (Invitrogen) or Mix&Go Competent cells (Zymo Research) for plasmid DNA amplification. Endotoxin-free plasmids were purified using the ZymoPURE II Plasmid Maxiprep Kit (Zymo) and filtered at 0.22 µm (Millipore). Nucleic acid concentration was measured based on the absorbance at 260nm using NanoDrop One/One (ThermoFisher Scientific).

Vaccine production and purification

NeoVLPs were produced by transient transfection using Expi293F cells and the Expiectamine293 Transfection Kit following manufacturer's instructions (Thermo Fisher). Cellular cultures were harvested 48h post-transfection by centrifugation at 400xg for 5 min. A protocol to extract intracellular neoVLPs was adapted from Titchener-Hooker et al^{326,327} (Figure 14). Cell pellet was resuspended in 1 PV of 20mM phosphate buffer with 2mM EDTA (ThermoFisher Scientific), 2mM EGTA (Merck) and a protease inhibitor cocktail (cOmplete ULTRA™ Tablets EDTA-free, Merck). Cell disruption was carried out manually using a Tissue Grinder (CS1, Kimble Chase) for 1 min on ice. Disrupted cells were collected by centrifugation (3000xg for 15 min at 4°C) and the cellular pellet resuspended in the phosphate buffer containing 0.2% Triton X-100 (Sigma) and incubated on a rotating wheel at 4°C for 4 hours. Then, samples were centrifuged at 4°C for 15 min at 3000xg and the supernatant was recovered, mixed with Amberlite XAD4 beads (Sigma) for detergent removal and incubated for 2 hours on a rotating wheel at 4°C. After that, samples were centrifuged for 5 min at 800xg, and the supernatant was recovered and loaded on a SepFastDUO5000Q column (BioToolomics) for a bimodal, ion exchange and size exclusion chromatography. Column flow through was recovered, filtered at 0.22µm and concentrated for further analysis (FischerScientific; Figure 14).

Materials and methods

A second purification protocol was developed for both intracellular and extracellular neoVLPs where the extracted fraction of neoVLPs or the transfection supernatants were recovered and neoVLPs were concentrated and purified by ultracentrifugation. NeoVLPs containing fractions were loaded on a 30% - 70% double sucrose cushion and centrifuged at 39,000 x g for 2 hours 30 mins at 4°C using a TH-641 rotor in a Sorvall RCM120EX centrifuge. Gradient was fractionated from top to bottom and neoVLPs were recovered from the 30/70 interphase. Extra sucrose was removed from the sample by dialysis using a Spectra-Por Float-A-Lyzer G2 (Merck) against 1xPBS. In the final preparation, remaining sucrose was expected to be lower than 5% (Figure 14).

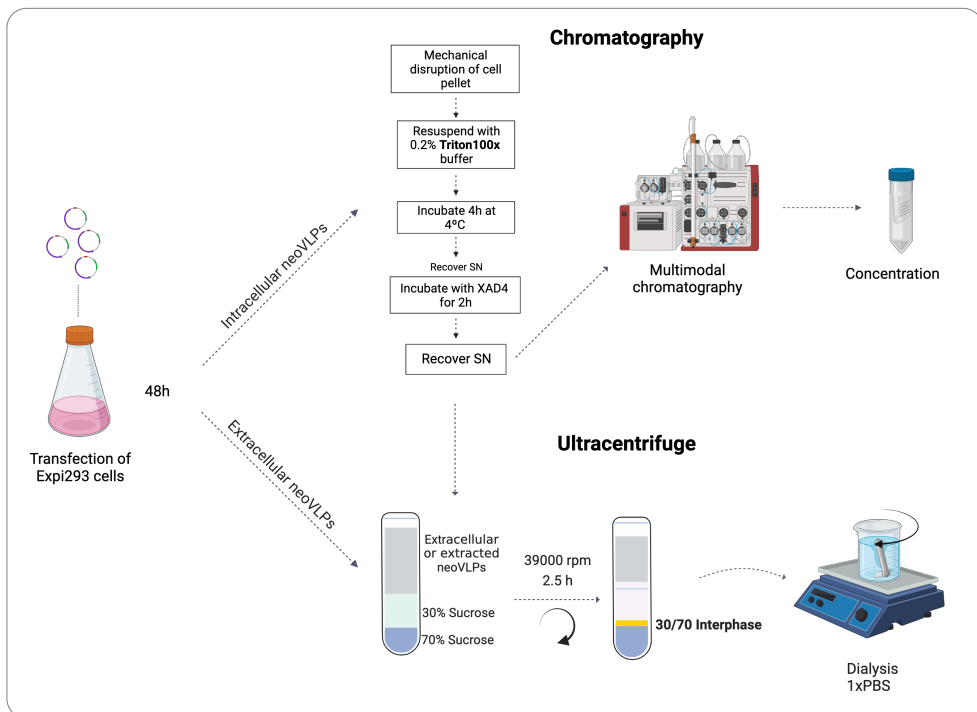


Figure 14. NeoVLP production and purification protocols. NeoVLPs were produced in Expi293F cells. Cells were transfected and harvested 48 hours later, and pellets and supernatants were recovered for intracellular or extracellular neoVLPs, respectively. To extract intracellular neoVLPs, cell pellets were mechanically disrupted and incubated with a Triton100X 0,2% buffer for 4 hours at 4°C. Then, detergent was removed by a second incubation with XAD4 resin, and supernatant was recovered for a further purification step. Extracted intracellular neoVLPs were either purified by chromatography or loaded on top of a 30%-70% double sucrose cushion. Intracellular neoVLPs were also purified by sucrose gradient. NeoVLPs were then recovered from the interphase and dialysed against 1xPBS to eliminate the excess sucrose.

Transmission electron microscopy (TEM)

VLP-producing cells were fixed with 2.5% glutaraldehyde in 1xPBS for 2 hours at 4°C, post-fixed with 1% osmium tetroxide with 0.8% potassium ferrocyanide for 2 hours and dehydrated in increasing concentrations of ethanol. Then, cell pellets were embedded in epon resin and polymerised at 60°C for 48 hours. Sections of 70 nm in thickness were obtained with a Leica EM UC6 microtome (Wetzlar) and stained with 2% uranyl acetate and Reynold's solution (0.2% sodium citrate and 0.2% lead nitrate). Sections were analysed using a JEM-1400 transmission electron microscope (JEOL) and imaged with an Orius SC1000 CCD Camera (Gatan).

Cryogenic electron microscopy (Cryo-EM)

VLP morphology was assessed by cryo-EM. Extracted or purified VLPs were deposited on a carbon-coated copper grid and prepared using an EM GP workstation (Leica). Vitrified VLPs were prepared on a Lacey Carbon TEM grid (copper, 400 mesh) and immediately plunge into liquid ethane. The grids were viewed on a JEOL 2011 transmission electron microscope operating at an accelerating voltage of 200 kV. Electron micrographs (Gatan US4000 CCD camera) were recorded with the Digital Micrograph software package (Gatan).

Flow cytometry

VLP-producing Expi293F cells were analysed by flow cytometry. Cells were recovered 48h post-transfection and washed with staining buffer (1xPBS with 1% FBS) twice. To detect cell surface protein expression, cells were stained with APC anti-FLAG (DYKDDDDK) tag antibody (Biolegend; dilution 1:500) for 20 mins at RT. After three washes, cells were fixed and permeabilised using the FIX&PERM Kit (Invitrogen) and stained intracellularly with the FITC-KC57 (anti-HIV p24) antibody (Beckman Coulter; dilution 1:200). For the intracellular detection of VLP expression, cells were first fixed and permeabilised before incubation with the same antibodies. All samples were acquired using a BD FACSCelesta™ Cell Analyzer with DIVA software. Data analysis was performed using the Flow-Jo v10.6.2 software (Tree Star Inc.).

Materials and methods

Western blot and Coomassie blue staining

For the western blot assay, samples were boiled at 95°C for 5 mins and proteins were separated by SDS-PAGE using 4-12% Bis-Tris Nu-PAGE gels (Invitrogen). Proteins were electro-transferred to a PVDF membrane using the Trans-Blot Turbo Transfer Pack (BioRad). Membranes were blocked (1xPBS pH 7.4, 0.05% Tween20, 5% non-fat skim milk) for 1 hour at RT and subsequently incubated with a rabbit polyclonal anti-HIV1 p55+p24+p17 antibody (Abcam, 1:2,000) or a rabbit polyclonal anti-GAPDH antibody (Abcam, 1:1000) overnight at 4°C. After washing, the membranes were incubated with Peroxidase AffiniPure Goat Anti-Rabbit IgG (H+L) antibody (Jackson ImmunoResearch, 1:10,000) for 1 hour at room temperature (RT), washed and developed using the SuperSignal West Pico PLUS Chemiluminescence Substrate (Thermo Scientific). Images were obtained using a Chemidoc™MP Imaging System (BioRad).

For the Coomassie blue staining samples were prepared and proteins separated by SDS-PAGE as detailed above. Gels were washed twice with 20mL of Milli-Q H₂O and in stained using SimplyBlue Safe Stain (Thermo Fisher) solution for 1 hour. Then, gels were rinsed and washed with 20mL of water overnight.

VLP and total protein quantification

Purified VLPs were quantified either by p24 ELISA (INNOTEST HIV antigen mAb, Fujirebio) following manufacturer's instructions or by western blotting. For western blot quantification samples were prepared as explained above and separated by SDS-PAGE under reducing conditions. For the standard curve, a Gag recombinant protein was used starting at 125 ng with 1:2 dilutions until 7,8 ng of protein. Blocked membranes were incubated overnight with the primary monoclonal antibody anti-HIV1 p24 antibody (Abcam, 39/5.4A; dilution 1:2,000). After washing the membranes with 1xPBS Tween-20 0.05%, membranes were incubated with the secondary antibody Peroxidase AffiniPure Donkey anti-Mouse IgG (H+L; Jackson ImmunoResearch, dilution 1:10,000). Membranes were then washed and developed using the SuperSignal West Pico PLUS Chemiluminescence Substrate (Thermo Scientific). Images were obtained using a Chemidoc™MP Imaging System (BioRad). The analysis of the bands detected and the interpolation of p24 protein in each sample was performed using the ImageLab software v 6.0 (BioRad). The total protein present in the

sample was assessed by Bicinchoninic Acid (BCA) Protein Assay following manufacturer's instructions.

In vivo experiments

Mice immunisation

Five-week-old male and female C57BL/6J01aHsd mice were purchased from Envigo. All experimental procedures were performed by trained researchers and approved by the competent authorities (Generalitat de Catalunya, Authorisation ID 9943). All protocols were conducted in accordance with the Spanish laws and the Institutional Animal Care and Ethics Committee of the Comparative Medicine and Bioimage Centre of Catalonia (CMCiB). Procedures were performed prioritising the welfare of the animals used and always following the three Rs principles.

Groups of 10 mice, male and female equally distributed, were immunised on week 0 with either naked DNA (coding for VLPs) or purified neoVLPs. 20 ug of naked DNA were electroporated at the hind of the leg and the protocol consisted of 8 pulses of 20 ms with 1s interval at 60V. Mice immunised with purified VLPs were injected a dose of 100ng of p24-Gag at the hock, which is a subcutaneous/intradermal administration³²⁸. This administration is comparable to footpad administration, draining to similar sites such as the popliteal and the iliac lymph nodes³²⁸. Three weeks after the first immunisation, a second dose of the vaccine was administered. DNA was electroporated or purified VLPs were injected as previously explained. When the purified VLPs were adjuvanted, 20ug of MPLA (Invivogen) were added to each dose. Before every vaccination and at end point, blood was collected by facial vein puncture or intracardiac puncture, respectively. In both cases, plasma was recovered from whole blood after coagulation (30 min to 4 hours) and centrifugation at 4000xg for 10 mins. Spleens were also recovered after mice were euthanised. Spleens were mechanically disrupted using a 70 µm cell strainer (DBiolab), and splenocytes were either cryopreserved in FBS/10% dimethyl sulfoxide (Merck) or used in fresh single cell mixtures for ELISpot assays. Before stimulation, single cell splenocyte mixtures were incubated 5 mins with 5 ml of RBC lysis buffer (ThermoFischer) for erythrocyte depletion and washed with 1xPBS+1%FBS.

Materials and methods

Tumour inoculation

Mice were inoculated subcutaneously at the right flank with either 10^5 of B16-F10 or 2×10^5 Pan02 cells in 100 μ L of sterile 1xPBS with 2mM EDTA. Tumour growth was measured with a caliper every two days and tumour volume (V) was estimated using the formula: $V = (\text{length} \times \text{width}^2) \times 0,5$, where length represents the largest tumour diameter and width represents the perpendicular tumour diameter. Human endpoint was considered when tumour volume was 1 cm^3 or over. At end point, blood samples and spleens were collected and processed as described previously.

To assess the antitumoral activity of the neoVLPs, an *in vivo* experiment with a tumour challenge was performed. In this case, mice were immunised with a DNA prime and a purified VLP boost, administered as detailed above. Two weeks after the second immunisation, neoVLP immunised and control mice were inoculated subcutaneously at the right flank with 10^5 B16-F10 cells (ATCC; CRL-6475) in 100 μ L of sterile 1xPBS with 2 mM EDTA. Tumour growth was followed until end point as described above.

Quantification of anti-HIV Gag antibodies by ELISA

The concentration of anti-Gag antibodies in sera of vaccinated mice was determined by ELISA. Nunc MaxiSorp 96-well plates (ThermoFisher Scientific) were coated with 100 ng of recombinant Gag/well³²¹ in 1xPBS (Gibco) and incubated overnight at 4°C in a wet chamber. Coated plates were blocked with 1xPBS, 0,05% Tween20 (Sigma) and 1% of bovine serum albumin (BSA, Miltenyi biotech) for 2 hours at RT. Sera from vaccinated animals was diluted (1:100 or 1:1,000) and 100 μ L/well of each sample were incubated over night at 4°C in a wet chamber. As standard reference, anti-HIV p24 antibody (Abcam) was used starting at 333 ng/mL and doing a serial dilution of 1:3 down to 0.46 ng/mL. Plates were washed and total bound IgG was determined with a secondary HRP-conjugated Donkey anti-mouse IgG Fc antibody (Jackson ImmunoResearch, 1:10,000) for one hour at RT. Plates were developed using O-phenylenediamine dihydrochloride (OPD; Sigma) and analysed at 492 nm with a noise correction at 620 nm.

Quantification of anti-host cell proteins by Flow cytometry

The presence of antibodies targeting host proteins from the Expi293F cell line was determined by flow cytometry. Expi293F cells were incubated with diluted mouse serum

samples (1:1,000) for 30 mins at RT. After washing, cells were incubated with a secondary AlexaFluor647 goat anti-mouse IgG Fc antibody at a 1:500 dilution (Jackson ImmunoResearch) for 15 minutes at RT. Cells were then washed three times with staining buffer (1xPBS/1% FBS) and fixated with a formaldehyde 1% solution. Cells were acquired using a BD FACSCelesta™ Cell Analyser with DIVA software. Data analysis was performed using the Flow-Jo v10.6.2 software (Tree Star Inc.).

Quantification of T-cell responses by IFN γ ELISpot

Multiscreen ELISpot white plates (Millipore) were coated overnight at 4°C with the anti-mouse IFN γ AN18 antibody (Biolegend) at 2 μ g/mL. The following day, plates were washed with sterile 1xPBS and 1% FBS and blocked with 100 μ L of RPMI 1640 medium supplemented with 10% FBS (R10) for at least 1 hour at 37°C. After blocking, 4 x 10⁵ splenocytes per well were added to the plate. Cells were stimulated with synthetic peptides corresponding to the individual neoantigens found in the neoVLPs. In the case of the frameshifts, these were pools of two overlapping peptides covering the entire frame shifts. Peptides were added at a final concentration of 14 μ g/mL/peptide in a total volume of 140 μ L per well. Cells were incubated overnight at 37°C and 5% CO₂. The next day, plates were washed and incubated with a biotinylated anti-mouse IFN γ monoclonal antibody R4-6A2 (Biolegend, 1:2,000) for 1 hour at RT, followed by an alkaline phosphatase conjugated streptavidin (Mabtech) incubation under the same conditions. IFN γ -specific spots were developed by addition of AP Conjugate substrate Kit (BioRad) and the reaction was stopped by aspiration and incubation for 10 min with 1xPBS (Gibson), 0.05% Tween-20 (Sigma). Concanavalin A (Merck) was used as a positive control at 7 μ g/mL and R10 alone as negative control. Spots were counted using an ELISpot reader S6 Macro M2 (ImmunoSpot, CTL).

Statistical analysis

Specific CTL responses against individual neoantigen peptides in ELISpot assays were analysed using Mann-Whitney U test. Multiple comparisons were adjusted by FDR method. Time to sacrifice in each condition were compared by Kaplan-Meier curves and log-rank test.

RESULTS

SECTION 1: Analysis and comparison of linker sequences and their effect in antigen processing and presentation in a neoantigen polypeptide vaccine

Neoantigens can be delivered to the immune system as unique long single molecules that concatenate the different peptides (polypeptide) spaced by linker sequences. Such polypeptides should be designed in a way that individual neoantigens are properly presented by MHC molecules after being processed by the antigen presentation machinery. However, during the trimming process, long peptides might generate a mix of non-relevant short peptides that may affect the presentation of the neoantigen of interest³²⁹. To avoid that, endogenous neoantigen flanking sequences may be replaced by specific designed ones that promote the processing and presentation of the selected epitopes.

No clear consensus is found in the literature about which type of linker sequence would be optimal, as a variety of linkers have been used so far^{330–340}. In our case, we designed an HIV-1 Gag-based VLP as a platform to display predicted immunogenic neoantigens. In this case, peptides were presented as a concatenated long polypeptide fused to the structural Gag protein that will self-assemble into VLPs, exposing the peptides on the surface of the particle. To study the impact that linker sequences may have in the processing and presentation of the different neoantigens included in our vaccine design, we performed an analysis comparing 5 different constructs, where the same neoantigens were spaced by 5 different linker sequences, using the surrogate peptide SIINFEKL (OVA peptide) as a reporter peptide.

1. Development of an epitope presentation assay

To estimate the impact of the spacer sequence on MHC-I antigen presentation, we have developed an *in vitro* assay that evaluates the presentation of the H-2K^b-restricted OVA peptide, SIINFEKL, on the surface of B16-F10 cells. After IFN γ treatment, B16-F10 cells express high levels of MHC-I molecules on their surface^{341,342}, making these cells suitable to study MHC-I-dependent antigen presentation (Figure 15). Binding of the SIINFEKL peptide to H-2K^b molecules was monitored by flow cytometry using the antibody 25-D1.16, which specifically recognises SIINFEKL only when bound to H-2K^b. As a proof-of-concept that the assay works, we incubated IFN γ stimulated B16-F10 cells with the SIINFEKL peptide and determined the presence of SIINFEKL/H-2K^b complexes at the cell surface (Figure 15).

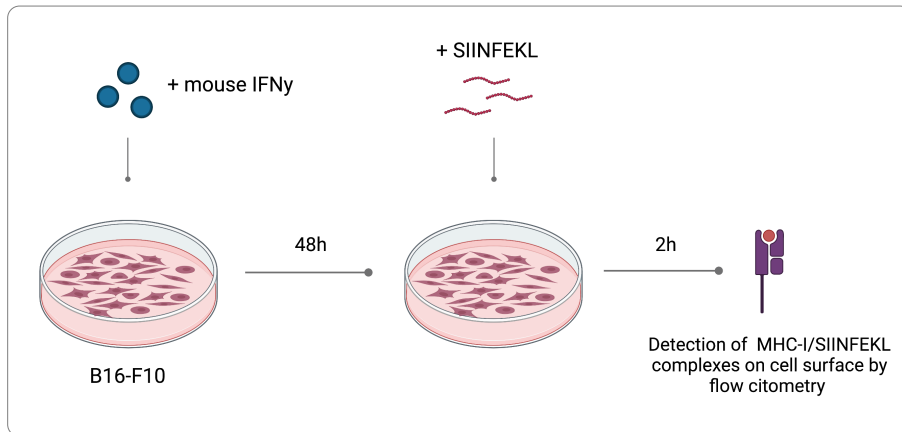


Figure 15. Experimental approach overview. B16-F10 cells were stimulated with IFN γ for 48 hours. After that, the SIINFEKL peptide was added. The expression of MHC-I and the presence of MHC-I/SIINFEKL complexes were analysed by flow cytometry. Created with Biorender.

2. Identification of the optimal spacer for MHC-I epitope presentation

With the aim of selecting the optimal spacer for a neoantigen polypeptide vaccine, we investigated the impact of five different spacers on the MHC-I neoantigen presentation. We designed a DNA plasmid encoding a single chain polypeptide containing a signal peptide and the FLAG tag at the N-terminus, followed by a total of thirteen putative B16-F10-specific MHC-I-restricted peptides in addition to the SIINFEKL peptide at the centre (Figure 16A). We then tested five different spacer sequences (AAA, AAL, ADL, A and GGGG). Of note, peptides in each construct were linked by the same spacer. The selection of the spacer sequence was based on cleavage preferences by the immunoproteasome and ERAP proteins and on previously published work^{331,335–337}.

All five plasmids, coding for surface expressed polypeptides, were separately transfected into B16-F10 cells. Six hours later, cells were treated with IFN γ to enhance both the expression of MHC-I molecules on the cell surface and the function of the immunoproteasome. Forty-eight hours later, the expression of the full-length proteins was evaluated and the formation of SIINFEKL/MHC-I complexes at the cell surface was determined by flow cytometry (Figure 16B)³⁴³.

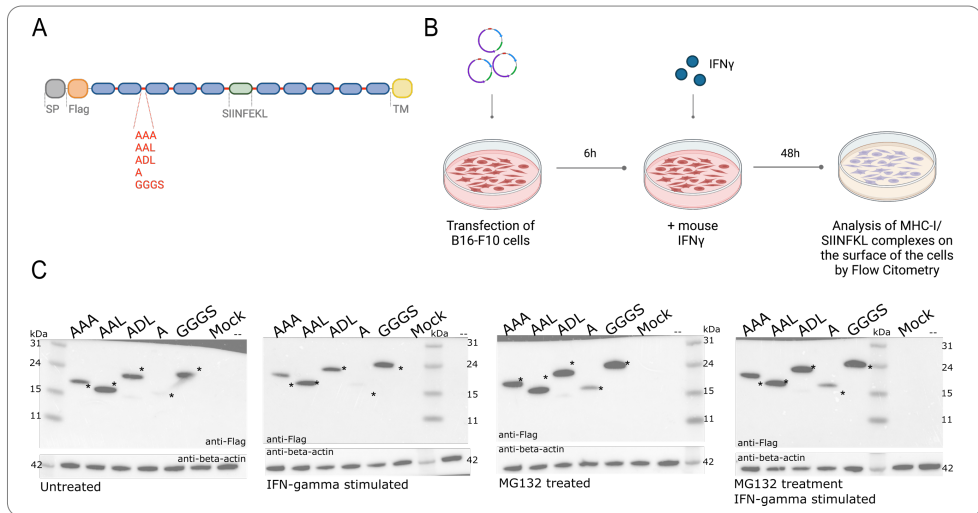


Figure 16. Construct design and western blot analysis. (A) Schematic representation of the constructs used. (B) Graphical scheme of the experimental procedure used for linker screening. A and B created with Biorender. (C) Western blot analysis of the expression of recombinant proteins. From left to right: untreated transfected cells, IFN γ stimulated B16-F10 cells, MG132 (proteasome inhibitor) treated cells and IFN γ + MG132 treated cells. Asterisk indicates expected molecular weight.

Expression of the full-length proteins was evaluated by western blot using an anti-Flag antibody. Polypeptide molecules containing spacers AAA, AAL, ADL and GGS were successfully expressed; while A-linked polyprotein was not detected (Figure 16C), suggesting that it is either not expressed or processed very rapidly. However, stimulation of transiently transfected B16-F10 cells with IFN γ showed a decreased intensity in the western blot bands for all polyproteins except for GGS-linked, compared to untreated samples (Figure 16C). In contrast, incubation of transiently transfected B16-F10 cells with MG132, a proteasomal inhibitor, showed an increased intensity in the western blot bands for all polyproteins, including the A-linked polyprotein, which becomes clearly detectable at its expected molecular weight (Figure 16C). At last, incubation of transiently transfected B16-F10 cells with MG132 allowed the increase or recovery of all polyprotein expression after IFN γ stimulation (Figure 16C). Taken together, these results suggest that proteasomal degradation may be a major contributor to the processing of the polypeptides.

Next, the antigen presentation efficiency was determined by the presence of MHC-I/SIINFEKL complexes on the surface of transfected and IFN γ stimulated B16-F10 cells. Flow cytometry data showed that the highest amount of the MHC-I/SIINFEKL complex was obtained with the alanine-based linkers, specifically the AAA-spacer, indicating that this

Results – Section 1

linker might be the most successful spacer for the processing and MHC-I presentation of the SIINFEKL peptide (Figure 17A to C). Conversely, the GGGs linker showed the lowest signal indicating that it was less efficient in peptide processing and presentation (Figure 17A to C).

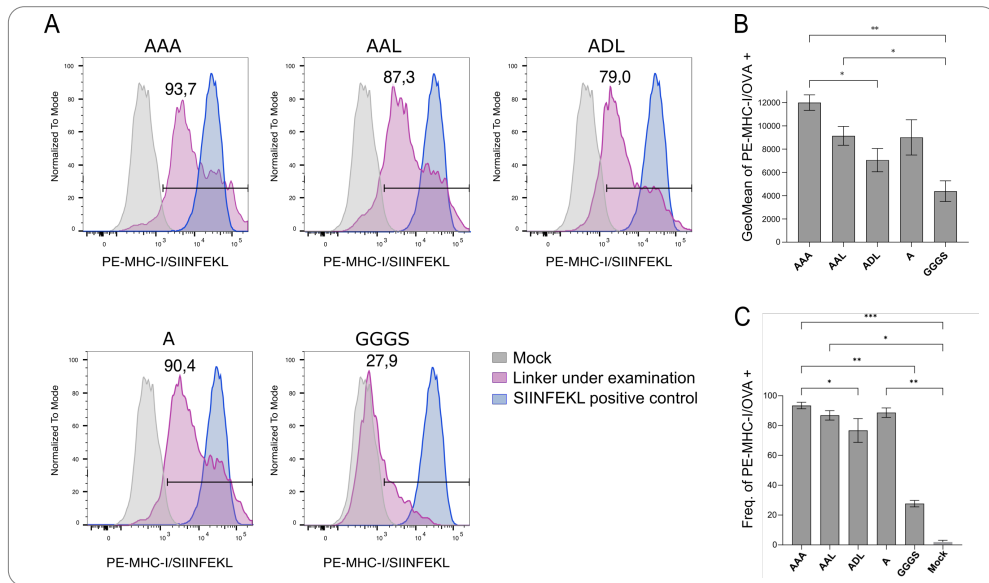


Figure 17. Flow cytometry analysis of MHC-I/SIINFEKL complexes on cell surface. (A) Representative flow cytometry panels of the detection of MHC-I/SIINFEKL complexes on the surface of B16-F10 cells. Frequency of positive cells for the linker under examination is represented on each panel. **(B)** Levels of MHC-I/SIINFEKL on cell surface expressed as geometric mean plus SD of three replicates. **(C)** Frequency of MHC-I/SIINFEKL positive cells. Mean plus SD of three replicates. Data were analysed using Dunn's test, * $P < 0.1$, ** $P < 0.01$, *** $P < 0.001$.

3. Transfection efficiency controls

Analysis of the frequencies of cells expressing MHC-I/SIINFEKL complexes confirmed a higher presentation and processing efficiency of peptides spaced by alanine-based linkers versus GGGs (Figure 17C). To determine if these differences were due to transfection efficiency variations, the same experiment was replicated adding a GFP-expressing plasmid in the transfections in a 1:4 ratio with the constructs. In this case, both the formation of MHC-I/SIINFEKL complexes and the frequency of expressing cells were selected within the GFP+ population, ensuring that all gated cells had been successfully transfected.

The frequency of GFP+ cells was similar in GGGs and AAL-transfected cells (52.7% vs 53.5% of GFP+ cells, respectively) and higher than in those cells transfected with AAA, ADL or A polypeptides (37.1%; 38% and 33.9% of GFP+ cells, respectively, Figure 18A). Analysis of

the frequencies of cells expressing MHC-I/SIINFEKL complexes, as well as their signal intensity on the surface of GFP⁺ cells, confirmed the more efficient presentation of the SIINFEKL peptide when neoantigens are concatenated using alanine-based linkers (Figure 18B and C).

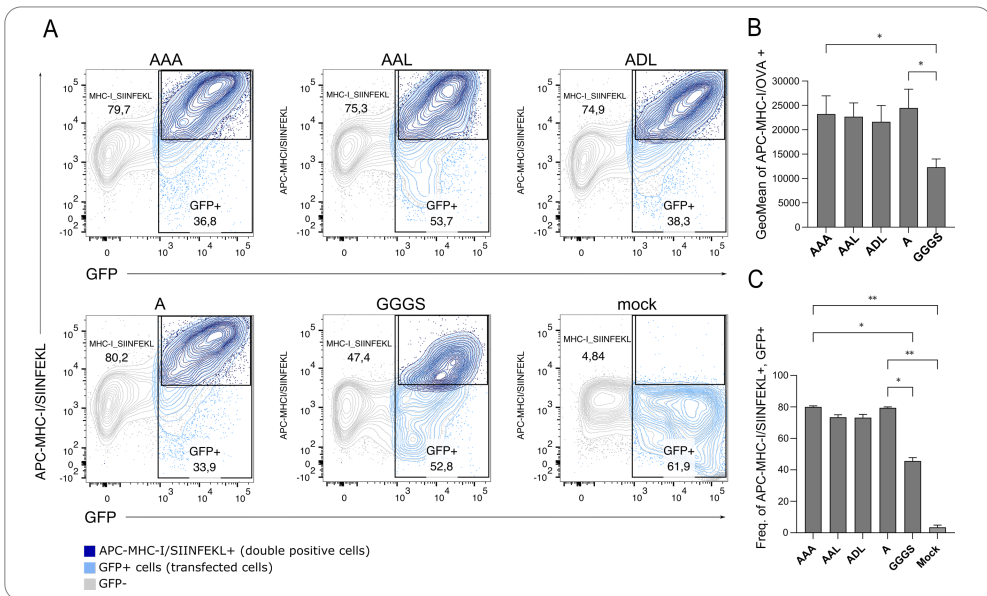


Figure 18. Recombinant proteins transfection controls. Surface expressed polypeptides. (A) Representative flow cytometry panels for the detection of MHC-I/SIINFEKL on co-transfected B16-F10 cells with both surface expressed polypeptide and GFP coding plasmid. Frequency of GFP⁺ and APC-MHC-I/SIINFEKL⁺ in GFP⁺ cells are indicated in each panel. Grey: GFP negative cells; light blue: GFP⁺ cells; dark blue: APC-MHC-I/SIINFEKL⁺ GFP⁺ cells. **(B)** Levels of detection of MHC-I/SIINFEKL on the surface of GFP⁺ B16-F10 co-transfected cells are shown as geometric mean. **(C)** Frequency of APC-MHC-I/SIINFEKL⁺ GFP⁺ co-transfected cells. Error bars represent SD of three independent experiments. All data were analysed using Kruskal-Wallis test corrected for multiple comparisons by original FDR method of Benjamin and Hochberg, * $P < 0.1$, ** $P < 0.01$.

Surface expressed proteins may require extra processing and transport steps compared to intracellularly expressed proteins, and this fact may affect to protein availability for proteasomal processing and epitope presentation. Therefore, we confirmed the results described above using intracellularly expressed polypeptides. We removed the signal peptide and the CD44-TM of the initial constructs (Figure 19A) and evaluated their expression in B16-F10-transfected MG132-treated cells by western blot (Figure 19B). Polypeptides containing spacers AAA, ADL and GGGG were successfully expressed; while AAL- and A-linked constructs showed a weaker signal (Figure 19B), suggesting that they were either less expressed or processed very rapidly. Then, the antigen presentation efficiency

Results – Section 1

was determined as previously described, including a co-transfection with a GFP coding plasmid for transfection efficiency evaluation. AAA-linked polypeptide showed the highest amount of the MHC-I/SIINFEKL complex by flow cytometry, while GGGS-linked polypeptide showed the lowest signal (Figure 19C and D). These results are comparable with those previously obtained with surface expressed polypeptides. Analysis of the frequencies of cells expressing MHC-I/SIINFEKL complexes confirmed a more efficient presentation and processing of the peptides concatenated by alanine-based linkers versus GGGS (Figure 19E).

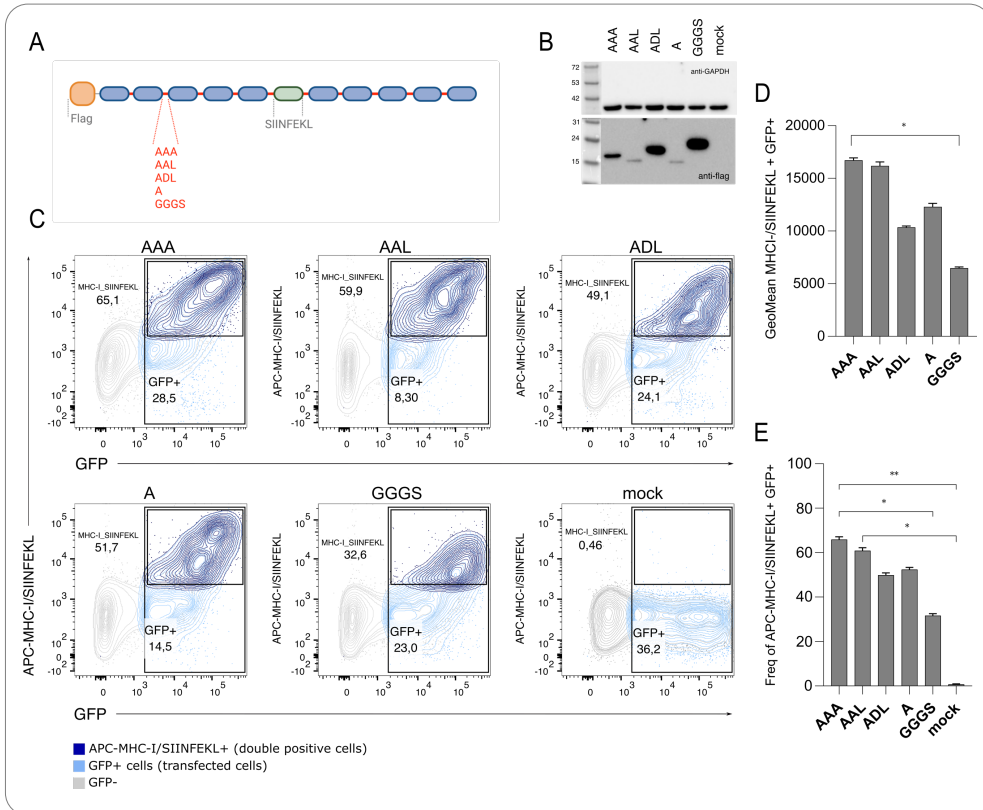


Figure 19. Recombinant proteins transfection controls. Intracellularly expressed polypeptides. (A) Schematic representation of the intracellularly expressed polyproteins used. Orange: FLAG tag; blue: neoantigens; and, green: SIINFEKL peptide. Created with Biorender. **(B)** Western blot image of the expression of recombinant intracellularly expressed polypeptides in MG132-treated transfected B16-F10 cells. **(C)** Representative flow cytometry panels for the detection of MHC-I/SIINFEKL on co-transfected B16-F10 cells with both intracellularly expressed polypeptide and GFP coding plasmid. Frequency of GFP⁺ and APC-MHC-I/SIINFEKL⁺ GFP⁺ cells are indicated in each panel. Grey: GFP negative cells; light blue: GFP⁺ cells; dark blue: APC-MHC-I/SIINFEKL⁺ GFP⁺ cells. **(D)** Levels of detection of MHC-I/SIINFEKL on the surface of GFP⁺ B16-F10 co-transfected cells are shown as geometric mean. **(E)** Frequency of APC-MHC-I/SIINFEKL⁺ GFP⁺ co-transfected cells. Error bars represent SD of three independent experiments. All data were analysed using Kruskal-Wallis test corrected for multiple comparisons by original FDR method of Benjamin and Hochberg, * $P < 0.1$, ** $P < 0.01$.

4. Activation and proliferation assay

To confirm that MHC-I/SIINFEKL complexes detected on the surface of B16-F10 cells can stimulate CD8⁺ T cells, we performed an antigen presentation and stimulation experiment using splenocytes from OT-I mice. This mouse model expresses a transgenic TCR that recognises the SIINFEKL peptide in the context of H2K^{b344}. With this aim, B16-F10 cells were transfected with surface expressed polypeptides and stimulated with IFN γ to promote protein processing and presentation. Then, transfected and stimulated B16-F10 cells were co-culture with splenocytes from OT-I mice. Activation of CD8⁺ T cells was evaluated 24 hours post-co-culture. The results showed higher frequency of CD25⁺ CD44⁺ CD8⁺ T cells in those co-cultures where B16-F10 cells were transfected with alanine-based linkers (Figure 20A and B). Similar results were obtained when the proliferating activity of CD8⁺ T cells was evaluated on day three (Figure 21A and B). Taken together, these results confirm that alanine-based linkers promote a more efficient processing and presentation of the peptides, generating a higher activation of CD8⁺ T cells.

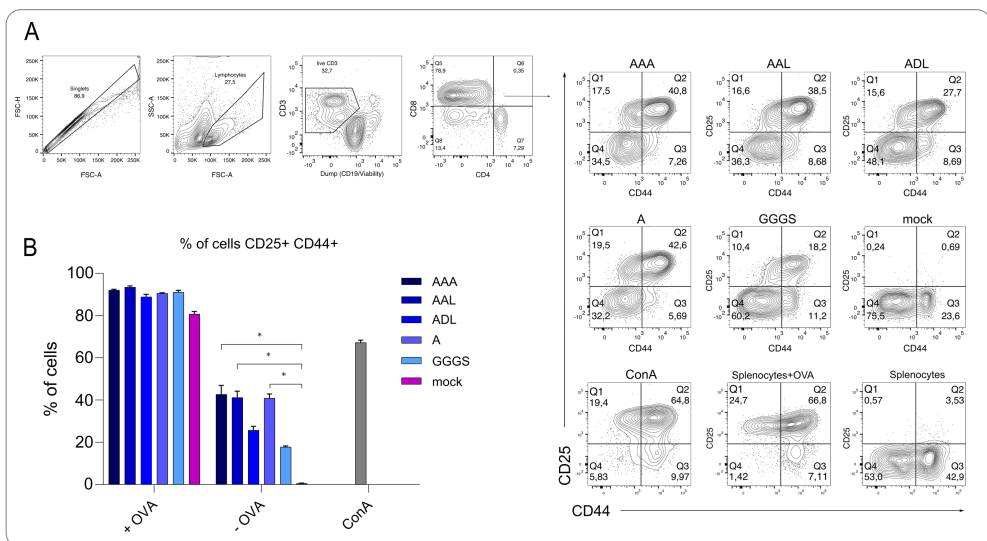


Figure 20. Effect of linker sequence in T-cell activation. (A) Gating strategy for the analysis of CD8⁺ T cells activation. **(B)** Frequency of CD8⁺ CD25⁺ CD44⁺ T cells, 24h post-co-culture of B16-F10 transfected cells with splenocytes from OT-I mice. Mean plus SD of three replicates is shown in all graphs. All data were analysed using Kruskal-Wallis test corrected for multiple comparisons by original FDR method of Benjamini and Hochberg, * $P < 0.1$.

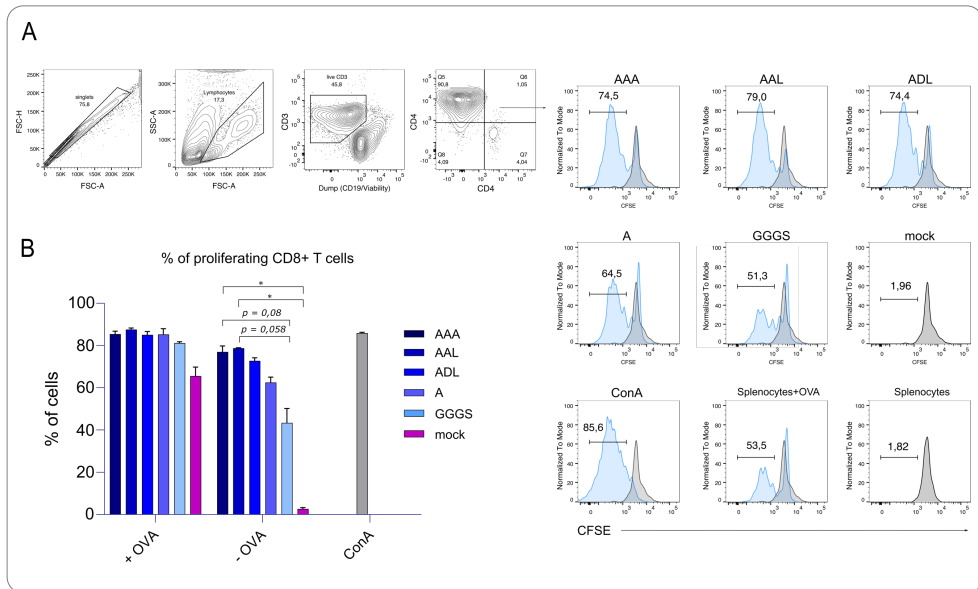


Figure 21. Effect of linker sequence in T-cell proliferation. (A) Gating strategy for the analysis of the CD8⁺ T cells proliferation. **(B)** Frequency of proliferating CD8⁺ T cells at 72h post-co-culture of B16-F10 transfected cells with splenocytes from OT-I mice. Mean plus SD of three replicates is shown in all graphs. All data were analysed using Kruskal-Wallis test corrected for multiple comparisons by original FDR method of Benjamini and Hochberg, * $P < 0.1$, ** $P < 0.01$.

5. Effect of neoantigen position on epitope presentation

Another open question is whether peptide position within the polypeptide might affect peptide processing and presentation. To investigate this possibility, three recombinant proteins were tested, where the SIINFEKL peptide was located at the N-terminal region, at the centre or close to the C-terminus of the polypeptide sequence (Figure 22A). All three constructs were designed using the AAA-spacer, since it was the most favourable linker. All resulting proteins were expressed by transient transfection in B16-F10 cells and detected at the expected molecular weight by western blot (Figure 16C and 22B). As before, presentation of the differently located SIINFEKL peptide on the MHC-I was assessed by flow cytometry (Figure 23A). The SIINFEKL peptide was detected on the surface of the B16-F10 cells in complex with MHC-I molecules in all cases. Similar levels of presentation were observed when the SIINFEKL peptide was expressed at the centre or close to the C-terminus of the recombinant protein. However, when expressed at the N-terminal region, the amount of the H2K^b/SIINFEKL complexes was lower compared to the rest (Figure 23A to C). These results suggested that processing and presentation of neoantigens at the middle or C-

terminus of the polypeptide could be more successful compared to neoantigens at the N-terminal region.

Alternatively, SIINFEKL presentation might depend on the surrounding amino acids. Since in the previous experiment, the SIINFEKL peptide located at the N-terminal region was flanked by the FLAG Tag (DYKDDDDK) and an AAA-linked neoantigen, we designed a new polypeptide where the N-terminal located SIINFEKL peptide was flanked by two neoantigens spaced by the AAA linker or the GGS (Figure 23D). In addition, a polypeptide sequence positioning the SIINFEKL peptide at the C-terminal region and spaced by one neoantigen from the transmembrane domain of CD44 was also analysed (Figure 23D). Expression of all new AAA- and GGS-linked recombinant proteins was confirmed by western blot, showing the expected molecular weight for all variants (Figure 23E). Remarkably, the detection of H2K^b/SIINFEKL complexes in transfected B16-F10 cells showed no differences among constructs (Figure 23F-G). Overall, the data suggests that the efficiency of neoantigen processing and presentation might depend on the environment of the flanking sequences (beyond the linker itself), but their position (N-, middle or C-terminal) does not necessarily play a major role. Moreover, these results support the idea that position of the neoantigen in the polypeptide sequence may not influence the processing and presentation of the neoantigens as much as the sequences flanking the epitopes.

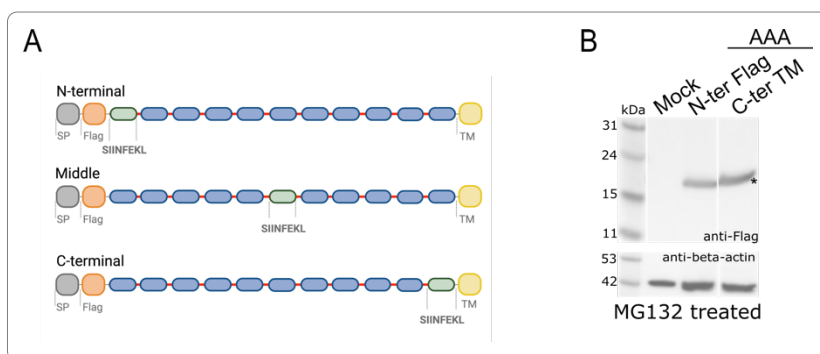


Figure 22. Role of peptide position in antigen presentation. (A) Schematic representation of the constructs used. Created with Biorender. **(B)** Western blot image of the expression of recombinant proteins in MG132-treated transfected B16-F10 cells. Asterisk indicates expected molecular weight.

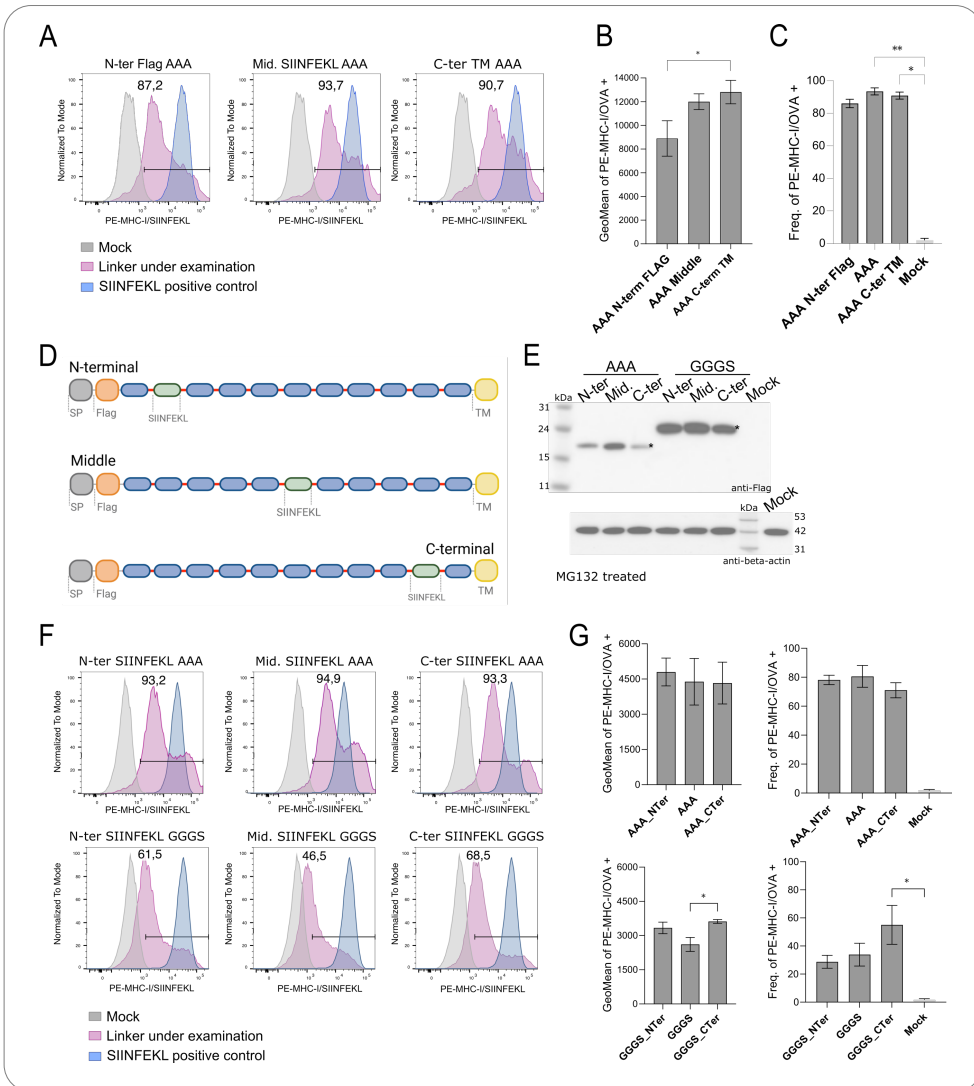


Figure 23. Role of peptide position in antigen presentation. (A) Representative flow cytometry panels for the presentation of MHC-I/SIINFEKL peptide on transfected B16-F10 cells. Frequency of positive cells is represented on each panel. **(B)** Geometric mean values for the presentation of SIINFEKL peptide on mouse MHC-I molecules from transfected B16-F10 cells with AAA N-term, AAA and AAA C-term TM. **(C)** Frequency of cells expressing MHC-I/SIINFEKL on the cell surface. Error bars represent SD of three independent experiments. Data were analysed using Dunn’s test, * $P < 0.1$, ** $P < 0.01$. **(D)** Schematic representation of the constructs used. Created with Biorender. **(E)** Western blot image of the expression of recombinant proteins in MG132-treated transfected B16-F10 cells. Asterisk indicates expected molecular weight. **(F)** Representative flow cytometry panels for the presentation of MHC-I/SIINFEKL peptide on transfected B16-F10 cells. **(G)** Levels of detection of MHC-I/SIINFEKL on the surface of B16-F10 transfected cells as well as the frequency of cells expressing these complexes are shown. Data from three independent experiments were analysed using Dunn’s test, * $P < 0.1$, * $P < 0.01$.

SECTION 2: Optimisation of HIV-1 Gag-based Virus-Like Particles to display melanoma neoantigens

Immunotherapeutic strategies aim to generate *de novo* or expand existing specific T-cell responses which have the potential to target and kill tumour cells¹⁶. Thus far, these novel therapies have proven clinical efficacy in a variety of malignant tumours^{301–303,345–347}, among which melanoma has been one of the most investigated. Melanoma has been historically an immune-reactive type of cancer, probably associated with its high mutational burden, and therefore high potential immunogenicity³⁴⁸. In this project, the B16-F10 murine melanoma cell line was the one chosen to select neoantigens that were loaded on the neoVLPs (Figure 24). This cell line derives from the C57BL/6 strain, and it represents a well established syngeneic tumour model for the evaluation of different immunotherapies^{349,350}.

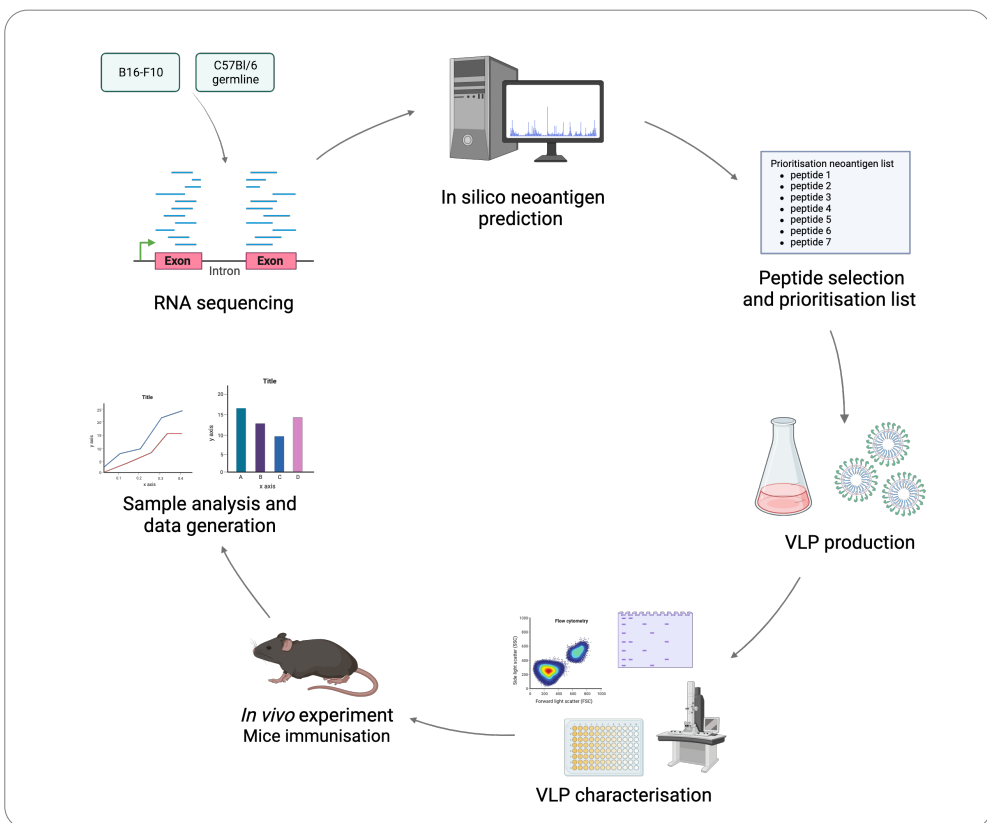


Figure 24. Graphical overview of the project. Neoantigens were selected *in silico* using a neoantigen prediction pipeline and classified in a prioritisation list. NeoVLPs were designed and produced displaying the selected neoantigens. NeoVLPs were characterised and their expression and morphology were confirmed. Immunogenicity of neoVLPs was tested *in vivo* using a C57BL/6 mouse model. The immunogenic capacity of neoVLPs was determined by their efficacy in generating neoantigen-specific CD8⁺ T-cell responses detected by ELISpot using splenocytes from vaccinated mice.

In cancer vaccine development, besides the difficulties in identifying the most suitable targets, the discovery of adequate vaccine delivery platforms has become one of the biggest challenges to elicit sustainable antigen specific T-cell responses³⁵¹. Within this framework, we developed HIV1 Gag-based neoantigen VLPs (neoVLPs) expressing on their surface a collection of selected neoantigens from the B16-F10 cell line. In total, 5 neoantigen-expressing HIV-1 Gag-based VLPs were fully characterised, as well as purified and formulated as vaccines. Their immunogenicity was evaluated in C57BL/6 mice and their T-cell response was analysed by ELISpot. In addition, one selected candidate was tested as a preventive vaccine in a tumour challenge *in vivo* experiment (Figure 24).

1. Identification of nonsynonymous mutations and frameshifts in B16-F10 mouse melanoma cell line*

The melanoma cell line B16-F10 was chosen as a tumour model for the development of NOAH and the selection of neoantigens. This work was performed in collaboration with the research group of Dr Victor Guallar at the Barcelona Supercomputing Centre (BSC). DNA and mRNA were prepared from B16-F10 cells and C57BL/6 healthy tissue and sequenced by WES and RNA-seq. Then, using the novel NOAH pipeline and the selection criteria previously described 41 peptides of 9 amino acids in length (short peptides) and three long peptides from frameshifts were selected and classified in different tiers (Figure 25). Tier1 emphasised the selection of neoantigens with larger differences on binding affinity between the wild-type (WT) and the mutated variant. Neoantigens included in this group showed mutations in MHC anchor residues that increased the binding to MHC class I molecules. Tier2 grouped neoantigens with high MHC binding affinity. Mutations in these peptides involve a significant change in physicochemical properties (such as polar to aliphatic, negative to positive charge, etc.) for those amino acids that are largely exposed to the solvent and, therefore, may be in contact with the TCR. Tier3 included those peptides that fulfil the binding and expression criteria as Tier2 but that presented less drastic mutations: with a similar predicted binding to that of the WT and less pronounced changes in a solvent exposed amino acid. In addition, three predicted frameshifts were also identified by NOAH and selected for further analysis (Figure 25).

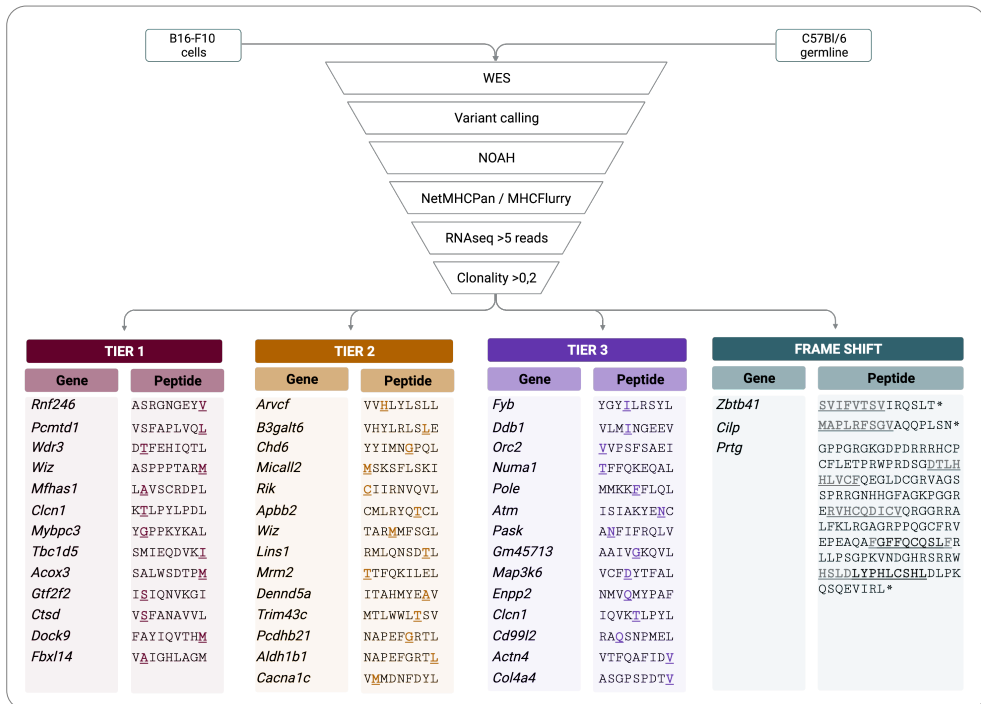


Figure 25. Scheme of the neoantigen selection strategy. Identified somatic mutations were filtered by structural features (NOAH), RNA expression, clonality and matched with NetMHCpan or MHCflurry. Neoantigens tiered according to structural features are shown with the mutation present in B16-F10 cells highlighted in bold. Created with Biorender.

2. Production and purification of neoVLPs

NeoVLPs were engineered to allow a high-density exposure of neoantigens on their surface. Such higher epitope density was obtained by fusing the concatenated neoantigen peptides to the HIV-1 structural Gag protein³²¹. Since it is estimated that there are approximately 2500 copies of Gag in one VLP³⁵², neoVLPs are expected to express a similar amount of each neoantigen (Figure 26A). NeoVLPs included a signal peptide and a FLAG tag at the N-terminus, followed by the concatenated neoantigen peptides separated by a spacer sequence (Figure 26B). This sequence was either an AAA or an SSS. Considering previous results shown in Section 1, a triple-alanine linker was included as this linker sequence promotes a more efficient peptide processing and presentation in MHC-I molecules³⁵³. When the addition of an AAA sequence generated alternative transmembrane domains, we substituted it for an SSS linker sequence to avoid it²⁹⁴. This polypeptide sequence was fused to the transmembrane domain of murine CD44 followed by the HIV-1 structural protein Gag

Results – Section 2

on the C-terminus (Figure 26B). From the results obtained from the identification of non-synonymous mutations in the B16-F10 cell line, three different neoVLP designs were generated including all neoantigens selected. The constructs were the following: (i) three different neoVLPs encoding concatenated neoantigens classified in Tiers 1 to 3 (Tier1-GAG, Tier2-GAG, Tier3-GAG), (ii) one neoVLP encoding three different Frameshifts (FS-GAG) and (iii) a NakedVLP without neoantigens used as control vehicle (Figure 26B). These different fusion constructs were then transfected into Expi293F cells, and the expression of the fusion proteins was determined by flow cytometry. To detect the presence of the fusion protein at the cell membrane, we performed an extracellular staining of FLAG tag and an intracellular staining of the HIV-1 Gag protein p24. A population of double positive cells could not be identified, suggesting that the fusion proteins are not reaching the cell membrane (Figure 26C). However, a double positive cell population was identified when intracellular staining of FLAG tag and p24 was performed, indicating that all the fusion proteins were being retained inside the transfected cells (Figure 26D). Formation of properly assembled neoVLPs in mammalian Expi293F cells was demonstrated by TEM for each of the fusion proteins tested (Figure 26E). TEM images suggested that the particles were budding from the rough endoplasmic reticulum, where the fusion protein was being synthesised, and were accumulating perinuclearly at the cytoplasm. No budding events were observed at the cellular membrane, thereby explaining the absence of extracellular FLAG tag staining by flow cytometry (Figure 26E).

Therefore, we adapted a protocol from Titchener-Hooker et al^{326,327} to extract and purify intracellular neoVLPs. Transiently transfected mammalian Expi293F cells were mechanically disrupted and neoVLPs were extracted by incubation with a low concentration of detergent (Triton X-100). After detergent removal, neoVLP samples were further purified by multimodal chromatography (strong anion-exchange with a size-exclusion effect). Samples from the VLP extracted fraction, prior to the chromatographic step, were imaged by cryo-EM (Figure 26F), showing the expected morphology for all neoVLPs. From the images, both the lipid bilayer of the enveloped VLP and the Gag ring inside the formed VLPs were distinguished (Figure 26F). Integrity of the fusion proteins in the cellular lysate (Pellet) and in the final vaccine preparation (Vax) was evaluated by western blot (Figure 26G). These results confirmed that fusion proteins were produced at the expected molecular weight,

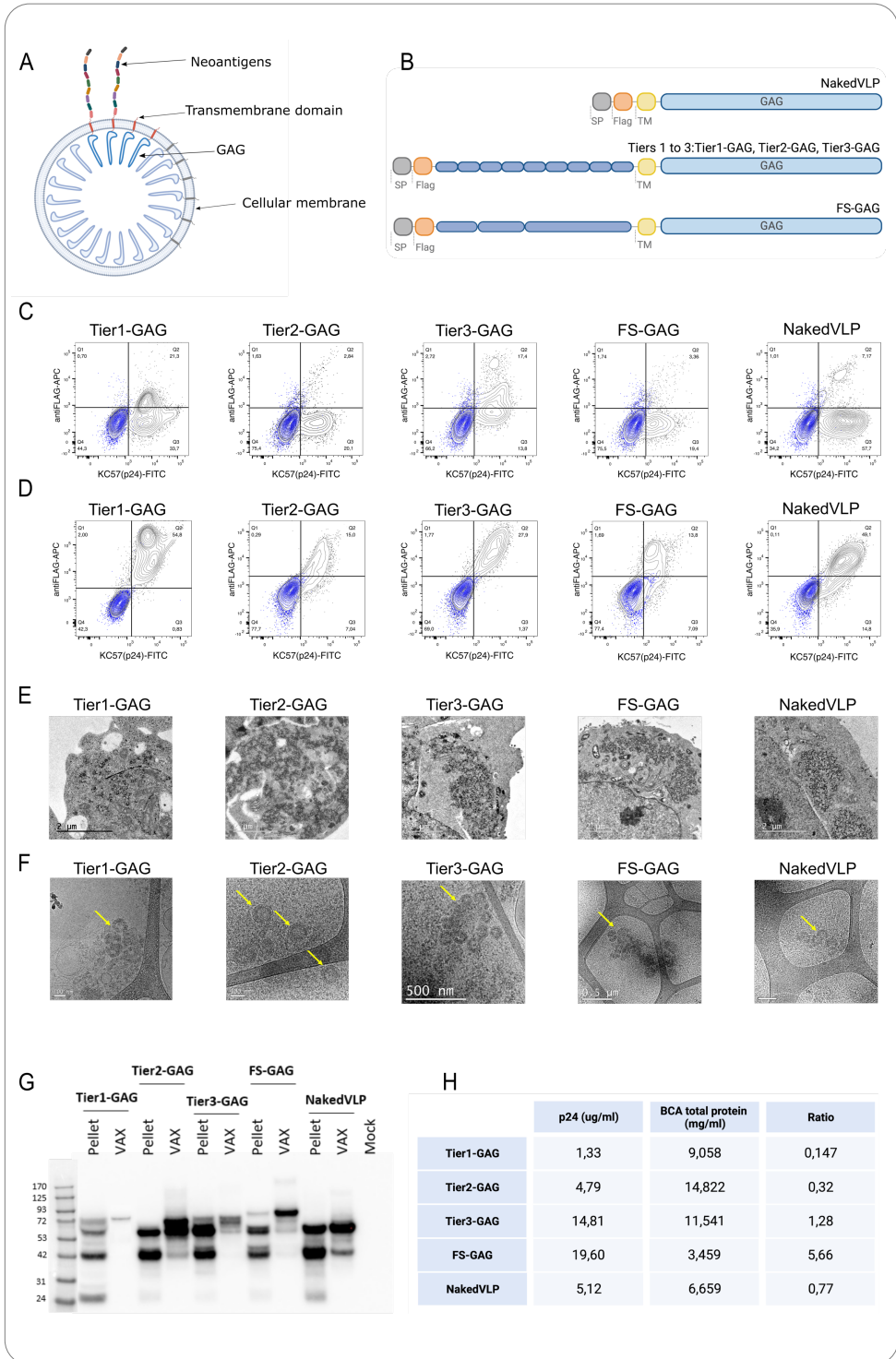


*Figure caption in the following page

even though several bands were shown in Tier2-GAG and Tier3-GAG, probably due to partial protein processing or degradation.

Final p24 concentration was determined by p24 ELISA or by western blot, and total protein quantification by BCA (Figure 26H). Purity of final formulations revealed p24/total protein ratios ranging from 0.1-5%. Despite these being consistent with previous VLP productions, a new purification protocol was optimised to try to reduce the presence of contaminants and increase the purity of the productions.

3. Determination of the optimal vaccine regime

After confirming the correct expression of our fusion-proteins and formation of neoVLPs, we proceeded to test whether the neoVLPs would elicit antigen specific T-cell responses upon vaccination. To that end, we first defined an optimal vaccination schedule by comparing the Gag-specific humoral and cellular responses generated from the three different vaccination regimes tested. C57BL/6 mice were immunised according to the following regimes: (i) two naked plasmid DNA doses (DD); (ii) one dose of naked plasmid DNA plus one dose of purified VLPs (DV); and (iii) two doses of purified VLPs (VV, Figure 27A). Analysis of the humoral response against HIV-1 Gag protein showed that DD and DV regimes elicited a higher antibody titre, compared to VV regime (Figure 27B). Regarding the generation of Gag-specific T-cell responses, IFN γ ELISpot analysis against six pools of ten overlapping peptides, each one covering the entire length of HIV-1 Gag protein, revealed a higher CTL response for the DV regime (Figure 27C). Therefore, the DNA prime/VLP boost regimen was chosen as the immunisation regime for all subsequent experiments.

Figure 26. VLP-based vaccine production and purification. (A) Drawing of a neoVLP. Neoantigens on the surface of the VLP, transmembrane domain in orange, HIV Gag in blue and cellular membrane in dark grey. Created with Biorender. (B) Scheme of the linear polyprotein that generates the neoVLP. Signal peptide in light grey and FLAG tag in orange. Created with Biorender. (C) Representative flow cytometry panels for the expression of neoVLP fusion proteins in transiently transfected Expi293F cells. Identification of FLAG tag at the surface of the cells and total p24-Gag. Population of mock transfected Expi293F cells in blue. (D) Representative flow cytometry panels for the expression of neoVLP fusion proteins in transiently transfected Expi293F cells. Identification of total FLAG tag and total p24-Gag. Population of mock transfected cells in blue. (E) TEM images of Expi293F cells producing neoVLP particles. (F) Cryo-TEM images of extracted (XAD4) neoVLPs. (G) Western blot image of the cell lysate (Pellet) and purified (Vax) of neoVLPs. (H) Quantification of p24 by ELISA and total protein by BCA in the final preparation.

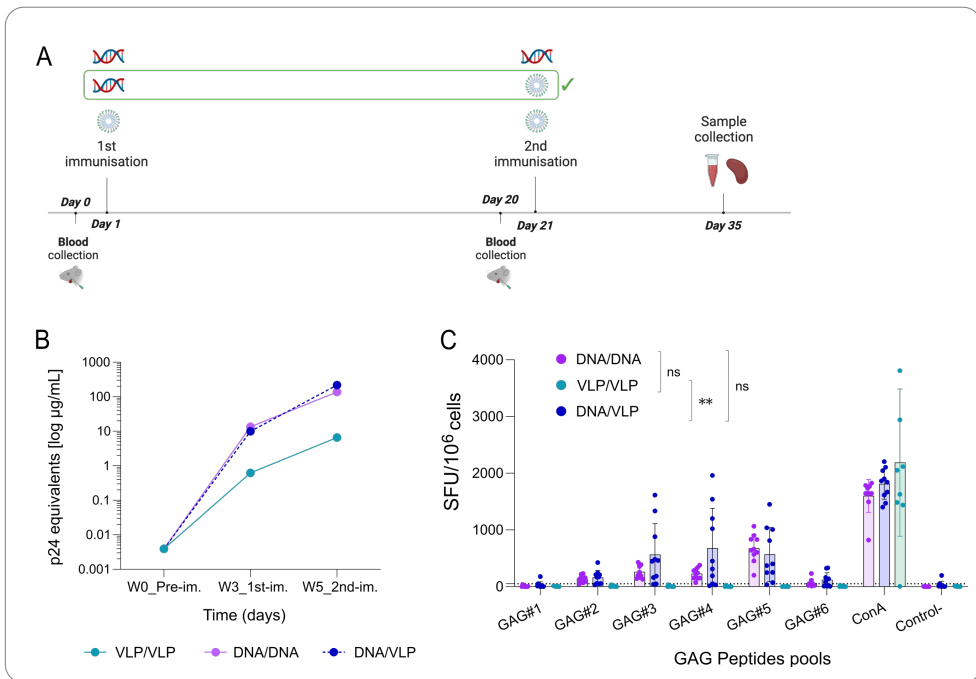


Figure 27. Selection of the optimal vaccination regime. (A) Experimental design of the different regimes tested. Created with Biorender. (B) Evaluation of the humoral response against Gag overtime. (C) Evaluation of the T-cell response against 6 pools of 10 overlapping peptides covering the entire HJIV-1 Gag protein overtime. Data represented as mean \pm SD. Data analysed using Mann-Whitney U test, * $P > 0.1$, ** $P > 0.01$.

4. Immunogenicity of neoVLPs in C57BL/6 mice

Having established the vaccination regime, three neoVLPs coding for concatenated neoantigens (Tier1-GAG, Tier2-GAG and Tier3-GAG) and one coding for three concatenated Frameshifts (FS-GAG), were tested along with a NakedVLP as a control.

a. Humoral response against Gag protein and Expi293 proteins

Two immunisations, a DNA prime and a purified VLP boost were administered with a 3-week interval (Figure 28A). Humoral response against the structural Gag protein was determined by ELISA. In all cases, higher levels of antibodies after the prime dose were observed, with considerable variability (Figure 28B). Purified VLP boost showed a strong effect increasing the humoral response against Gag (Figure 28B and C). These results indicate that the differential expression of the constructs induced some variability after the

Results – Section 2

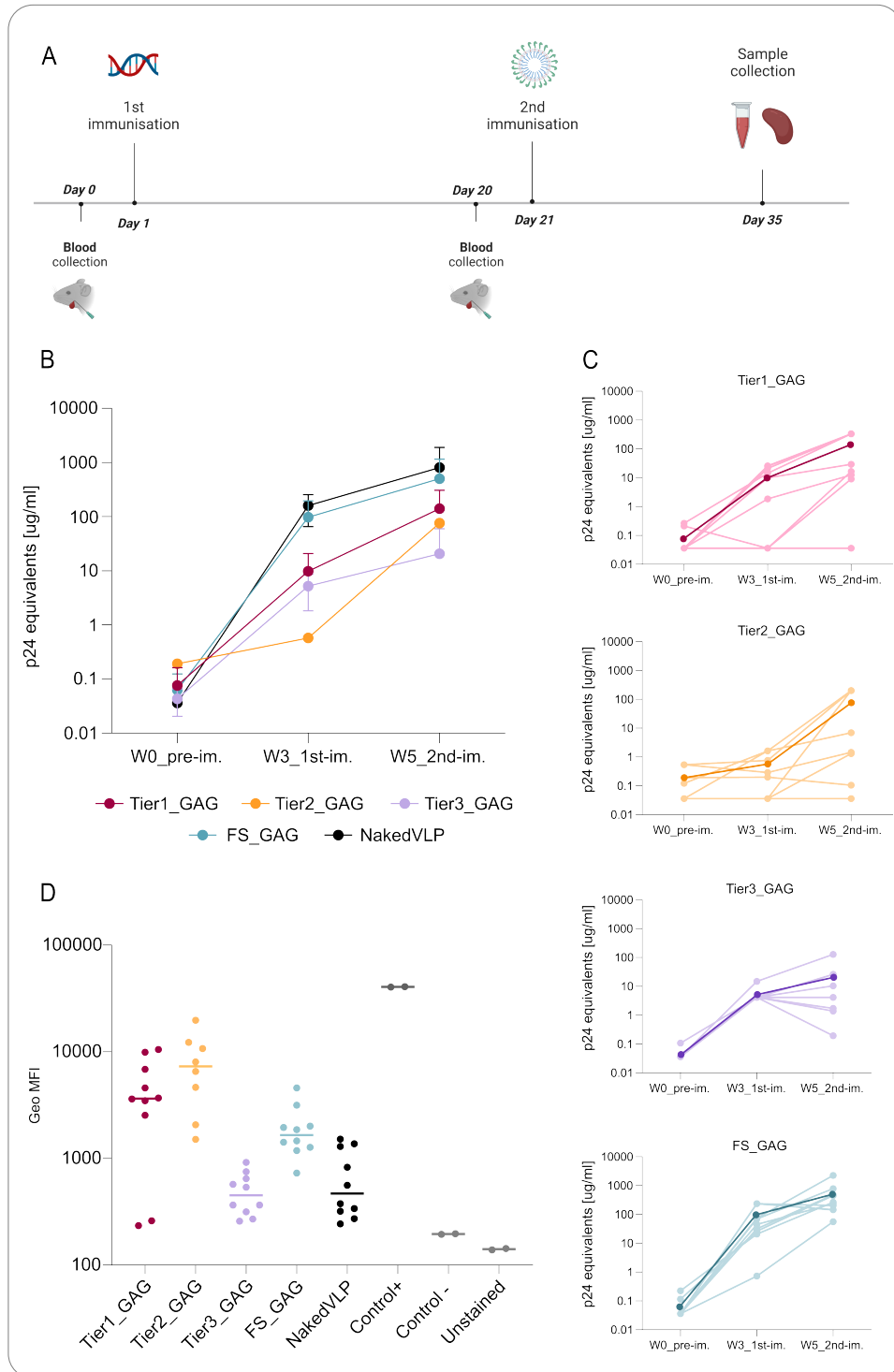


*Figure caption in the following page

first DNA immunisation, but antibody levels of all groups were comparable after the boost with purified neoVLPs (Figure 28B and C).

Purified neoVLPs were produced in Expi293F cells and thus, they can incorporate on their membranes proteins from this cell line. These proteins are considered contaminants in the neoVLP preparations, together with small vesicles such as exosomes that can also be present in the final formulation. VLP size exosomes, or other vesicles, may not be removed in the purification steps and their presence can also elicit a specific humoral response against host proteins. Hence, the humoral response against the Expi293F proteins was also analysed. Non-transfected Expi293F cells were incubated with serum from vaccinated mice at endpoint. Anti-human mouse antibodies were detected with an anti-mouse fluorochrome-conjugated secondary antibody by Flow Cytometry (Figure 28D). Antibodies against host proteins were detected in all cases, indicating that the presence of human proteins is also eliciting a humoral response.

Taken all together, the humoral response against Gag suggests the correct expression of the fusion-proteins after DNA electroporation in the muscle of the animals. In addition, the humoral response observed against host cell proteins reveals the capacity of neoVLPs to elicit a rapid humoral responses after two doses.

b. Neoantigen specific CD8+ T-cell response

To identify IFN γ -producing CD8+ T cells, splenocytes from vaccinated animals were stimulated with individual peptides from Tier1, Tier2, Tier3 and with pools of two overlapping peptides covering the entire Frameshifts. In addition, one single pool of HIV-1 Gag overlapping peptides covering residues 314 to 412 was used as a vaccination positive control for all neoVLPs. Antigen specific CD8+ T-cell responses were detected against five neoantigens from Tier2-GAG neoVLP and one from Tier3-GAG neoVLP (Figure 29A).

Figure 28. Humoral response against GAG and host cell proteins. (A) Schematic representation of the experimental design. (B) Evaluation of humoral response against GAG over time for all groups vaccinated with the neoVLPs. Tier1-GAG in dark red, Tier2-GAG in yellow, Tier3-GAG in purple, FS-GAG in light blue and in black mice vaccinated with the NakedVLP. (C) Evaluation of the humoral response against Gag individually represented with each replicate corresponding to each vaccinated mouse. (D) Evaluation of the humoral response against host proteins at end point for all groups vaccinated with neoVLPs. Tier1-GAG in dark red, Tier2-GAG in yellow, Tier3-GAG in purple, FS-GAG in light blue and in black mice vaccinated with the NakedVLP. In grey two internal controls representing the maximum and minimum signals obtained.

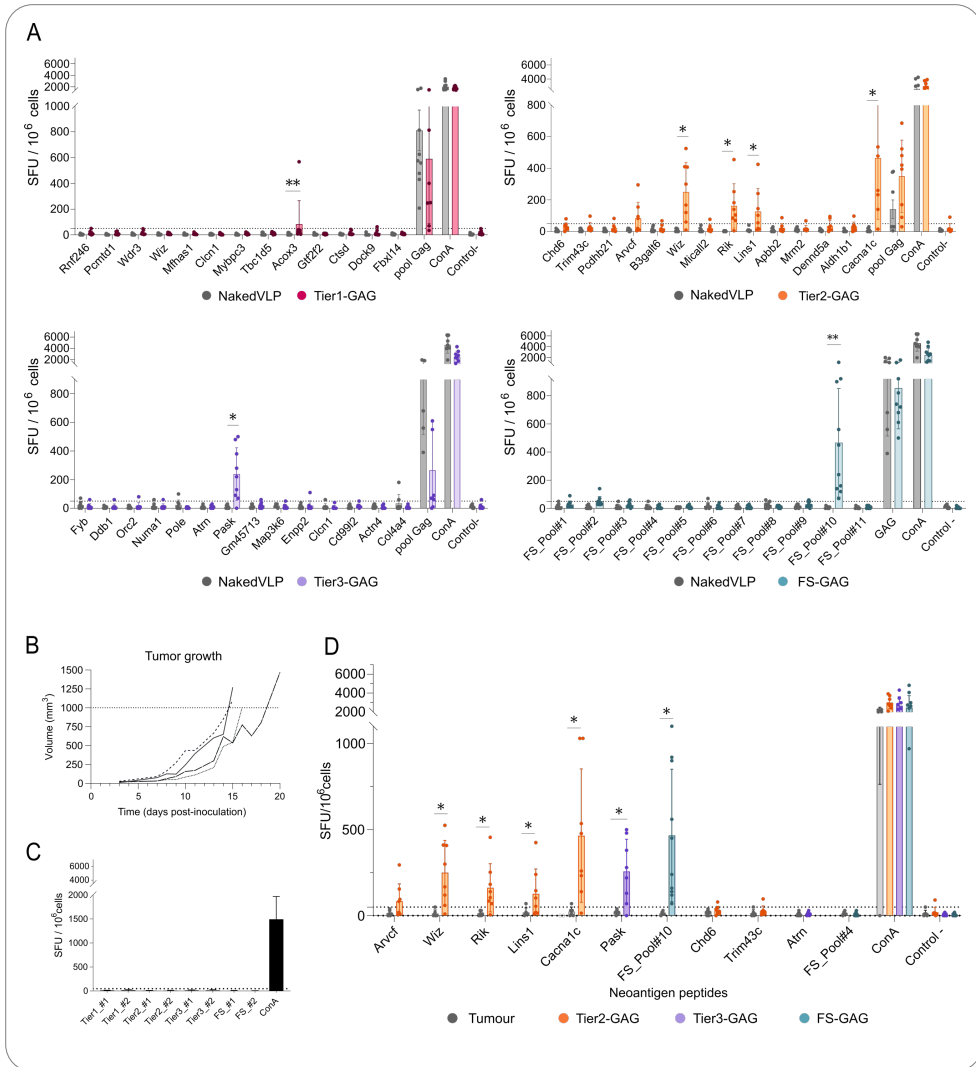


Figure 29. T-cell response against selected neoantigen included in the neoVLPs. (A) Evaluation of cellular response generated against the selected neoantigens. Tier1-GAG in dark red, Tier2-GAG in yellow, Tier3-GAG in purple, FS-GAG in light blue and NakedVLP in grey. **(B)** Tumour growth in mice inoculated with 10⁵ B16-F10 cells. **(C)** Evaluation of the cellular response against selected neoantigens in mice inoculated with B16-F10 cells. **(D)** Comparison of cellular response against the selected neoantigens in vaccinated animals vs tumour inoculated animals. Data represented as mean \pm SD. Data analysed using Mann-Whitney U test, * $P > 0.1$, ** $P > 0.01$.

Additionally, we also detected CD8+ T-cell responses against one out of the three frame shifts fragment tested (Prtg; Figure 29A). CD8+ T-cell responses against one peptide from

Tier1-GAG were also detected, but only one animal responded positively. Therefore, identified neoantigens in the Tier2 category were confirmed as the most immunogenic.

To determine whether neoVLP therapeutic vaccination would elicit *de novo* responses or potentiate already existing T cell specificities derived from the tumour presence, we inoculated four syngeneic C57BL/6 animals (two males and two females) with 10^5 B16-F10 cells subcutaneously at the right flank. Mice were euthanised when the tumour volume reached 1000 mm^3 , between day 15 and day 20 post-inoculation (Figure 29B), and splenocytes were collected. Cells were tested for CD8+ T-cell activity by ELISpot, and no IFN γ producing CD8+ T cells were detected after splenocyte stimulation with the pools of peptides covering all neoantigens included in the 4 neoVLPs (Figure 29C). When comparing the CD8+ T-cell responses obtained after vaccination with response obtained after tumour inoculation, we confirm that neoVLPs successfully generate *de novo* tumour-specific T-cell immune responses (Figure 29D).

5. Design, production, and purification of a new VLP containing 7 proven immunogenic neoantigens (Cippa7-GAG)

After confirming that vaccination with neoVLPs could generate *de novo* neoantigen-specific T-cell responses, we hypothesised that the formulation of a new VLP containing the 7 proven immunogenic neoantigens could elicit optimal T-cell responses with anti-tumoral effect. Therefore, we designed a new neoVLP containing the top immunogenic neoantigens from Tier2-GAG, Tier3-GAG and FS-GAG. These were the following: 5 positive neoantigens from Tier2-GAG: Arvcf, Wiz, Rik, Lins and Cacna1c; one positive neoantigen from Tier3-GAG, Pask; and one long peptide from the Frameshift fragment Prtg (Figure 30A). No peptides from Tier1-GAG were included. Only one animal generated a detectable T-cell response against Acox3; and thus, we considered that it was not biologically relevant.

This new neoVLP, hereafter called Cippa7-GAG, was produced in Expi293F cells and purified following the same protocol detailed above. A flow cytometry intracellular staining of HIV-1 Gag (anti-p24) was performed simultaneously with an extracellular staining of FLAG tag, to detect the presence of the fusion protein at the membrane, which would result in budding of the VLPs.

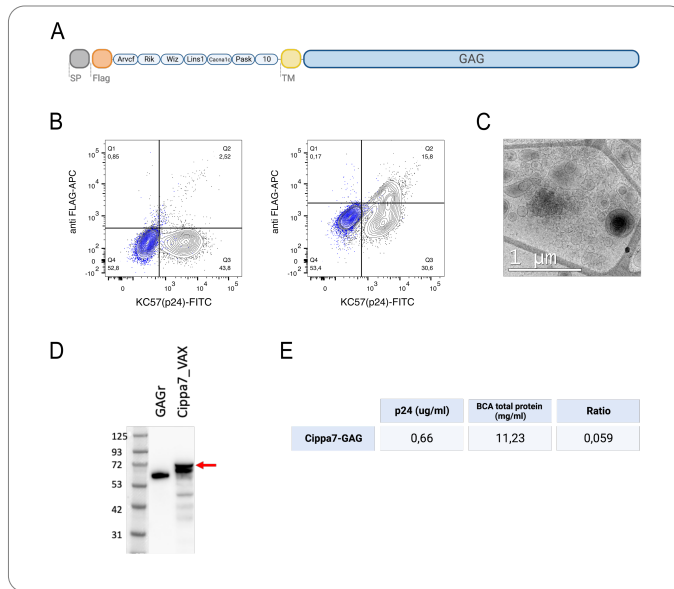


Figure 30. Cippa7-GAG production and characterisation. **A)** Scheme of the linear polyprotein that generates the Cippa7-GAG. Signal peptide in light grey and FLAG tag in orange. Created with Biorender. **(B)** Representative flow cytometry panel for the expression of the Cippa7-GAG fusion protein in transiently transfected Expi293F cells. Identification of FLAG tag at the surface of the cells and total p24-Gag in the left panel. Identification of total FLAG tag and total p24-Gag in the right panel. Population of mock transfected Expi293F cells in blue. **(C)** Cryo-TEM images of the extracted fraction of Cippa7-GAG. **(D)** Western blot image of the final VAX preparation (anti-HIV1 p55+p24+p17 antibody, Abcam). **(E)** Quantification of p24 by ELISA and total protein by BCA in the final preparation.

As expected, no presence of the fusion protein at the surface of producing cells was detected, indicating once again that the fusion protein was being retained in the cytosol of the cells (Figure 30B). NeoVLPs were purified following the same protocol, and the neoVLP extracted fraction, prior to the chromatography step, was imaged by cryo-EM (Figure 30C). The presence of correctly self-assembled Cippa7-GAG VLPs was lower than expected. The integrity of the protein was analysed by western blot using an anti-p55+p24+p17 polyclonal antibody. Two bands of very similar molecular weight were consistently detected by western blot, probably because of some degree of protein degradation (Figure 30D).

a. Immunogenicity of Cippa7-GAG in C57BL/6 mice

Even though the expression level and purification yield of Cippa7-GAG was considerably low (Figure 30E), we decided to proceed with an *in vivo* experiment to test the immunogenic capacity of this new neoVLP. Here, DNA electroporation was followed by administration of

a 20 ng dose of HIV-1 Gag p24 (purified VLPs) with a 3-week interval, for both Cippa7-GAG and NakedVLP (Figure 31A).

i. Humoral response against Gag and host proteins

The anti-Gag antibody response was detected by ELISA as explained above. We obtained a very low humoral response against Gag from the group vaccinated with Cippa7-GAG, compared to the antibody titres obtained from the NakedVLP group, that were equivalent to the previous immunisations (Figure 31B and 28B). Cippa7-GAG vaccination did not elicit antibodies against the structural Gag protein after the DNA electroporation nor after the administration of purified VLPs (Figure 31B), probably due to the suboptimal expression of the protein already observed *in vitro*. However, antibody titres obtained after the administration of NakedVLP were comparable to the ones obtained in previous experiments, indicating that 20 ng of HIV-1 p24 is enough to elicit a detectable humoral response (Figure 31B).

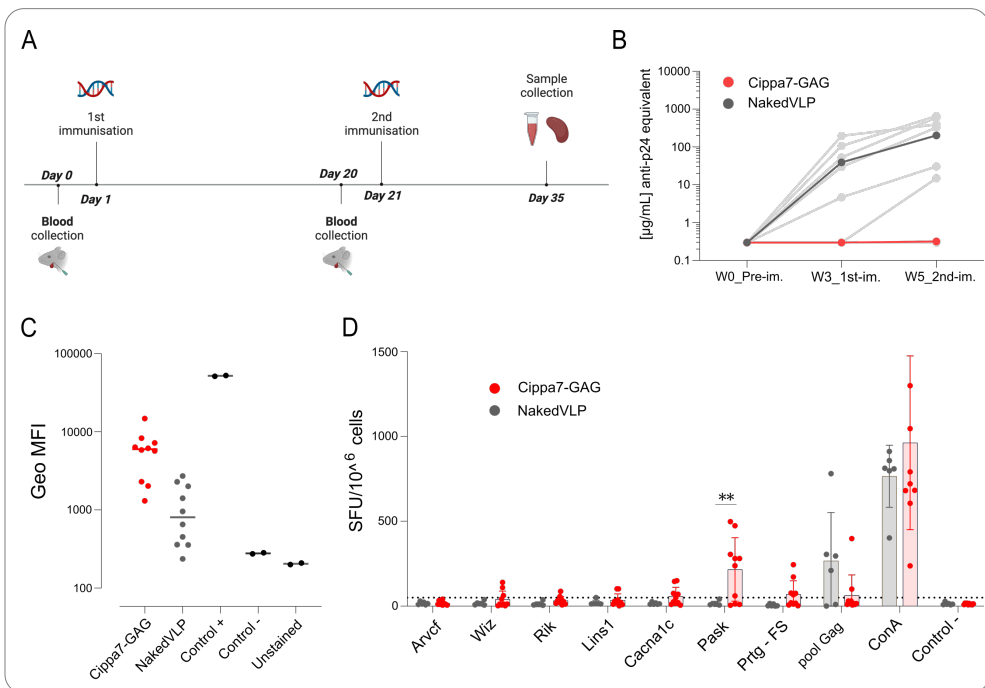


Figure 31. Cippa7-GAG immunogenicity *in vivo*. (A) Schematic representation of the experimental design used to evaluate the immunogenicity of the Cippa7-GAG VLP. Created with Biorender. (B) Evaluation of the humoral response against Gag. (C) Evaluation of the humoral response against host proteins at end point. In black two internal controls representing the maximum and minimum signals obtained. (D) Evaluation of the T-cell response generated upon vaccination. Cippa7-GAG in red, NakedVLP in grey in all graphs. Data analysed using Mann-Whitney U test, * $P > 0.1$, ** $P > 0.01$.

Humoral response against host proteins was also analysed by Flow Cytometry. As before, mouse anti-Expi293F antibodies were detected by incubating non-transfected Expi293F cells with mice sera and detecting the specific antibodies with a fluorochrome conjugated anti-mouse antibody. The MFI obtained from the animals vaccinated with Cippa7-GAG was about 10x fold compared to the control group (NakedVLP; Figure 31C). All together, these results indicate that the presence of contaminants compared to viable VLP particles is much higher in the Cippa7-GAG formulation compared to the NakedVLP (Figure 31C).

ii. Neoantigen specific CD8+ T-cell response

To detect CD8+ T-cell responses generated after Cippa7-GAG vaccination, splenocytes from vaccinated animals were stimulated overnight with the 7 immunogenic peptides displayed on the Cippa7-GAG to detect IFN γ producing CD8+ T cells. Only the neoantigen *Pask*, from the Tier3 classification category, was positive, with 6 animals out of 10 showing values over the threshold (Figure 31D). When comparing the T-cell response against HIV-1 Gag, parameter used as an experimental control, only the control group vaccinated with the NakedVLP had elicited a cellular response (Figure 31D). From the group vaccinated with the Cippa7-GAG neoVLP only two animals with Gag-specific CD8+ T cells were found (Figure 31D). These results show that the expression of the Cippa7-GAG VLP was very low, which might be due to a poor translation of the fusion protein, or it being degraded very rapidly, preventing the correct formation of neoVLPs and thus, the generation of a potent immune response.

Taken all together, the Cippa7-GAG was not a suitable vaccine candidate. Its expression was low *in vitro* and *in vivo*, which resulted in a poor immunogenicity overall.

6. Prophylactic vaccination with neoVLPs delays tumour growth.

To determine whether immune responses elicited by neoVLPs were protective against B16-F10-derived tumours, we performed a prophylactic vaccination followed by a B16-F10 tumour challenge assay in syngeneic C57BL/6 mice. In view of the previous results, we discarded the Cippa7-GAG candidate and chose the Tier2-GAG as a most promising vaccine candidate. In addition, a separate experimental group vaccinated with Tier2-GAG adjuvanted with Monophosphoryl Lipid A (MPLA) was included to maximise the response.

MPLA is a toll-like receptor 4 agonist that enhances strong Th1 responses in mice ³⁵⁴. Rhee *et al.* reported an augment in antigen-specific CD8+ T-cell responses post vaccination³⁵⁵. Animals were immunised following a DNA/VLP (DV) regime with Tier2-GAG, with or without MPLA as adjuvant (Figure 32). Continuing with a boost/prime regime, a first DNA electroporation of a plasmid coding for the neoVLP was performed, followed by a second immunisation with purified Tier2-GAG neoVLP with or without MPLA (Figure 32). Finally, the control group was immunised with NakedVLP plus MPLA. Two weeks after the boost (day 35 post first immunisation), all mice were inoculated with 10^5 B16-F10 cells and tumour growth was followed until the tumour reached 1000 mm^3 (Figure 32).

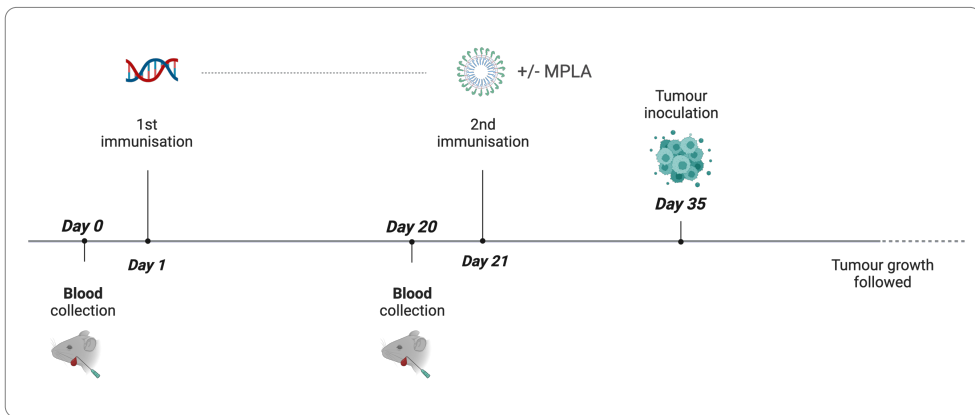


Figure 32. Schematic representation of the tumour challenge experiment performed to evaluate the antitumour potential of neoVLP vaccination. A first DNA prime was followed by a boost with purified VLPs with or without adjuvant (MPLA). Two weeks after the second immunisation (on day 35) animals were inoculated with 10^5 B16-10 cells and the tumour growth was followed until end point.

a. Humoral response against Gag and host proteins

Detection of antibodies against HIV-1 Gag protein showed consistent results with the previous experiment. Low titres of antibodies were detected after the first DNA immunisation, indicating that the expression *in vivo* is not as optimal. It was not after the boost with purified VLPs that we could observe expected levels of anti-Gag antibodies, comparable to those observed in the group vaccinated with NakedVLP (Figure 33A). Regardless of the presence of MPLA, antibodies decayed after the second immunisation and until end of experiment, which ranged from 2-6 weeks after the boost. Contrarily, in the

Results – Section 2

control group, the generation of anti-Gag antibodies reached a plateau after the first immunisation with DNA, and it was maintained until end point (Figure 33A). Regarding the humoral response against Expi293F proteins, we could not observe relevant differences between vaccinated groups (Figure 33B). These data suggests that all vaccine preparations contained similar amounts of host proteins coming from either exosomes or proteins incorporated in the neoVLPs membranes (Figure 33B).

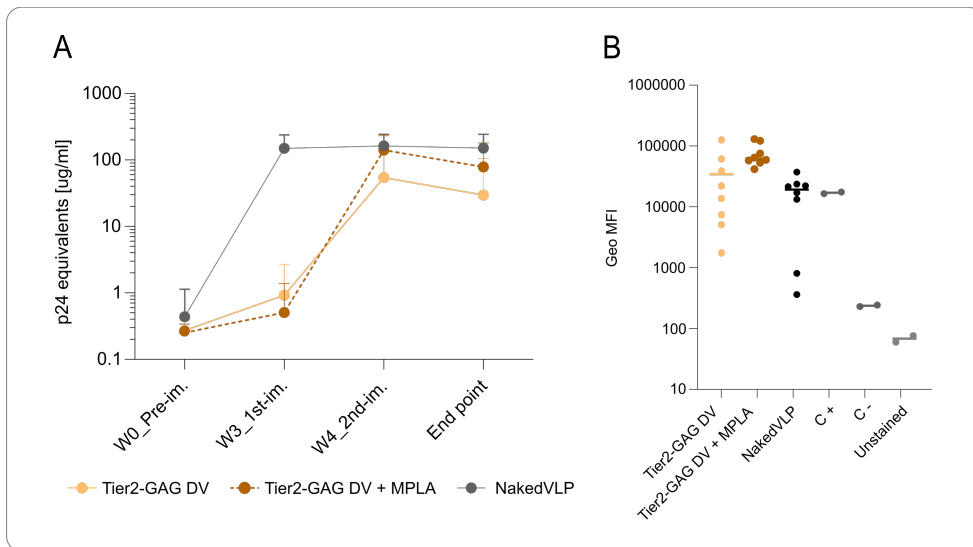


Figure 33. Evaluation of Tier2-GAG humoral response in a tumour challenge experiment to test the anti-tumour capacity of the neoVLPs. (A) Evaluation of the humoral response against Gag. Tier2-GAG in yellow, Tier2-GAG + MPLA in brown, NakedVLP in grey. **(B)** Evaluation of the humoral response against host proteins at end point in all vaccinated groups. Tier2-GAG in yellow, Tier2-GAG + MPLA in brown, NakedVLP in black.

b. Neoantigen specific CD8+ T-cell response

IFN γ producing CD8+ T-cells were detected by ELISpot. Five neoantigens generated specific T-cell responses in both vaccinated groups, such neoantigens were the same as previously identified (Figure 34A). When comparing groups with or without MPLA as adjuvant, no significant differences were detected, but a trend in all positive neoantigen indicates that the adjuvant MPLA is not inducing a statistically significant more potent CD8+ T-cell response (Figure 34A).

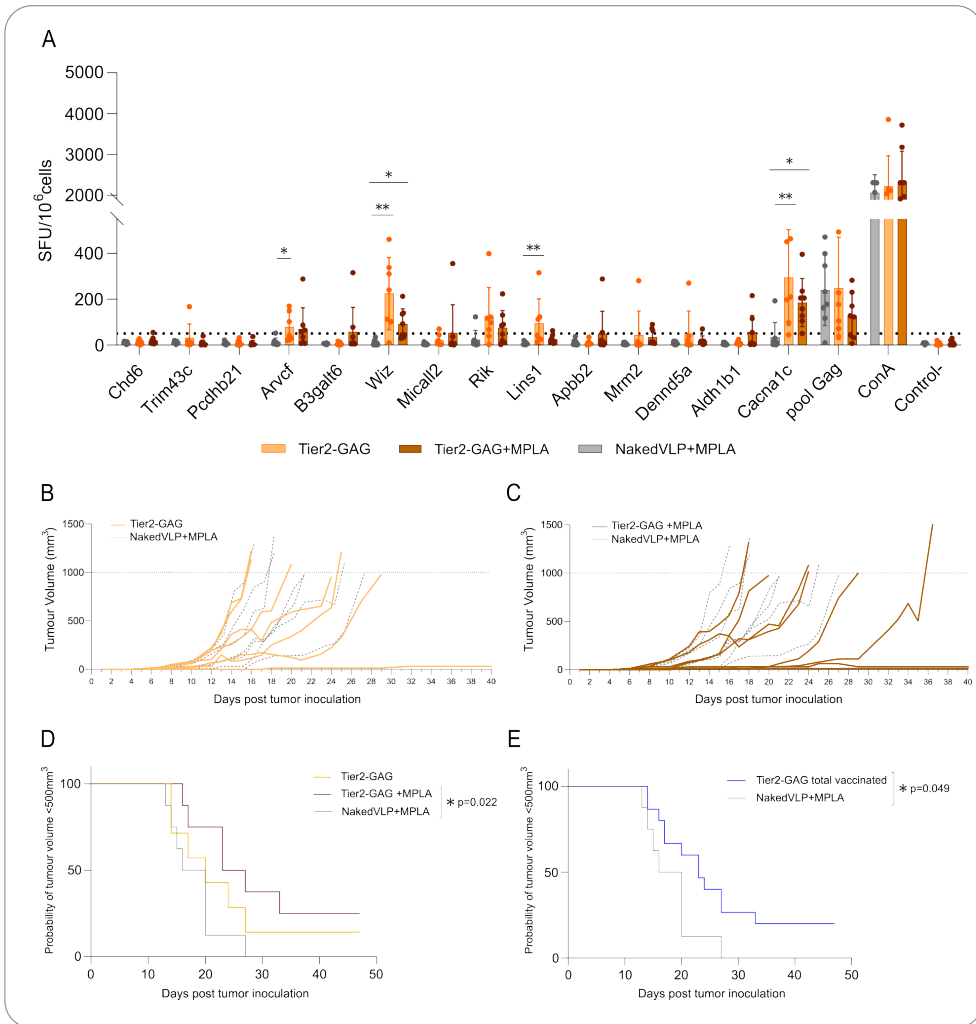


Figure 34. Tumour growth delay and control by neoVLP vaccinated animals. (A) Evaluation of cellular responses generated against the selected neoantigens and Gag peptides. **(B)** Tumour growth curves of each animal in the Tier2-GAG group in yellow. **(C)** Tumour growth curves of each animal in the Tier2-GAG+MPLA group in brown. Animals vaccinated with NakedVLP are represented by grey dotted lines in both C and D. **(D)** Kaplan-Meier graph representing the time before mice reach a tumor volume equal or over 500 mm³. Tier2-GAG group in yellow, Tier2-GAG+MPLA group in brown and naked-VLP vaccinated mice in grey. **(E)** Kaplan-Meier graph representing the time before mice reach a tumour volume equal or over 500mm³. Vaccinated with Tier2-GAG in blue (with or without adjuvant) and NakedVLP vaccinated mice in grey.

c. Tumour growth and mice survival after tumour inoculation

Finally, we assessed the functional activity of the immune response generated upon vaccination. To determine the antitumoral impact of neoVLP vaccination, vaccinated animals were inoculated with 10^5 B16-F10 cells and tumour growth was followed overtime until end point (volumes reached 1000 mm^3), when animals were euthanised. Both vaccinated groups (DV and DV+MPLA) showed a delay in tumour growth compared to the control group (vaccinated with NakedVLP; Figure 34B and C). Moreover, three animals, one from the DV and two from the DV+MPLA group, did not develop any detectable B16-F10 derived tumour (Figure 34B and C). In addition, neoVLP-vaccinated animals showed an increased survival rate compared to control animals (Figure 34D and E). Results indicate that vaccination with neoVLPs can generate *de novo* neoantigen-specific CD8+ T-cell responses with potential to become protective against tumour development.

7. Optimisation of the neoVLP purification protocol

Parallel to the immunogenicity analysis of our neoVLPs, a new purification strategy was optimised to increase the yield of neoVLPs and reduce the presence of contaminants in the final formulation. The new approach involved purifying neoVLPs by ultracentrifugation (UC) using a double sucrose cushion (Figure 35A). Discontinuous sucrose gradients have been used extensively to purify VLPs used as immunogens, as there is a necessity to minimise host cell protein contamination^{356–359}. The purification was performed with the same batch of extracted Tier2-GAG neoVLPs and they were either purified by chromatography as explained previously or loaded on top of a 30%-70% double sucrose cushion. Samples were centrifuged at $39,000 \times g$ for 2.5 hours at 4°C and neoVLPs were recovered from the 30/70% interphase (Figure 35A). Then, neoVLPs were dialysed to remove the excess of sucrose. Analysis of HIV-1 Gag p24 protein concentration by ELISA revealed a higher concentration of Gag in samples purified by ultracentrifugation (UC) than samples purified by chromatography (Figure 35B). Moreover, quantification of total protein by BCA assay showed a total protein concentration 3 times lower in the fraction purified by UC compared to the one purified by chromatography, resulting in a ratio p24:total protein ($\mu\text{g/mL}:\text{mg/mL}$) almost 4x fold higher (Figure 35B). The differences in total protein content were clearly observed comparing the VAX fraction after the chromatography with the post-dialysed fraction of the UC by

Coomassie blue staining, where the chromatography fraction showed a higher content of total protein (Figure 35C).

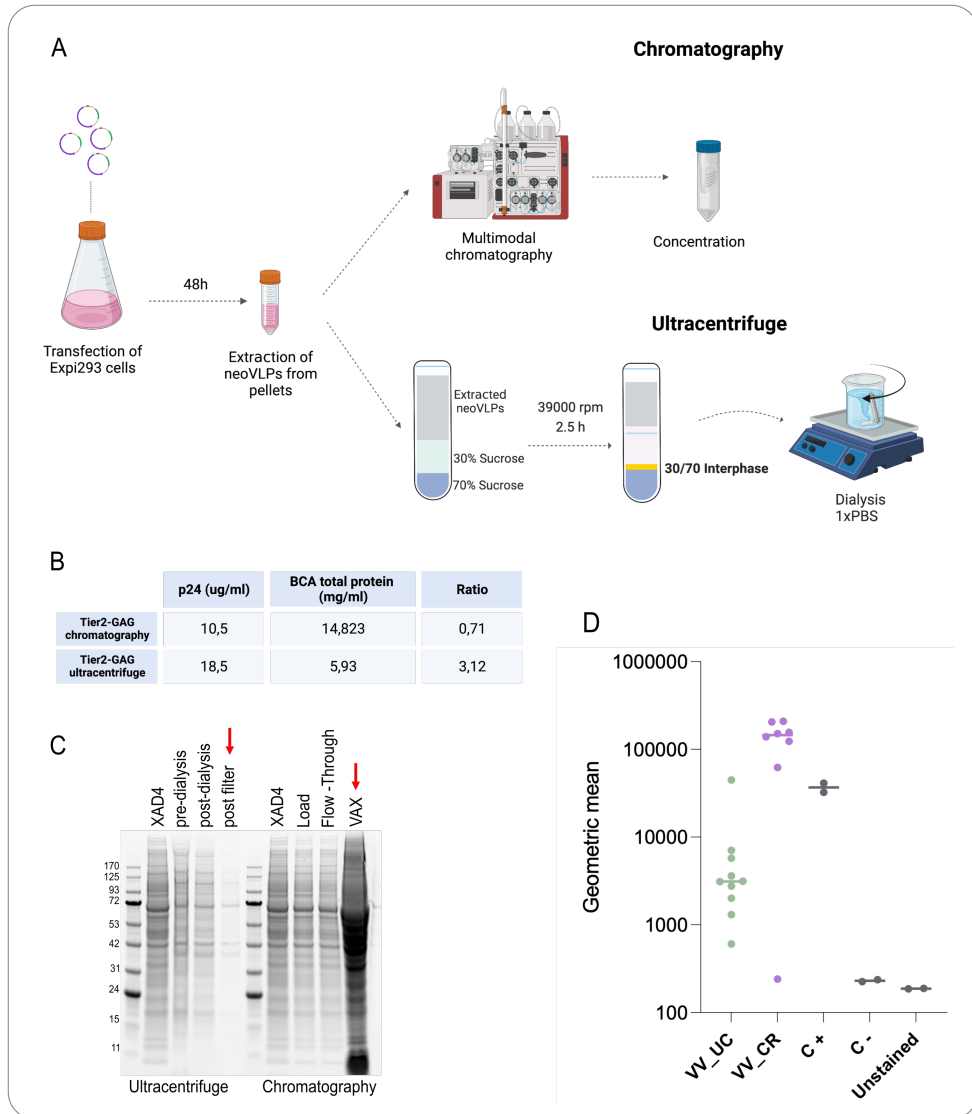


Figure 35. Optimisation of the neoVLP purification strategy. (A) Schematic representation of the comparison between the chromatography purification protocol and the sucrose cushion. Created with Biorender. (B) Quantification of the p24 concentration and the total protein in samples purified following the two purification strategies. (C) Coomassie blue staining of four purification steps of each of the two purification strategies used with neoVLPs. (D) Evaluation of the humoral response against host proteins after vaccination with two doses of purified VLPs following the two different purification strategies.

Results – Section 2

Additionally, we analysed the humoral response against host proteins from different immunisations with intracellular neoVLPs purified by ultracentrifugation or by chromatography with MPLA. As before, mouse anti-Expi293F antibodies were detected by incubating non-transfected Expi293F cells with mice sera and detecting the specific antibodies with a fluorochrome conjugated anti-mouse antibody. Results revealed that animals vaccinated with purified neoVLPs by UC showed an MFI 20x fold lower than animals vaccinated with neoVLPs purified by chromatography (Figure 35D). These results confirm that the presence of contaminants and extracellular vesicles decreased exponentially when neoVLPs were purified by ultracentrifugation.

Taken together, neoVLP purification by double sucrose cushion and UC guarantees a higher purity of the proteins and an increased neoVLP recovery.

SECTION 3: Development of second generation neoVLPs displaying cancer neoantigens. Proof of concept with the Pan02 murine model

HIV-1 Gag-based VLPs generated from the fusion protein between HIV-1 Gag and an antigen of interest have given excellent results when the antigen had a known structure^{321,322}. When the antigen presented is a polypeptide, generated by concatenating different peptides, its lack of structure can bring increased instability to the platform, and the inability to conform a minimal secondary structure can sometimes fail to generate VLPs. Results from section 2 show that the success in generating and expressing neoVLPs can depend on the peptides conforming the polypeptide and probably their order within the construct. Furthermore, fusion-protein neoVLPs were being retained inside the producing cells which hinders the purification process and increases the number of contaminants present in the final formulation. Consequently, here we present a second-generation HIV-1 Gag-based VLPs for the delivery of cancer neoantigens (C_neoVLPs), where the peptides will be expressed at the C-terminal of the Gag protein, instead of at the N-terminal. Whereas in the classical N-terminal neoVLPs the neoantigens remained outside of the VLP and fused to the Gag protein through a transmembrane domain, in C_neoVLPs epitopes will be expressed in the core of the particle (Figure 36).

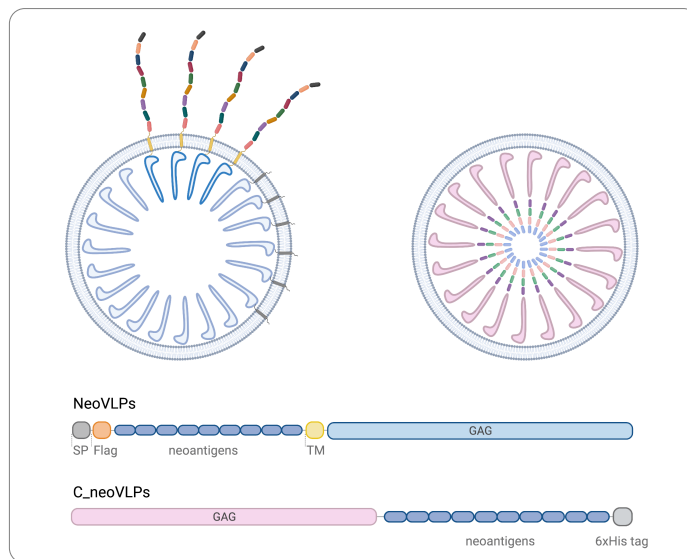


Figure 36. Schematic drawing comparing classical neoVLPs and second-generation C_neoVLPs. First generation neoVLPs are engineered as fusion-proteins, where the HIV-1 Gag protein is fused to the polypeptide by a transmembrane domain. Contrarily, C_neoVLPs express the concatenated neoantigens at the C-terminal of the Gag protein, and thus they lack the transmembrane domain. Created with Biorender.

C_neoVLPs were generated with neoantigens from the pancreatic adenocarcinoma mouse model (C57BL/6), the Pan02 cell line. Pancreatic cancer is one of the most highly aggressive and poorly immunogenic types of cancer, and the necessity to develop new treatment strategies against it made us reconsider and adapt the tumour model previously used (B16-F10). The pipeline used to identify and select Pan02 neoantigens included some improvements from the previous one. Despite the promising results regarding the immunogenicity of the predicted neoantigens from the B16-F10 tumour, only 7 out of 44 were able to generate specific CD8+ T-cell responses upon vaccination. Therefore, the neoantigen identification pipeline could still be refined.

1. Identification of nonsynonymous mutations in Pan02, a murine pancreatic adenocarcinoma cell line*

DNA and mRNA were prepared from Pan02 cells and C57BL/6 tissue and sequenced by WES and RNA-seq. This work was performed in collaboration with Dr Victor Guallar's group at the BSC. After sequences from WES of the tumoral cell line and healthy tissue were matched, somatic mutations were identified. Then, a list of neoantigens was predicted using the PredIG pipeline, which includes a structural filter (NOAH) and NetCleave²⁹⁴, an algorithm for predicating C-terminal antigen processing. The selected neoantigens included in the C_neoVLPs were the top 15 ranked as most immunogenic (highest score; Figure 37). Whereas in the neoantigen selection of B16-F10 only peptides of 9 amino acids (aa) long were included, in this case there was not a length restriction, and the list comprised peptides ranging from 8 to 11 aa long. Furthermore, after the selection was performed based on the algorithm immunogenicity score, the structural features of the mutations found in the neoantigens were classified in the three tiers as done previously, although in this case it was not considered as an immunogenicity criterion.

*Work carried out by the BSC

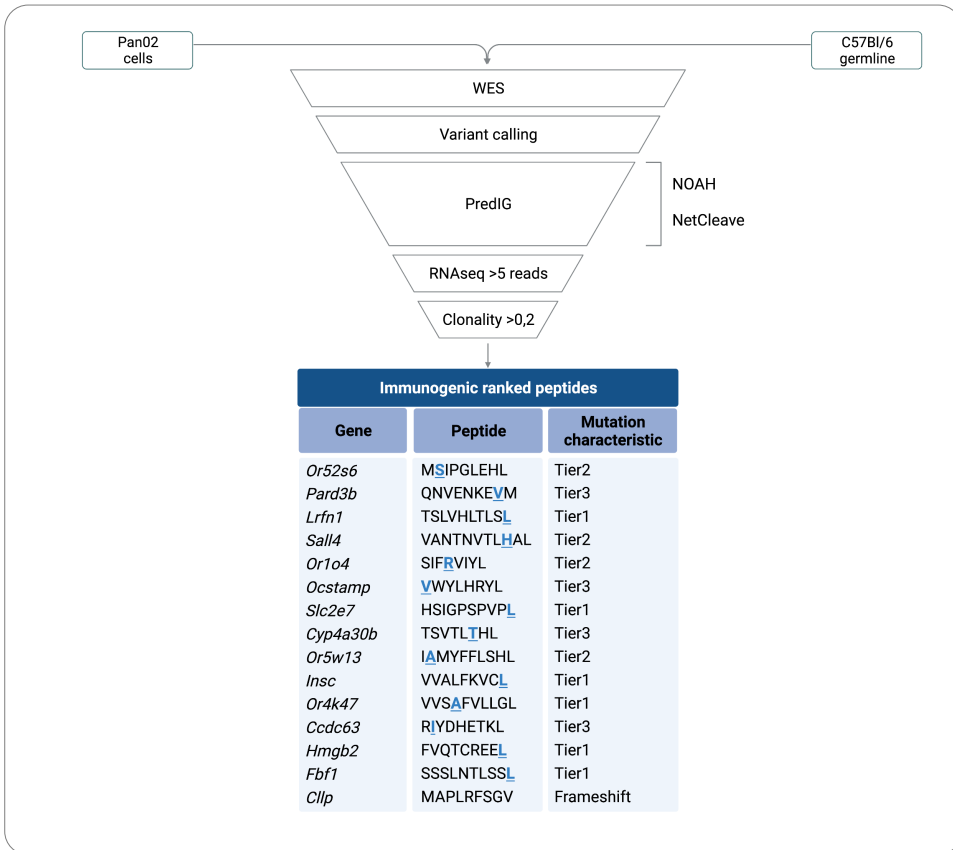


Figure 37. Scheme of the new neoantigen selection strategy. Identified somatic mutations were filtered using PredIG. Neoantigens selected were ranked according to immunogenicity score and the top 15 most immunogenic neoantigens were considered for the VLP design. Mutations present in Pan02 cells are highlighted and underlined in bold. Created with Biorender.

2. Production and characterisation of C_neoVLPs

C_neoVLPs, lacking the transmembrane domain, were engineered to increase their budding at the plasma membrane and hence promote their extracellular release. With the classical fusion-protein approach, neoVLPs were being trapped intracellularly, and a protocol to extract them had to be developed. With this second generation neoVLPs for the delivery of cancer neoantigens, their release to the extracellular medium and an increased yield were expected. Pan02 neoantigens previously selected with PredIG were loaded on both neoVLP platforms, classical and second-generation neoVLPs. In both approaches, neoantigen were concatenated and separated by linker sequences. This sequence was

Results – Section 3

either an AAA or an SSS, as described previously^{294,353}. One neoVLP and three different C_neoVLPs were designed: (i) N_Top15, containing the 15 most predicted immunogenic neoantigens at the N-terminus of the VLP fused to the Gag protein (first generation neoVLP), (ii) C_Top15 containing the same 15 neoantigens at the C-terminus of Gag (second-generation neoVLP), (iii) C_Top7 containing the first 7 among these 15 peptides (second-generation neoVLP), and (iv) C_Top8 containing the last 8 peptides of these 15 (second-generation neoVLPs; Figure 38A). As controls, two separate VLPs working as empty carriers were generated only expressing the structural Gag protein without the neoantigens. One corresponding to the NakedVLP, with the signal peptide directly fused to the Gag protein by the murine CD44 transmembrane domain and a FLAG-tag, and the other one was a VLP only expressing HIV1-Gag and a 6xHis tag (C_Gag; Figure 38A).

These constructs were then transfected into Expi293F cells and harvested 48h later, and the expression of the proteins was determined by flow cytometry (Figure 38B and C). To detect the presence of N_Top15 neoVLP at the cell membrane, we performed an extracellular staining of FLAG tag and an intracellular staining of Gag p24. A population of double positive cells could not be identified, suggesting that the fusion proteins were not reaching the cell membrane, as seen previously with the B16-F10 neoVLPs (Figure 38B). As expected, the fusion-protein was being retained inside the transfected cells, as a double positive cell population was only identified when intracellular staining of FLAG tag and p24 was performed (Figure 38C). In the case of C_neoVLPs, expressing the neoantigens at the C-terminus, we could only confirm the correct expression of the Gag protein inside the cells. Flow cytometry results show that all four C_neoVLPs, including C_Gag, were expressing the Gag and it could be detected (Figure 38C).

To determine the increased release of VLPs to the extracellular medium when using the C-terminus approach, the cell lysate and the supernatant of each transfection were analysed by western blot. Results show no detectable protein in the supernatant of the two classical VLPs, N_Top15 and NakedVLP (Figure 38D). Contrarily, we were able to detect equally or more protein in the supernatant of all C_neoVLPs compared to the cell lysates (Figure 38D). Furthermore, the levels of expression of C_Top7 and C_Top8 were considerably higher than C_Top15, indicating that probably a construct containing a higher number of neoantigens at the C-terminus is poorly translated or degraded rapidly (Figure 38D).

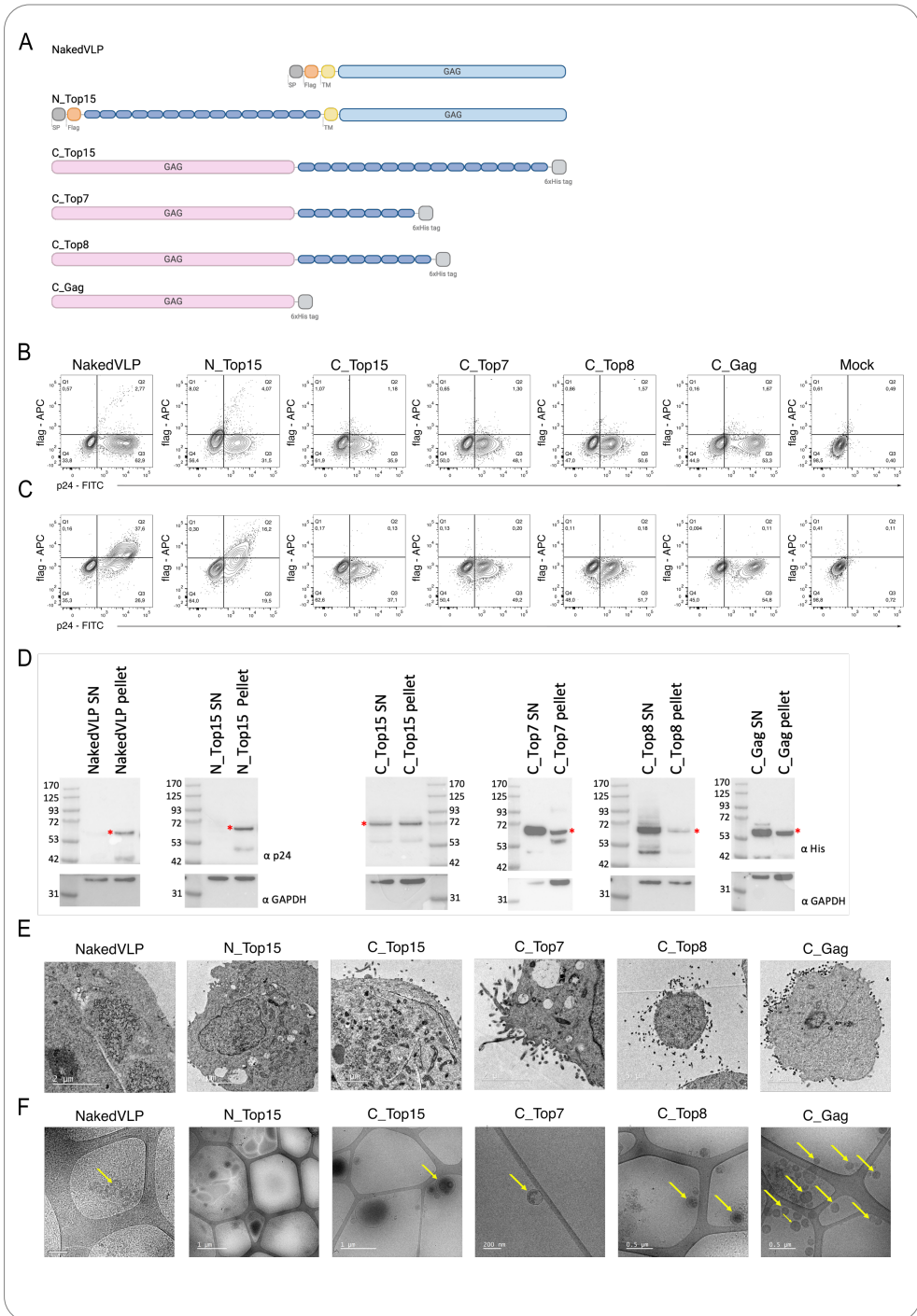


*Figure caption in the following page

Results – Section 3

To confirm if the expression of the proteins that were being detected by flow cytometry and western blot were properly assembled VLPs, we analysed the VLP producing Expi293F cells by TEM. Images showed budding events at the cellular membrane of all C_neoVLP transfections, and formation of VLPs with a lipid bilayer and a structural Gag ring could be clearly identified in all C_neoVLPs transfections (Figure 38E and F). However, as expected from results obtained from the B16-F10 neoVLPs, when analysing the formation of VLPs in the N_Top15, TEM images suggested that the VLP particles were budding from the rough endoplasmic reticulum, where the fusion proteins were being synthesised, and were accumulating perinuclearly at the cytoplasm (Figure 38E). No budding events were observed at the cellular membrane of N_Top15 nor the NakedVLP producing cells (Figure 38E), confirming the results seen in the flow cytometry and in the western blot analysis, where we could not detect p24 protein in the cell membrane nor in the supernatant, respectively.

Altogether, C_neoVLPs were being expressed and assembled properly into VLPs and were being released to the extracellular media as expected. Therefore, we decided to continue with the purification of C_Top7 and C_Top8, as results show a higher level of expression compared to C_Top15. Chosen C_neoVLPs constructs were transiently transfected in Expi293F cells and recovered from the supernatant 48h later. Supernatants from transfection were loaded onto a 30%/70% double sucrose cushion and samples were centrifuge. Then, the 30%/70% interphase was recovered and dialysed against 1xPBS, and all fractions were analysed by Coomassie blue staining and western blotting (Figure 39A). A sample clarification could be observed clearly when comparing the post-dialysed interphase with the supernatant of all C_neoVLP (Figure 39B-D), where the total protein concentration is clearly higher. Furthermore, when detecting the specific protein by western blot, result show equivalent protein bands in the supernatant compared to the dialysed 30%/70%

Figure 38. C_neoVLP-based vaccine production and purification. (A) Scheme of the linear polyprotein that generates the neoVLPs. With Gag in blue, classical neoVLPs expressing Pan02 neoantigens Signal peptide in light grey, FLAG tag in orange and TM domain in yellow. With Gag in pink, second generation C_neoVLPs carrying Pan02 neoantigens. In grey 6xHis tag. Created with Biorender. (B) Representative flow cytometry panels for the expression of neoVLP fusion proteins in transiently transfected Expi293F cells. Identification of FLAG tag at the surface of the cells and total p24-Gag. (C) Representative flow cytometry panels for the expression of neoVLP fusion proteins in transiently transfected Expi293F cells. Identification of total FLAG tag and total p24-Gag. (D) Western blot image of the cell lysate (Pellet) and the supernatant (SN) of all transfected VLPs. Asterisk indicates expected molecular weight. (E) TEM images of Expi293F cells producing neoVLP particles. (F) Cryo-TEM images of purified N_neoVLPs and C_neoVLPs.

interphase, indicating that most of the protein of interest is recovered after purification (Figure 39B-D).

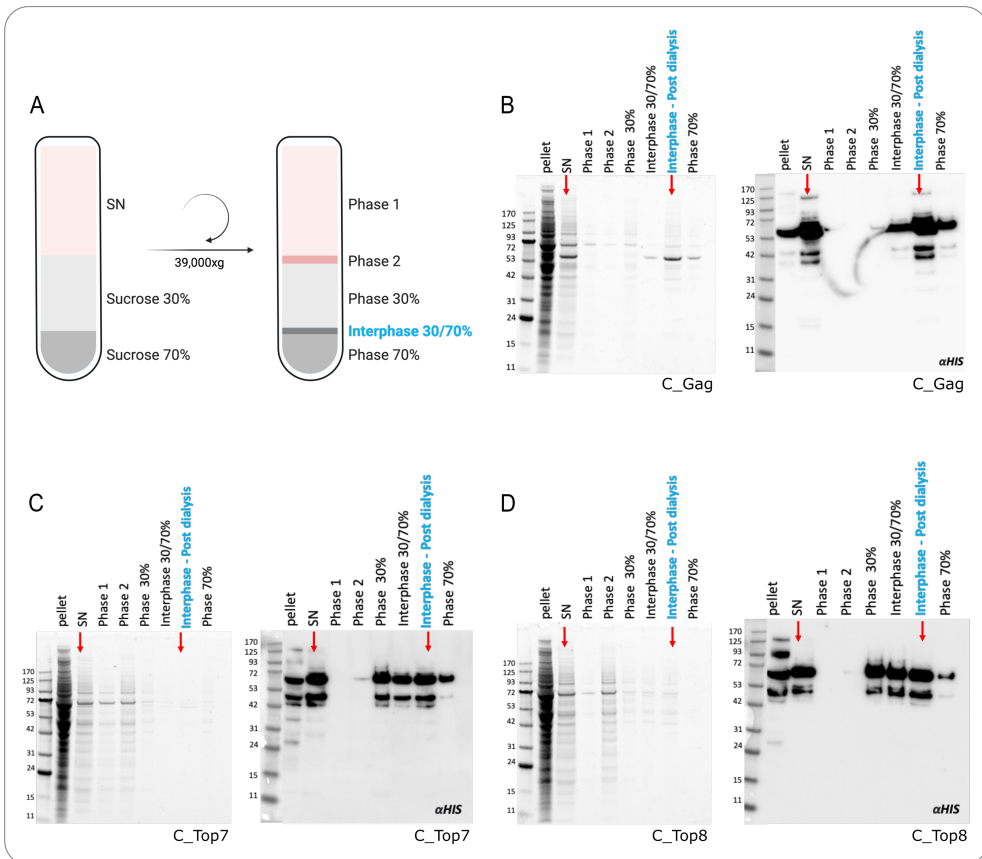


Figure 39. Optimisation of the VLP purification strategy. (A) Diagram of the sucrose cushion used for the purification and the different density phases that appear after centrifugation. Created with Biorender. (B) Coomassie blue staining and western blot analysis of all the purification steps of the C_Gag VLP production. In blue the final preparation after dialysis. (C) Coomassie blue staining and western blot analysis of all the purification steps of the C_Top7 VLP production. In blue the final preparation after dialysis. (D) Coomassie blue staining and western blot analysis of all the purification steps of the C_Top8 VLP production. In blue the final preparation after dialysis.

3. Preliminary immunogenicity assay of C_neoVLPs

To validate the new selection of neoantigens and their delivery with the second-generation neoVLPs, we performed a preliminary immunogenicity assay with only one candidate. To perform the screening assay, we select the C_Top8 as it had shown the highest expression by flow cytometry and western blot analysis. The *in vivo* assay performed

Results – Section 3

followed a homologous regime of two doses of naked DNA encoding for the neoVLP construct (Figure 40A). A homologous DNA regime was chosen as it is the most straightforward vaccination method, and it does not involve purification and formulation of a large batch of soluble neoVLPs.

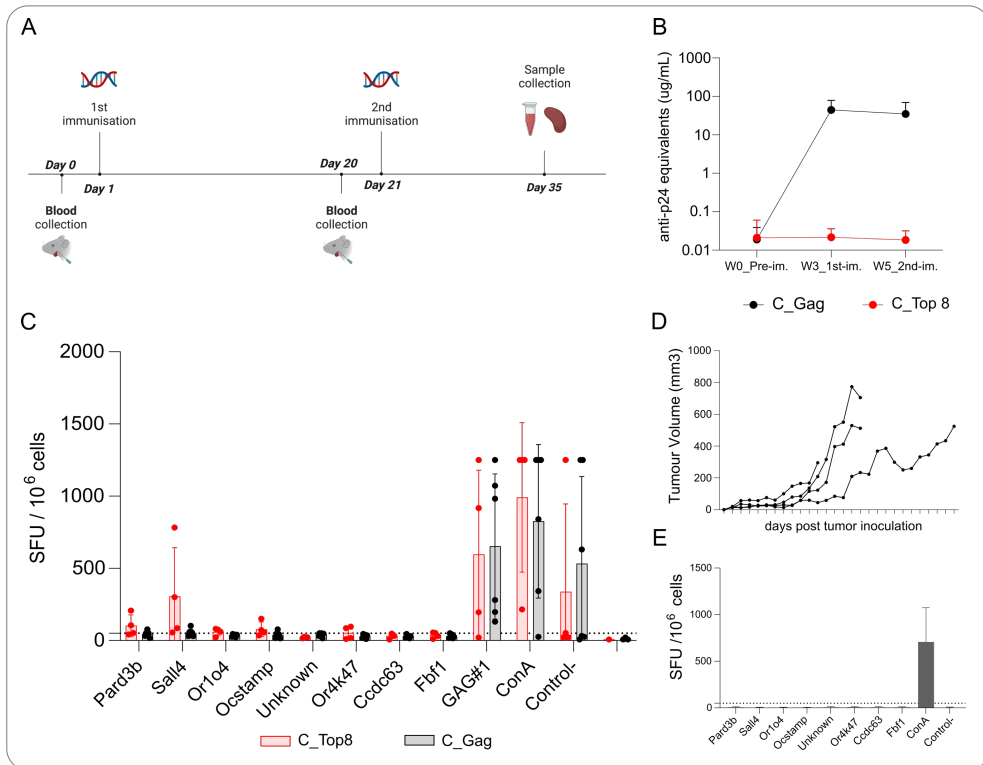


Figure 40. Preliminary immunogenicity assay of C_Top8. Schematic representation of the experimental designed used to evaluate the immunogenicity of C_Top8. Created with Biorender. **(B)** Evaluation of the humoral response against Gag. **(C)** Evaluation of the T-cell response generated upon vaccination. C_Top8 in red, C_Gag in grey in all graphs. **(D)** Tumour growth in mice inoculated with 2×10^5 Pan02 cells. **(E)** Evaluation of T-cell responses against selected neoantigens in mice inoculated with Pan02 cells.

Animals were electroporated with two doses of naked DNA as previously explained and they were sacrificed two weeks after the second immunisation. Blood and spleens were recovered and processed for further analysis. We could not detect antibodies against the HIV-1 Gag protein in the group vaccinated with C_Top8 neoVLP, probably because the protein was being degraded rapidly after synthesis and was not able to elicit a detectable humoral response (Figure 40B). On the contrary, the control group vaccinated with C_Gag

showed a peak after the first immunisation and the antibody titre was stable until endpoint, confirming the stability of empty Gag VLPs and their increased production *in vivo* (Figure 40B). To identify IFN γ -producing CD8 $^+$ T-cell responses, splenocytes from vaccinated animals were stimulated with all the individual peptides included in the C_Top8 VLP. In addition, one single pool of HIV-1 Gag overlapping peptides covering residues 314 to 412 was used as a vaccination positive control. Antigen specific CD8 $^+$ T-cell responses were detected against 2 neoantigens: Pard3b and Sall4 (Figure 40C).

To determine whether these responses detected upon immunisation were *de novo* responses or already existing T-cell specificities against the tumour, we inoculated four syngeneic C57BL/6 animals (two males and two females) with 2×10^5 Pan02 cells subcutaneously at the right flank. Mice were euthanised when the tumour volume reached 1 cm 3 and splenocytes were collected (Figure 40D). Cells were tested for CD8 $^+$ T cell activity by ELISpot, and no IFN γ producing CD8 $^+$ T cells were identified after splenocyte stimulation with the pools of peptides covering all neoantigens included in the C_Top8 (Figure 40E). These results suggest that the responses detected after immunisation were new T-cell specificities.

DISCUSSION

In the last 20 years the field of immuno-oncology has been entirely transformed with the emergence and establishment of immunotherapies as a standard approach for cancer treatment¹⁹¹. Immunotherapies harness the individual's own immune system to purposely recognise and eliminate cancer cells, as it would normally do with a viral or bacterial infection³⁶⁰. This approach represents an incredible breakthrough in the field and has allowed many patients to achieve long-term responses and even complete remission¹³⁸. However, a complete understanding of all the elements that participate in the orchestrated immune response against tumours is still needed, and despite the advances, immunotherapies do not yet represent the principal and most effective therapy for all cancer patients^{138,191}.

Among cancer immunotherapies, vaccines have become one of the most novel and promising strategies. Vaccines aim to sensitise the immune system against tumour-specific antigens and drive tumour-reactive T cells to the tumour site³⁶¹. However, when administered therapeutically, they can face significant challenges as there is a need to overcome an immune system that has been restrained by mechanisms promoting self-tolerance, which sustain tumour development³⁶¹. Other immunotherapies such as IC blockade contribute to fight this by releasing immunosuppression and halting the negative signals that limit the effector function of the immune system, but this does not have any benefit if the availability of tumour-reactive T cells is low¹⁵⁰. For that reason, vaccines are key in the development of cancer immunotherapeutic strategies as they promote T cell priming and activation with tumour antigens³⁶¹. Nonetheless, while the use of cancer vaccines has shown some benefits, the number of patients who truly benefit from such treatments, along with their overall survival rates, remain suboptimal¹³⁸. Therefore, to achieve better outcomes, it is crucial to carefully select antigens, explore and improve vaccine design regarding platform usage and delivery, and study appropriate combinations of treatment. By addressing immunosuppression mechanisms within the tumour microenvironment and stimulating or modulating the immune system in a targeted manner, the performance of vaccines can be significantly enhanced¹³⁸.

With regards to antigen selection, there has been a significant shift in the cancer vaccine field with the recent focus on neoantigens²². Advances in technologies like next-generation sequencing have made it possible to examine all somatic mutations in tumour cells to predict highly immunogenic neoantigens, that are completely tumour-specific¹²³. Unlike

Discussion

tumour-associated antigens, neoantigens are commonly unique to each patient and thus their identification must be personalised²². The generation of neoantigen-specific T cells that contribute to tumour elimination upon vaccination has been demonstrated repeatedly, both in animal models and in clinical trials, and there is considerable evidence supporting efficacy, safety and potential of neoantigen vaccines^{244,247,301,303,308,362–366}. In this context, neoantigens from the B16-F10 and the Pan02 cell lines were chosen as appropriate immunogenic candidates to test on the design of our neoVLPs.

Virus-like particles represent a suitable platform for the display of vaccine antigens^{309,310}. VLPs are virus-mimicking structures made up of one or more structural proteins capable of self-assembly³⁰⁹. They imitate the size and form of actual viral particles, but they lack the genetic material, rendering them incapable of infecting host cells³⁰⁹. VLPs are becoming increasingly popular in the field of preventive medicine. To date, besides the FDA approved VLP-based vaccines^{367–369}, several candidates are being explored against infectious agents and solid tumours^{370–376}.

Among the different structural proteins that VLPs can take advantage from, the HIV-1 Gag polyprotein is one of them³¹⁷. HIV-1-based VLPs can self-assemble from the sole expression of the p55 Gag protein and are able to accommodate different antigens on their surface³¹⁷. On this basis, we aimed to display the selected cancer neoantigens on the surface of our VLP design by fusing the neoantigen-polypeptide to the HIV-1 Gag protein through a transmembrane domain and a linker sequence. Our group had previously demonstrated the successful development of these fusion-protein HIV-1 based VLP platform expressing a high density of immunogens on the surface³²¹. These VLPs were produced, purified and able to elicit a potent and functional humoral response in a mouse model³²¹. Furthermore, following the same rationale, novel fusion-protein VLPs were produced using the structural Gag protein from the Feline Leukaemia Virus (FeLV) that confirmed a strong elicitation of T-cell responses³²². In the present work, we aimed to apply this knowledge and generate functional HIV-1-based Gag VLPs expressing on the surface the predicted immunogenic neoantigens from the B16-F10 and Pan02 cell lines.

Optimisation of the VLP design involved studying the spacer sequences that would separate neoantigens in the polypeptide fused to the Gag protein. Epitope flanking sequences strongly influence peptide processing by proteasomes and understanding the proteasome cleavage mechanisms can be extremely helpful when predicting possible

epitopes^{329,377,378}. In a cancer vaccine context, it can be determining on the processing and MHC-I presentation of neoantigens, especially in RNA or DNA-based vaccines, where peptides are concatenated in single molecules. Velders and colleagues demonstrated the impact that linker sequences can have on the induction of a CTL response in a DNA vaccine³⁷⁹. They generated two constructs that only differed in the presence or absence of linker sequences separating the epitopes³⁷⁹. While vaccination with the construct that did not include defined epitope spacers resulted in protection of 50% of tumour challenged mice, 100% of mice were protected when the vaccine construct had the epitopes spaced by linkers³⁷⁹. They concluded that vaccination with a DNA vaccine adding defined spacers to separate epitopes benefits the peptide processing and presentation, and in turn results in better anti-tumour immunity³⁷⁹.

Here, five different linker sequences used to separate neoantigens were compared, and their effect in peptide processing and presentation was analysed. Five different constructs were designed expressing 13 irrelevant neoantigens with the SIINFEKL epitope in the centre as a reporter peptide. Neoantigens were spaced by five different linker sequences: AAA, AAL, ADL, A and GGGG. The expression of the protein was determined by western blotting, and detection of all proteins was only achieved when the cells were incubated with a proteasome inhibitor. The construct with a single alanine linker was not detected unless the proteasome was inhibited. These results suggested that the protein was being degraded very rapidly after its synthesis, but it does not necessarily correlate with a more efficient MHC-I presentation of the target peptide. When analysing the SIINFEKL/MHC-I complexes on the surface of cells, the construct containing a single alanine as linker did not significantly increase the presentation of the SIINFEKL peptide compared to the rest. This shows that a rapid processing does not necessarily translate into an enhanced presentation, suggesting that the proteasome could be cleaving the protein in unexpected sides and thus, generating different peptides from the expected ones.

When analysing the MHC-I/SIINFEKL I complexes on the surface of transfected cells, constructs where epitopes were spaced by alanine-based sequences were being presented more efficiently on the MHC-I molecules, and hence more MHC-I/p complexes were being detected on the cell surface. This was confirmed when we analysed the functionality of the peptide presentation in a T-cell activation and proliferation assay with splenocytes from OT-I mice. These cells, containing engineered TCRs that recognise specifically SIINFEKL bound to

Discussion

the MHC-I, were co-culture with cells transfected with each of the different constructs. We wanted to confirm that the MHC-I/p complexes detected on the surface of transfected cells could stimulate T cells. Results showed a higher T-cell activation and proliferation when OT-I splenocytes were co-cultured with transfected cells expressing constructs where neoantigens were spaced by alanine residues, confirming the results obtained previously. This is not the first time that alanine flanking sequences are shown to promote epitope processing and T-cell recognition. Koszinowski and colleagues demonstrated that flanking an epitope with oligo-alanines could increase the yield of antigenic peptides generated³⁸⁰. They inserted a known antigenic sequence in different positions within a carrier protein and analysed the recovery of peptides processed by the cells. When the insert was in an unfavourable area where the processing of the optimal antigenic peptide could be expected to be lower, this was reverted by separating the epitope from the neighbouring sequences with alanine residues. This resulted in an increased recovery yield of the tested peptide³⁸⁰. In a separate study, they compared the processing and presentation of minigenes with or without alanine spacers. The presence of flanking sequences with alanine residues resulted in an improved yield of the final antigenic peptides³⁸¹.

Taken together, we performed a comparative analysis of five different peptide flanking sequences and evaluated their impact on antigen processing and presentation. Moreover, as our constructs contained a transmembrane domain and hence, were surfaced expressed, they could require extra processing and transport steps, which could affect protein availability for proteasomal processing and epitope presentation. For that reason, we also compared the five same linker sequences with intracellularly expressed polypeptides, and confirmed the results obtained. Our data suggest that linkers based on alanine residues would allow more efficient processing and presentation of the peptides compared to linker sequences containing combinations of glycine and serine.

After selecting the optimal spacer, we proceeded to assess how the position of the peptide and the flanking sequence within the polypeptide molecule affected peptide processing and presentation efficiency. Initially, our results showed that despite the peptide being presented regardless of its position in the polypeptide, its presentation was reduced when located at the N-terminal portion of the polypeptide. On the contrary, peptides from the centre to the C-terminus of the molecule were presented to a similar higher level. However, re-arrangement of the peptides at the N-terminus of the molecule showed that

the amino acid environment surrounding the peptide might be more relevant than the position in the polypeptide sequence for peptide processing and presentation through the MHC-I pathway. This information should be taken into consideration for the design of neoantigen-based polypeptide or the evaluation of their immunogenicity.

Altogether, epitope flanking sequences can have a decisive role in processing and presentation efficiency, and thus it should be taken into consideration when designing polypeptide vaccines. Proteasomes do not always cleave molecules on the same sites, if it was like this, every time a protein was degraded a set of repeated non-overlapping peptides would be generated³⁸². Contrarily, proteasomes generate a wide set of overlapping peptides that cover the entire protein³⁸². This means that an antigenic peptide will not necessarily be produced each time an antigen molecule is degraded, therefore adding spacers that force cleavage sites can help get desired outcomes and enhance the presentation of the epitopes of interest, in this case neoantigens. Taken all together, proteasomal degradation is a decisive step that can modulate the immune surveillance of T cells and therefore the immune response elicited against specific targets.

Having selected the linker sequences to concatenate neoantigens in the polypeptide and having observed a relatively low impact of peptide position in presentation and T-cell activation, we proceeded to produce the full-length Gag-based VLPs expressing a high-density of neoantigen-polypeptides on their surface. In total, 4 neoVLPs plus a NakedVLP (working as a vehicle) were produced and purified. The candidates were selected based on confirmed expression of VLPs by flow cytometry staining of the producing cells, optimal detection of all the proteins by western blotting, and VLP visualisation by TEM and Cryo-EM.

NeoVLPs were designed based on the previous fusion-protein VLPs engineered by the group. Tarrés-Freixas *et al.* showed the successful production and purification of a MinGag VLP, a Gag-based VLP expressing an HIV antigen on the surface³²¹. Similar to MinGag VLPs, neoVLPs were designed with a signal peptide at the N-terminal to translocate the protein to the cell membrane and promote its budding. Contrarily to regular Gag-VLPs, which are produced in the cytosol and migrate to the membrane directly, neoVLPs are most probably synthesised in the ER and migrate to the membrane through Golgi. However, 48h post-transfection, fusion-proteins were being retained inside the ER and could not migrate to the membrane to be released. This was observed first by flow-cytometry staining of the Gag

Discussion

protein, that could not be detected at the cell membrane. It was also confirmed by the TEM analysis on the VLP-producing cells, where neoVLPs could be seen inside the cells and no budding events were observed on any of the producing cells. For that reason, neoVLPs had to be extracted from within cells and could not be purified directly from the supernatant. Extraction of neoVLPs from inside the cells adds more steps to the purification process and increases the quantity of possible contaminants. The extracted fraction of neoVLPs was further purified by ion-exchange chromatography (with a size-exclusion effect). Ion-exchange chromatography is a suitable technique to purify neoVLPs as most phospholipids are negatively charged at physiological pH and thus neoVLPs budding from the host cell generating a phospholipid bilayer will have a negative net charge³⁸³. The size-exclusion effect contributes to separate neoVLPs from other extracellular vesicles. However, the purity of the final preparation was not as optimal as desired, as the presence of host cell proteins and other contaminants was still high. For that reason, an improved purification protocol was developed, loading the extracted VLP fraction on top of a 30%-70% double sucrose cushion and concentrating the VLPs by ultracentrifugation. Then, the recovered VLP fraction was dialysed to remove the sucrose excess and the ratio of Gag/total protein was determined. VLPs purified by ultracentrifugation (UC) showed an increased ratio of Gag/total protein, indicating higher purity. From then onwards, this protocol was used to purify the second-generation C_neoVLPs. Despite this, other contaminants such as extracellular vesicles are probably being recovered as well from the UC density ring, and a second purification step would be necessary. Separating VLPs from extracellular vesicles is probably one of the biggest challenges in the downstream process of VLP production. Steppert *et al.* developed a protocol where clarified and filtered cell culture supernatants containing HIV-1 VLPs were purified using strong anion-exchange monoliths³⁸³. They succeeded in eluting most particles achieving a 90.9% depletion of host cell proteins³⁸³. Hence, adding an anion-exchange chromatography after the UC could result in more pure yields and better recovery ratios, and it could be explored in the future to purify neoVLPs. Nonetheless, in a personalised vaccine application, delivering neoVLPs as purified soluble particles is probably not the most adequate approach. In a personalised vaccine context, each neoVLP developed will be different and will require a large-scale production and purification. For that reason, a high throughput purification protocol that results in a high concentration of particles in a very pure formulation would need to be optimised for every

neoVLP developed. Therefore, a delivery system based on nucleic acid-based vaccines coding for the neoVLPs is probably more adequate. Up until now, we have successfully tested the delivery of our neoVLPs as a DNA-based vaccine, despite the limitations regarding a possible inefficient uptake from somatic cells when DNA is administered naked. To overcome that, DNA needs to be electroporated or administered encapsulated by liposomes³⁸⁴. Tarrés-Freixas *et al.* developed a DNA electroporation protocol with a luciferase-encoding plasmid and reported a 3-log higher production of bioluminescence after electroporation compared to regular administration, and the stable expression of luciferase up until 3 months post electroporation. Following this protocol we confirmed the correct electroporation of DNA-based neoVLPs and their optimal expression *in vivo*. However, and more so after the COVID19 pandemic, mRNA vaccines have emerged as powerful alternatives to DNA-based approaches due to their high effectiveness, cost-effective production, and safe delivery³⁸⁵. Recent technological advances, forced by the Sars-CoV-2 pandemic, have resolved the challenges regarding their potential instability and inefficient delivery, making mRNA vaccines the newest and most promising vaccine delivery system³⁸⁵. Pivoting towards mRNA vaccines in the context of neoVLPs would be the optimal strategy and thus, personalised neoVLPs would not require a systematic large-scale production and purification.

Further characterisation of VLPs included cryo-EM analysis of purified VLPs, and it revealed an expected rounded-shape morphology with an identified electron-dense core formed by the p55 Gag protein for all neoVLPs, similar to the ones observed in regular Gag VLPs^{383,386,387}. This confirms that the presence of neoantigens can allow the correct generation of Gag-based VLPs. Taken together, fusion-protein neoVLP constructs assembled into well-formed VLPs that were expected to be displaying the neoantigens on the surface. Flow-cytometry staining targeting the FLAG-tag at the N-terminal of the protein showed the detection of the FLAG-tag at the surface of producing cells and intracellularly most probably co-localised with the Gag protein, which suggests the correct expression of neoantigens located C-terminal from the FLAG-tag.

Considering all the results, 4 neoVLPs expressing the selected neoantigens and 1 NakedVLP working as an empty carrier were selected to test their immunogenicity *in vivo*, in the C57BL/6 mouse model. We performed an experiment comparing homologous (DNA/DNA or VLP/VLP) and heterologous regimens (DNA/VLP) and analysed the T-cell

Discussion

response generated against the Gag protein. The combination of two delivery strategies of the same immunogen has been demonstrated to elicit higher responses^{321,388}. As seen previously, higher T-cell responses were obtained when the VLP administration was a combination of DNA and purified particles. Thereupon, all the immunisations were performed following a heterologous regime.

After the immunisation with the selected neoVLPs, the humoral response against HIV-1 Gag protein was evaluated by ELISA. Anti-Gag antibodies were detected after the DNA prime in all immunised groups, and a clear effect of the purified VLP boost was observed. In parallel, CD8+ T-cell responses were analysed by ELISpot. Splenocytes from vaccinated mice were stimulated overnight with all the neoantigens included in the neoVLPs. In total, 7 positive responses were detected out of the 44 prioritised neoantigens. This correlates with the prediction accuracy observed in different neoantigen identification pipelines using the C57BL/6 mouse model which tends to be around 20-30%^{349,366}. Unfortunately, the accuracy of neoantigen prediction in humans from mutations identified by exome sequencing is still very low, typically around 5%³⁸⁹⁻³⁹³.

Furthermore, none of the positive neoantigens belonged to the Tier1 neoantigen class. Neoantigens from the Tier1 classification presented mutations in HLA anchor residues which increased their binding affinity. Peptides selected from this group acquired HLA presentation through mutations, and their WT counterpart should not be presented in HLA molecules because they lacked the anchor residue needed. HLA-binding affinity is probably one of the dominant contributors to neoantigen immunogenicity and currently it represents one of the primary factors of peptide prioritisation. For that reason, Tier1 predicted neoantigens were expected to be the most immunogenic, but none of these 12 neoantigens were able to generate detectable responses. Interestingly, 6 out of the 7 positive neoantigens belonged to the Tier2/Tier3 classification, which comprised neoantigens with high HLA binding affinity that had acquired mutation in exposed residues which could be in contact with the TCR, and thus be involved in TCR recognition. These peptides were prioritised according to the structural features of the mutated residues, and all presented high affinity for HLA molecules. Acquired mutations in these peptides were located in the TCR contact surface and probably modified recognition by cognate T cell clones, which could result in higher immunogenicity compared to Tier1 neoantigens. These results highlight the importance of including TCR recognition in neoantigen selection pipelines. *In silico* prediction algorithms

primarily focus on MHC-I binding, which probably represents the most selective and comprehensively understood step in antigen presentation^{292,394}. Some of these tools also take advantage of other processes such as peptide cleavage and transport²⁹⁴, gene expression and clonality to refine and enhance the accuracy in neoantigen prediction. However, it is well known that not all peptides presented by MHC molecules will trigger T cell activation³⁹⁵, therefore being able to determine which MHC/p complexes will be recognised by TCRs is a crucial step. Several approaches have been developed to try to predict MHC-peptide-TCR binding such as TCRex, NetTCR or Repitope^{396–398}. TCRex, for example, is based on a machine learning algorithm that analyses common patterns among different TCRs that have the same specificity for an epitope³⁹⁷. In contrast, Repitope recapitulates the concept of epitope immunodominance and hypothesises that epitopes targeted by different individuals with different T cell repertoires have probably some intrinsic patterns that increase their probability to be recognised by different TCRs³⁹⁸. This rationale could be adapted in the neoantigen selection strategies and study inherent characteristics from predicted neoantigens that have been proven immunogenic and study if the occurrence of these characteristics can help predict immunogenicity. This approach has been followed by Gfeller and colleagues when developing PRIME, a predictor of immunogenic epitopes that correlates neoantigen prioritisation with T-cell potency and provides insights into the biophysical factors governing T-cell recognition³⁹⁴.

Another question that arises from evaluating these results is the possibility of the different filters applied in the neoantigens selection pipelines becoming limitations. A clear example of these was filtering the selection of peptides only focusing on minimal epitopes (9-mers) which correspond to peptides bound to MHC-I, disregarding MHC-II binding peptides. Selecting short or long neoantigens is still an open question in the field and there is not a clear consensus. Using short sequences ensures MHC-I binding, which can lead to TCR recognition and the generation of a functional CD8+ T-cell response capable of eliminating tumour cells^{399–402}. Vaccination with a mixture of short peptides induces CD8+ T-cell responses in patients⁴⁰³. However, using short peptides can have several limitations. If the peptide is too short, it can bind exogenously to the MHC-I molecule of both professional APC and other cell types⁴⁰⁴. The presentation of peptides without appropriate co-stimulation and bypassing intracellular processing and presentation can be tolerogenic and hence, lead to T cell anergy⁴⁰⁴. Furthermore, shorter peptides tend to be HLA-restricted,

Discussion

which does not represent the high polymorphisms of HLA molecules in the population. This can be a problem when developing “off-the-shelf” vaccines, as the peptides selected would ideally be recognised by different HLA allotypes. On the other hand, long peptides must be internalised and processed by the proteasome, which will not always necessarily result in the presentation of the identified epitope. Despite this, internalised and processed long peptides can be cross-presented to CD8+ T cells and presented in MHC-II molecules to be recognised by CD4+ T cells, what elicits a complete CTL response⁴⁰⁵. Moreover, long peptides are not HLA-restricted and thus they allow for a wider population coverage of HLA-types⁴⁰⁵. For that reason, nowadays the most common neoantigen-based immunogens include identified CD8 epitopes surrounded by an extension of up to 25-30 aa long, to include CD4 possible epitopes⁴⁰⁶. In our case, filtering the selection of peptides included in our neoVLPs to CTL minimal epitopes and considering only 9-mers can be a limitation. Not regarding the induction of tolerance because of an inappropriate presentation, as our neoVLPs will be internalised by APCs and peptides should be cross-presented to CD8+T cells, but because of the lack of CD4+ T cell epitopes. CTL activation in the absence of CD4+ help can result in T cell dysfunction, for that reason adding helper epitopes in neoantigen vaccines can promote CTL responses with the suitable help. Despite this, there is a possibility that CD4+ T cell are being primed and activated upon vaccination, and this could be explored by performing an immunophenotyping of the splenocytes recovered and exploring if the IFN γ production observed in the ELISpot is being released only by CD8+T cells or also by CD4+ T cells.

Finally, something to take into consideration when selecting neoantigen-specific T cells is the low percentage of reactive-T-cell clones available in fresh single-cell suspension such as splenocytes and thus, the sensitivity limit of the techniques used to detect them⁴⁰⁷. Despite ELISpot being a highly sensitive technique, there is a possibility that the number of clones reactive to certain neoantigens was too low to be detected. To overcome this, T cell enrichment strategies have been developed to try to enrich the neoantigen T-cell population prior to analysis. Some examples are detecting the neoantigen T-cell population by identification of surface marker expression, isolating individual T-cell clones via multimer staining or expanding a whole neoantigen T-cell population by sensitisation, co-culturing them with loaded APCs⁴⁰⁷. This could be an interesting approach to consider for further experiments analysing the T-cell response against neoVLPs.

After analysing the CD8+ T-cell response and confirm that our neoVLPs were able to elicit *de novo* T-cell responses against the neoantigens included, we performed a tumour challenge experiment administering the candidate neoVLPs (Tier2-GAG) as a prophylactic vaccine. Two weeks after the second vaccine dose, we inoculated the animals with B16-F10 cells and followed tumour growth. We wanted to determine if the response elicited after immunising with neoVLPs was potent enough to control tumour development. We included a group vaccinated with neoVLP plus and adjuvant, MPLA, to evaluate if the response could be enhanced when administered with an adjuvant. Results showed a similar neoantigen-specific CD8+ T-cell response in all vaccinated groups, and no significant differences could be observed when animals were vaccinated with or without adjuvant.

Additionally, three animals did not develop a detectable tumour, one animal vaccinated with neoVLPs and two animals vaccinated with the adjuvanted neoVLPs. The B16-F10 tumour model is considered a non-immunogenic and immune suppressive tumour, and in our case once the tumour was established it did not elicit any detectable CD8+ T-cell response against the selected neoantigens. The immune profile of the B16-F10 tumour model is characterised by a poor T-cell infiltration, decreased expression of chemokines and cytokines and a downregulation of adaptive immune-related genes⁴⁰⁸. Furthermore, it presents an upregulation of CTNNB1 (b-catenin), which is linked to the suppression of chemokine production from tumour cells and a reduced T-cell infiltration⁴⁰⁹. Despite this fact, vaccination with our neoVLPs was able to prevent tumour development in 3 out of 16 animals as monotherapy, i.e. not combining the vaccination with any immune-modulators or ICI therapies. Probably, to confirm the potential of our neoVLPs, vaccination should be administered in a therapeutic context. Animals are vaccinated once the tumour has been inoculated and established, mimicking a natural cancer progression. In this situation, a poorly infiltrated and immune-suppressive tumour will escape immunosurveillance and grow uncontrollably unless vaccination is effective. Moreover, the anti-tumour potential of neoVLPs could be tested in combination with other immunotherapies such as ICI. It could be happening that neoVLPs can elicit neoantigen-specific T-cell responses, but these activated T cells cannot infiltrate the tumour. Priming tumour reactive T cells will not be effective if these cannot penetrate the tumour, or if the tumour is highly immunosuppressive and has a low expression of inflammatory cytokine or a downregulated MHC-I presentation. Combining vaccination with an ICI therapy will probably potentiate the effect of the vaccine

Discussion

and result in better outcomes. Furthermore, in a therapeutic context, tumours can enter a phase of equilibrium compared to tumours that completely escape the immune response. Comparing and visualising the T-cell infiltration and distribution of TILs in these kinds of tumours by microscopy would also be interesting to explore post-vaccination.

The production of neoVLPs also presents some limitations. The polypeptide of concatenated neoantigens fused to the Gag protein lacks a secondary structure, this hampers the proper expression of the protein that is probably subjected to a higher level of degradation. In addition, RNA and protein half-life will depend on the order of the peptides in the polypeptides. If this vaccine platform aims to become a delivery system for personalised neoantigens, the production of the proteins needs to be optimised and highly effective. The fact that the impact of secondary structure in the polypeptide stability is hard to predict can become problematic to upscale this platform as it has great effect on the VLP formation. For that reason, we developed a second generation VLPs where the neoantigens are expressed at the C-terminal of the protein. This results in the synthesis of the neoantigens after the Gag proteins has been fully synthesised, guaranteeing the full expression of the Gag protein, indispensable for the VLP assembly. Furthermore, not having the neoantigens expressed on the VLP surface allows for the elimination of the transmembrane domain that linked the fusion-protein, and that we think contributed to retain the VLPs intracellularly. With this changes, the second generation of C-neoVLPs are expected to express the neoantigens in the core of the particle, and to be released to the extracellular media. Purifying VLPs from the extracellular media instead of extracting them from within cells reduces drastically the presence of contaminants in the sample.

C_neoVLPs were produced with neoantigens from the Pan02, a murine pancreatic adenocarcinoma cell line. Until then we had worked with the B16-F10 melanoma cell line, which is one of the most investigated tumour models in mice and very established⁴¹⁰. Despite this, pancreatic cancer represents one of the most aggressive types of cancer and the 85% of diagnosed patients have a survival rate lower than 5 years⁴¹¹. Furthermore, many patients are diagnosed at later stages, which hinders the effective treatment and categorises most tumours as incurable. This type of cancer is also characterised by a high resistance to chemotherapy. Therefore, the necessity to develop novel and effective therapies has arisen, and immunotherapies represent an optimal approach.

Three C_neoVLPs were produced containing the 15 most immunogenic neoantigens predicted. A fourth classical VLP was also produced for comparison, containing the 15 neoantigens at the N-terminal of Gag. All VLPs were produced in Expi293F cells and the pellets and supernatants from the transfections were recovered after 48h. Analysis of the supernatants of all three C_neoVLP by western blotting showed that they were being released effectively to the extracellular media compared to the N-terminal classical neoVLPs. However, the C_Top15 was being expressed at much lower levels, probably because these C_neoVLP had 15 peptides in total, and the expression of a bigger concatenated polypeptide diffculted the generation of fully formed VLPs. This was also confirmed by the TEM analysis, where less budding events were being detected on the C_Top15 producing cells, compared to the C_Top7 and C_Top8. Most probably, HIV-1 Gag based VLPs have a maximum number of aa they can tolerate without compromising VLP assembly. Results obtained suggest that addition of polypeptides ranging around 70-80 aa are well incorporated, and longer additions below 150 aa should be thoroughly investigated. There is a possibility that the protein is being degraded due to the unknown structure the polypeptide chain has, but it is also possible that the particles are not self-assembling successfully due to steric hindrance at the core of the particle. Steric hindrance can occur when large amino acids obstruct the proper arrangement of the protein's secondary structure, preventing the correct folding into its native conformation⁴¹². Therefore, polypeptide secondary structures should be considered when displaying the neoantigens in a specific order, and probably exploring linker sequences to separate peptides can also help reduce steric restrictions⁴¹². In some cases, it can also be addressed by reducing the antigen content⁴¹³, for example, generating VLPs by the co-transfection of constructs fused to the polypeptide and constructs expressing only HIV-1 Gag protein. In that way, only a known proportion of structural Gag proteins will be expressing the neoantigens at the C-terminal. This could be investigated for C_neoVLPs but a possible decrease in immunogenicity due to the reduction in antigen content should be taken into consideration.

One candidate, the C_Top8, was chosen to screen the immunogenicity of the Pan02 neoantigens through their delivery loaded on second-generation neoVLPs. We wanted to perform a preliminary assay to confirm the correct formation of the C_neoVLPs *in vivo* and their capacity to generate a neoantigen-specific CD8+ T-cell response. Animals were

Discussion

immunised with two doses of electroporated naked DNA. Two weeks after the second immunisation animals were euthanised and spleens recovered as previously explained.

The humoral response against the Gag protein was evaluated by ELISA. Only detectable antibodies against Gag were detected in the control group, where animals were vaccinated with C_Gag VLP. Animals vaccinated with the C_Top8 VLP did not elicit a humoral response against the structural Gag protein probably because the neoVLPs was being degraded very rapidly after its synthesis *in vivo*. Splenocytes were stimulated overnight with the 8 neoantigens included in the neoVLP and neoantigen-specific CD8+T cells producing IFN γ were detected by ELISpot. Two neoantigens elicited detectable responses, Pard3b and Sall4. Both peptides were categorised in the Tier2 and Tier3 classification according to the structural features of the mutated residues. Both had mutations in exposed residues that are probably in contact with the TCR and thus can mediate TCR recognition. This observation is consistent with the results obtained with B16-F10 neoantigens and reinforces the idea of needing to include T-cell recognition and binding in neoantigen prediction tools.

While in the B16-F10 neoantigen selection all peptides were 9-mers because of a length restriction filter applied, in this case one peptide was 9 aa long and the other one was 11 aa long. It is certain that traditionally MHC-I binding prediction tools have mainly focused on 9-mers but it has been demonstrated that peptides of other lengths can bind to MHC-I molecules and elicit a potent T-cell response⁴¹⁴. Hence, when considering peptides of all lengths in personalised neoantigen prediction tools, these need to reflect two aspects: the ability of different MHC specific alleles to bind to different length peptides; and the availability and frequency of different length peptides generated by the processing and presentation machinery⁴¹⁴.

CONCLUSIONS

Objective I: To design neoantigen concatenated polypeptide sequences that enhance antigen processing and MHC-I presentation.

The neoantigen concatenates were successfully designed and screened. Alanine-based linkers used as neoantigen spacers promoted enhanced functional presentation in MHC-I molecules.

Objective II: To adapt the HIV-1 Gag-based VLP platform to display concatenated neoantigens by optimising the design and production of Gag-neoantigen fusion proteins.

Novel neoVLPs expressing cancer neoantigens on their surface were successfully produced, confirming the adaptability of the VLP platform to a cancer context. Furthermore, a second-generation of neoVLPs was designed where neoantigens were expressed at the C-terminal of the HIV-1 Gag protein, promoting their release to the extracellular media.

Objective III: To test the immunogenicity of neoVLPs in a mouse model, assessing their capacity to generate detectable neoantigen-specific T-cell responses.

NeoVLPs induced a potent CD8+ T-cell response in C57BL/6 mice against 7 out of the 44 neoantigens included in the tested neoVLPs. The majority of immunogenic neoantigens showed mutations in exposed residues predicted to mediate TCR recognition.

Objective IV: To study the antitumoral efficacy of neoVLP vaccination in a tumour challenge in vivo experiment in a mouse model.

The neoantigen-specific CD8+ T-cell responses elicited upon vaccination could delay the growth of the B16-F10 melanoma tumour in C57BL/6 mice compared to the control group. Moreover, 3 animals were able to completely eliminate inoculated B16-F10 cells and did not develop a detectable tumour by endpoint.

DISSEMINATION



Publications related to this thesis project

Barajas, Ana*, Armengol, Pep*, *et al.* VLP-mediated delivery of structure-selected neoantigens demonstrates immunogenicity and antitumoral activity in mice. *In preparation* (2023).

Aguilar-Gurrieri, C*., **Barajas, A***, Rovirosa, C. *et al.* Alanine-based spacers promote an efficient antigen processing and presentation in neoantigen polypeptide vaccines. *Cancer Immunol Immunother* 72, 2113–2125 (2023). <https://doi.org/10.1007/s00262-023-03409-3>

Publications related to other projects

Ortiz R, **Barajas A**, Pons-Grífols A, Trinité B, Tarrés-Freixas F, Rovirosa C, Urrea V, Barreiro A, Gonzalez-Tendero A, Cardona M, Ferrer L, Clotet B, Carrillo J, Aguilar-Gurrieri C, Blanco J. Exploring FeLV-Gag-Based VLPs as a New Vaccine Platform-Analysis of Production and Immunogenicity. *Int J Mol Sci.* 2023 May 19;24(10):9025. doi: 10.3390/ijms24109025. PMID: 37240371; PMCID: PMC10219511.

Tarrés-Freixas F, Aguilar-Gurrieri C, Rodríguez de la Concepción ML, Urrea V, Trinité B, Ortiz R, Pradenas E, Blanco P, Marfil S, Molinos-Albert LM, **Barajas A**, Pons-Grífols A, Ávila-Nieto C, Varela I, Cervera L, Gutiérrez-Granados S, Segura MM, Gòdia F, Clotet B, Carrillo J, Blanco J. An engineered HIV-1 Gag-based VLP displaying high antigen density induces strong antibody-dependent functional immune responses. *NPJ Vaccines.* 2023 Apr 6;8(1):51. doi: 10.1038/s41541-023-00648-4. PMID: 37024469; PMCID: PMC10077320.

Trinité B, Tarrés-Freixas F, Rodon J, Pradenas E, Urrea V, Marfil S, Rodríguez de la Concepción ML, Ávila-Nieto C, Aguilar-Gurrieri C, **Barajas A**, Ortiz R, Paredes R, Mateu L, Valencia A, Guallar V, Ruiz L, Grau E, Massanella M, Puig J, Chamorro A, Izquierdo-Useros N, Segalés J, Clotet B, Carrillo J, Vergara-Alert J, Blanco J. SARS-CoV-2 infection elicits a rapid neutralizing antibody response that correlates with disease severity. *Sci Rep.* 2021 Jan 28;11(1):2608. doi: 10.1038/s41598-021-81862-9. PMID: 33510275; PMCID: PMC7843981.

Poster presentations

Barajas, Ana; Aguilar-Gurrieri, Carmen; Rovirosa, Carla; Ortiz, Raquel; Urrea, Victor; de la Iglesia, Nuria; Clotet, Bonaventura; Blanco, Julià; Carrillo, Jorge. Short alanine-based spacers included in poly-neoantigen vaccines improve peptide processing and presentation to CD8+ T cells. **EACR Defence is the Best Attack: Immuno-Oncology Breakthroughs. Barcelona 2023.**

Aguilar-Gurrieri, Carmen; **Barajas, Ana**; Rovirosa, Carla; de la Iglesia, Nuria; Clotet, Bonaventura; Blanco, Julià; Carrillo, Jorge. Alanine-based spacers promote a more efficient antigen processing and presentation in neoantigen polypeptide vaccines. **EACR 2022 Congress: Innovative Cancer Science - Translating Biology to Medicine (Seville, Spain).**

Aguilar-Gurrieri, Carmen*; **Barajas, Ana***; Varela, Ismael; Amengual-Rigo, Pep; Vazquez, Miguel; Dos Anjos, Carla; Blanco-Heredia, Juan; de Mattos-Arruda, Leticia; Guallar, Victor; Carrillo, Jorge; Blanco, Julià. High immunogenic VLP-based vaccines elicit new T cell specificities against melanoma neoantigens in mice. **8th ImmunoTherapy of Cancer Conference (ITOC8). Virtual congress 2021.**

Aguilar-Gurrieri, Carmen; **Barajas, Ana**; Varela, Ismael; Amengual-Rigo, Pep; Vazquez, Miguel; Lapore, Alba; de Mattos-Arruda, Leticia; Guallar, Victor; Carrillo, Jorge; Blanco, Julià. A new and flexible VLP vaccine platform for personalized cancer immunotherapy. **EACR Virtual Conference (09-12 June 2021).**

REFERENCES

1. Cancer. <https://www.who.int/news-room/fact-sheets/detail/cancer>.
2. Danaei, G., Vander Hoorn, S., Lopez, A. D., Murray, C. J. L. & Ezzati, M. Causes of cancer in the world: comparative risk assessment of nine behavioural and environmental risk factors. *Lancet* **366**, 1784–1793 (2005).
3. Sarkar, S. *et al.* Cancer Development, Progression, and Therapy: An Epigenetic Overview. *International Journal of Molecular Sciences* 2013, Vol. 14, Pages 21087–21113 **14**, 21087–21113 (2013).
4. Loeb, K. R. & Loeb, L. A. Significance of multiple mutations in cancer. *Carcinogenesis* **21**, 379–385 (2000).
5. Greaves, M. & Maley, C. C. Clonal evolution in cancer. *Nature* 2012 **481**:7381 **481**, 306–313 (2012).
6. Cantor, D. Introduction: cancer control and prevention in the twentieth century. *Bull. Hist. Med.* **81**, 1–38 (2007).
7. Bode, A. M. & Dong, Z. Cancer prevention research — then and now. *Nature Reviews Cancer* 2009 **9**:7 **9**, 508–516 (2009).
8. Hill, M. J. Changes and developments in cancer prevention. *J. R. Soc. Health* **121**, 94–97 (2001).
9. Schiffman, J. D., Fisher, P. G. & Gibbs, P. Early Detection of Cancer: Past, Present, and Future. *American Society of Clinical Oncology Educational Book* 57–65 (2015) doi:10.14694/edbook_am.2015.35.57.
10. Zugazagoitia, J. *et al.* Current Challenges in Cancer Treatment. *Clin Ther* **38**, 1551–1566 (2016).
11. Chen, H. H. W. & Kuo, M. T. Improving radiotherapy in cancer treatment: Promises and challenges. *Oncotarget* **8**, 62742 (2017).
12. Wyld, L., Audisio, R. A. & Poston, G. J. The evolution of cancer surgery and future perspectives. *Nature Reviews Clinical Oncology* 2014 **12**:2 **12**, 115–124 (2014).
13. Chabner, B. A. & Roberts, T. G. Chemotherapy and the war on cancer. *Nature Reviews Cancer* 2005 **5**:1 **5**, 65–72 (2005).
14. Yang, Y. Cancer immunotherapy: Harnessing the immune system to battle cancer. *Journal of Clinical Investigation* **125**, 3335–3337 (2015).
15. Hanahan, D. & Weinberg, R. A. Hallmarks of Cancer: The Next Generation. *Cell* **144**, 646–674 (2011).
16. Chen, D. S. & Mellman, I. Oncology meets immunology: the cancer-immunity cycle. *Immunity* **39**, 1–10 (2013).
17. Dranoff, G. Cytokines in cancer pathogenesis and cancer therapy. *Nature Reviews Cancer* 2004 **4**:1 **4**, 11–22 (2004).
18. Tang, D., Kang, R., Coyne, C. B., Zeh, H. J. & Lotze, M. T. PAMPs and DAMPs: signal 0s that spur autophagy and immunity. *Immunol Rev* **249**, 158–175 (2012).
19. Krysko, D. V. *et al.* Immunogenic cell death and DAMPs in cancer therapy. *Nature Reviews Cancer* 2012 **12**:12 **12**, 860–875 (2012).
20. Galluzzi, L., Buqué, A., Kepp, O., Zitvogel, L. & Kroemer, G. Immunogenic cell death in cancer and infectious disease. *Nature Reviews Immunology* 2016 **17**:2 **17**, 97–111 (2016).
21. Garg, A. D., Krysko, D. V., Vandenabeele, P. & Agostinis, P. PERSPECTIVE DAMPs and PDT-mediated photo-oxidative stress: exploring the unknown †. (2011) doi:10.1039/c0pp00294a.
22. Schumacher, T. N., Scheper, W. & Kvistborg, P. Cancer Neoantigens. <https://doi.org/10.1146/annurev-immunol-042617-053402> **37**, 173–200 (2018).

References

23. Kroemer, G., Galluzzi, L., Kepp, O. & Zitvogel, L. Immunogenic Cell Death in Cancer Therapy. <https://doi.org/10.1146/annurev-immunol-032712-100008> **31**, 51–72 (2013).
24. Green, D. R., Ferguson, T., Zitvogel, L. & Kroemer, G. Immunogenic and tolerogenic cell death. *Nature Reviews Immunology* 2009 9:5 **9**, 353–363 (2009).
25. Ma, Y. *et al.* Anticancer chemotherapy-induced intratumoral recruitment and differentiation of antigen-presenting cells. *Immunity* **38**, 729–741 (2013).
26. Saccheri, F. *et al.* Bacteria-induced gap junctions in tumors favor antigen cross-presentation and antitumor immunity. *Sci Transl Med* **2**, (2010).
27. Obeid, M. *et al.* Calreticulin exposure dictates the immunogenicity of cancer cell death. *Nature Medicine* 2006 13:1 **13**, 54–61 (2006).
28. Schlitzer, A., McGovern, N. & Ginhoux, F. Dendritic cells and monocyte-derived cells: Two complementary and integrated functional systems. *Semin Cell Dev Biol* **41**, 9–22 (2015).
29. Joffre, O. P., Segura, E., Savina, A. & Amigorena, S. Cross-presentation by dendritic cells. *Nature Reviews Immunology* 2012 12:8 **12**, 557–569 (2012).
30. Taylor, B. C. & Balko, J. M. Mechanisms of MHC-I Downregulation and Role in Immunotherapy Response. *Front Immunol* **13**, 771 (2022).
31. Wieczorek, M. *et al.* Major Histocompatibility Complex (MHC) Class I and MHC Class II Proteins: Conformational Plasticity in Antigen Presentation. *Front Immunol* **8**, 1 (2017).
32. Neefjes, J., Jongstra, M. L. M., Paul, P. & Bakke, O. Towards a systems understanding of MHC class I and MHC class II antigen presentation. *Nature Reviews Immunology* 2011 11:12 **11**, 823–836 (2011).
33. Bobisse, S. *et al.* Sensitive and frequent identification of high avidity neo-epitope specific CD8 + T cells in immunotherapy-naïve ovarian cancer. *Nat Commun* **9**, (2018).
34. McGranahan, N. *et al.* Clonal neoantigens elicit T cell immunoreactivity and sensitivity to immune checkpoint blockade. *Science* **351**, 1463–1469 (2016).
35. Robbins, P. F. *et al.* Mining exomic sequencing data to identify mutated antigens recognized by adoptively transferred tumor-reactive T cells. *Nat Med* **19**, 747–752 (2013).
36. Wells, D. K. *et al.* Key Parameters of Tumor Epitope Immunogenicity Revealed Through a Consortium Approach Improve Neoantigen Prediction. *Cell* **183**, 818–834.e13 (2020).
37. Wieczorek, M. *et al.* Major Histocompatibility Complex (MHC) Class I and MHC Class II Proteins: Conformational Plasticity in Antigen Presentation. *Front Immunol* **8**, 1 (2017).
38. Pishesha, N., Harmand, T. J. & Ploegh, H. L. A guide to antigen processing and presentation. *Nature Reviews Immunology* 2022 22:12 **22**, 751–764 (2022).
39. Kovacovics-Bankowski, M. & Rock, K. L. A phagosome-to-cytosol pathway for exogenous antigens presented on MHC class I molecules. *Science* **267**, 243–246 (1995).
40. Shen, L., Sigal, L. J., Boes, M. & Rock, K. L. Important role of cathepsin S in generating peptides for TAP-independent MHC class I crosspresentation in vivo. *Immunity* **21**, 155–165 (2004).
41. Tiberio, L. *et al.* Chemokine and chemotactic signals in dendritic cell migration. *Cell Mol Immunol* **15**, 346 (2018).

42. Wculek, S. K. *et al.* Dendritic cells in cancer immunology and immunotherapy. *Nature Reviews Immunology* 2019 20:1 **20**, 7–24 (2019).
43. Nace, G., Evankovich, J., Eid, R. & Tsung, A. Dendritic Cells and Damage-Associated Molecular Patterns: Endogenous Danger Signals Linking Innate and Adaptive Immunity. *J Innate Immun* **4**, 6–15 (2012).
44. Shah, K., Al-Haidari, A., Sun, J. & Kazi, J. U. T cell receptor (TCR) signaling in health and disease. *Signal Transduction and Targeted Therapy* 2021 6:1 **6**, 1–26 (2021).
45. Takaba, H. & Takayanagi, H. The Mechanisms of T Cell Selection in the Thymus. *Trends Immunol* **38**, 805–816 (2017).
46. Oh, J. *et al.* Single variable domains from the t cell receptor β chain function as mono-and bifunctional cARs and tcRs. doi:10.1038/s41598-019-53756-4.
47. Klein, L., Kyewski, B., Allen, P. M. & Hogquist, K. A. Positive and negative selection of the T cell repertoire: what thymocytes see and don't see. *Nat Rev Immunol* **14**, 377 (2014).
48. Raskov, H., Orhan, A., Christensen, J. P. & Gögenur, I. Cytotoxic CD8+ T cells in cancer and cancer immunotherapy. *British Journal of Cancer* 2020 124:2 **124**, 359–367 (2020).
49. Togashi, Y., Shitara, K. & Nishikawa, H. Regulatory T cells in cancer immunosuppression — implications for anticancer therapy. *Nature Reviews Clinical Oncology* 2019 16:6 **16**, 356–371 (2019).
50. Dustin, M. L. The immunological synapse. *Cancer Immunol Res* **2**, 1023 (2014).
51. Huppa, J. B. & Davis, M. M. T-cell-antigen recognition and the immunological synapse. *Nature Reviews Immunology* 2003 3:12 **3**, 973–983 (2003).
52. Shaw, S. *et al.* Two antigen-independent adhesion pathways used by human cytotoxic T-cell clones. *Nature* **323**, 262–264 (1986).
53. Mchugh, R. S., Ahmed, S. N., Wang, Y. C., Sell, K. W. & Selvaraj, P. Construction, purification, and functional incorporation on tumor cells of glycolipid-anchored human B7-1 (CD80). *Proceedings of the National Academy of Sciences* **92**, 8059–8063 (1995).
54. Meier, S. L., Satpathy, A. T. & Wells, D. K. Bystander T cells in cancer immunology and therapy. *Nature Cancer* 2022 3:2 **3**, 143–155 (2022).
55. Simoni, Y. *et al.* Bystander CD8+ T cells are abundant and phenotypically distinct in human tumour infiltrates. *Nature* 2018 557:7706 **557**, 575–579 (2018).
56. Zhang, Y., Guan, X. Y. & Jiang, P. Cytokine and Chemokine Signals of T-Cell Exclusion in Tumors. *Front Immunol* **11**, 3093 (2020).
57. Jiang, P. *et al.* Signatures of T cell dysfunction and exclusion predict cancer immunotherapy response. *Nat Med* **24**, 1550–1558 (2018).
58. Van Allen, E. M. *et al.* Genomic correlates of response to CTLA-4 blockade in metastatic melanoma. *Science* **350**, 207–211 (2015).
59. Nakamura, Y. *et al.* Poor Lymphocyte Infiltration to Primary Tumors in Acral Lentiginous Melanoma and Mucosal Melanoma Compared to Cutaneous Melanoma. *Front Oncol* **10**, 2884 (2020).
60. Mori, H. *et al.* The combination of PD-L1 expression and decreased tumor-infiltrating lymphocytes is associated with a poor prognosis in triple-negative breast cancer. *Oncotarget* **8**, 15584 (2017).
61. Aires, D. J. *et al.* T-cell trafficking plays an essential role in tumor immunity. *Laboratory Investigation* 2018 99:1 **99**, 85–92 (2018).

References

62. Slaney, C. Y., Kershaw, M. H. & Darcy, P. K. Trafficking of T cells into tumors. *Cancer Res* **74**, 7168–7174 (2014).
63. Bellone, M. & Calcinotto, A. Ways to Enhance Lymphocyte Trafficking into Tumors and Fitness of Tumor Infiltrating Lymphocytes. *Front Oncol* **3**, (2013).
64. Zhang, F. *et al.* Inhibition of TNF- α induced ICAM-1, VCAM-1 and E-selectin expression by selenium. *Atherosclerosis* **161**, 381–386 (2002).
65. Fisher, D. T. *et al.* IL-6 trans-signaling licenses mouse and human tumor microvascular gateways for trafficking of cytotoxic T cells. *J Clin Invest* **121**, 3846–3859 (2011).
66. Lieberman, J. The ABCs of granule-mediated cytotoxicity: new weapons in the arsenal. *Nat Rev Immunol* **3**, 361–370 (2003).
67. Gordy, C. & He, Y. W. Endocytosis by target cells: an essential means for perforin- and granzyme-mediated killing. *Cell Mol Immunol* **9**, 5–6 (2012).
68. Lieberman, J. Granzyme A activates another way to die. *Immunol Rev* **235**, 93–104 (2010).
69. Lucken-Ardjomande, S. & Martinou, J. C. Granzyme a, a stealth killer in the mitochondrion. *Cell* **133**, 568–570 (2008).
70. I, R. & E, K. Granzyme B-induced apoptosis in cancer cells and its regulation (review). *Int J Oncol* **37**, (2010).
71. Barry, M. & Bleackley, R. C. Cytotoxic T lymphocytes: all roads lead to death. *Nature Reviews Immunology 2002 2:6* **2**, 401–409 (2002).
72. Thibodeau, J., Bourgeois-Daigneault, M. C. & Lapointe, R. Targeting the MHC Class II antigen presentation pathway in cancer immunotherapy. *Oncoimmunology* **1**, 908 (2012).
73. Richardson, J. R., Schöllhorn, A., Gouttefangeas, C. & Schuhmacher, J. CD4+ T Cells: Multitasking Cells in the Duty of Cancer Immunotherapy. *Cancers 2021, Vol. 13, Page 596* **13**, 596 (2021).
74. Zhou, L., Chong, M. M. W. & Littman, D. R. Review Plasticity of CD4 + T Cell Lineage Differentiation. *Immunity* **30**, 646–655.
75. Tay, R. E., Richardson, E. K. & Toh, H. C. Revisiting the role of CD4+ T cells in cancer immunotherapy—new insights into old paradigms. *Cancer Gene Therapy 2020 28:1* **28**, 5–17 (2020).
76. König, R., Huang, L. Y. & Germain, R. N. MHC class II interaction with CD4 mediated by a region analogous to the MHC class I binding site for CD8. *Nature 1992 356:6372* **356**, 796–798 (1992).
77. Owen, D. L., Sjaastad, L. E. & Farrar, M. A. Regulatory T Cell Development in the Thymus. *The Journal of Immunology* **203**, 2031–2041 (2019).
78. Spits, H. Development of $\alpha\beta$ T cells in the human thymus. *Nature Reviews Immunology 2002 2:10* **2**, 760–772 (2002).
79. Khelil, M. Ben *et al.* Harnessing Antitumor CD4+ T Cells for Cancer Immunotherapy. *Cancers 2022, Vol. 14, Page 260* **14**, 260 (2022).
80. Borst, J., Ahrends, T., Bąbała, N., Melief, C. J. M. & Kastenmüller, W. CD4+ T cell help in cancer immunology and immunotherapy. *Nature Reviews Immunology 2018 18:10* **18**, 635–647 (2018).
81. Schoenberger, S. P., Toes, R. E. M., Van Dervoort, E. I. H., Offringa, R. & Melief, C. J. M. T-cell help for cytotoxic T lymphocytes is mediated by CD40–CD40L interactions. *Nature 1998 393:6684* **393**, 480–483 (1998).

82. Bennett, S. R. M. *et al.* Help for cytotoxic-T-cell responses is mediated by CD40 signalling. *Nature* 1998 393:6684 **393**, 478–480 (1998).
83. Bennett, S. R. M., Carbone, F. R., Karamalis, F., Miller, J. F. A. P. & Heath, W. R. Induction of a CD8+ Cytotoxic T Lymphocyte Response by Cross-priming Requires Cognate CD4+ T Cell Help. *J Exp Med* **186**, 65 (1997).
84. Basu, A. *et al.* Differentiation and Regulation of TH Cells: A Balancing Act for Cancer Immunotherapy. *Frontiers in immunology* vol. 12 669474 Preprint at <https://doi.org/10.3389/fimmu.2021.669474> (2021).
85. Hor, J. L. *et al.* Spatiotemporally Distinct Interactions with Dendritic Cell Subsets Facilitates CD4+ and CD8+ T Cell Activation to Localized Viral Infection. *Immunity* **43**, 554–565 (2015).
86. Gerner, M. Y., Casey, K. A., Kastenmuller, W. & Germain, R. N. Dendritic cell and antigen dispersal landscapes regulate T cell immunity. *J Exp Med* **214**, 3105 (2017).
87. Calabro, S. *et al.* Differential Intrasplenic Migration of Dendritic Cell Subsets Tailors Adaptive Immunity. *Cell Rep* **16**, 2472 (2016).
88. Ferris, S. T. *et al.* cDC1 prime and are licensed by CD4+ T cells to induce anti-tumour immunity. *Nature* **584**, 624–629 (2020).
89. Filatenkov, A. A. *et al.* CD4 T cell-dependent conditioning of dendritic cells to produce IL-12 results in CD8-mediated graft rejection and avoidance of tolerance. *J Immunol* **174**, 6909–6917 (2005).
90. Pan, Y., Yu, Y., Wang, X. & Zhang, T. Tumor-Associated Macrophages in Tumor Immunity. *Front Immunol* **11**, 3151 (2020).
91. Xie, Y. *et al.* Naive tumor-specific CD4+ T cells differentiated in vivo eradicate established melanoma. *Journal of Experimental Medicine* **207**, 651–667 (2010).
92. Quezada, S. A. *et al.* Tumor-reactive CD4+ T cells develop cytotoxic activity and eradicate large established melanoma after transfer into lymphopenic hosts. *Journal of Experimental Medicine* **207**, 637–650 (2010).
93. Kitano, S. *et al.* Enhancement of tumor-reactive cytotoxic CD4+ T cell responses after ipilimumab treatment in four advanced melanoma patients. *Cancer Immunol Res* **1**, 235–244 (2013).
94. Bald, T., Krummel, M. F., Smyth, M. J. & Barry, K. C. The NK cell–cancer cycle: advances and new challenges in NK cell–based immunotherapies. *Nature Immunology* 2020 21:8 **21**, 835–847 (2020).
95. Li, Z. Y. *et al.* The transcriptional repressor ID2 supports natural killer cell maturation by controlling TCF1 amplitude. *J Exp Med* **218**, (2021).
96. Shimasaki, N., Jain, A. & Campana, D. NK cells for cancer immunotherapy. *Nature Reviews Drug Discovery* 2020 19:3 **19**, 200–218 (2020).
97. Myers, J. A. & Miller, J. S. Exploring the NK cell platform for cancer immunotherapy. *Nature Reviews Clinical Oncology* 2020 18:2 **18**, 85–100 (2020).
98. Béziat, V. *et al.* CD56brightCD16+ NK Cells: A Functional Intermediate Stage of NK Cell Differentiation. *The Journal of Immunology* **186**, 6753–6761 (2011).
99. Melsen, J. E., Lugthart, G., Lankester, A. C. & Schilham, M. W. Human Circulating and Tissue-Resident CD56bright Natural Killer Cell Populations. *Front Immunol* **7**, 262 (2016).
100. De Maria, A., Bozzano, F., Cantoni, C. & Moretta, L. Revisiting human natural killer cell subset function revealed cytolytic CD56dimCD16+ NK cells as rapid producers of abundant IFN- γ on activation. *Proc Natl Acad Sci U S A* **108**, 728–732 (2011).

References

101. Carrega, P. *et al.* Natural killer cells infiltrating human nonsmall-cell lung cancer are enriched in CD56^{bright}CD16⁻ cells and display an impaired capability to kill tumor cells. *Cancer* **112**, 863–875 (2008).
102. Carrega, P. *et al.* CD56^{bright}perforin^{low} noncytotoxic human NK cells are abundant in both healthy and neoplastic solid tissues and recirculate to secondary lymphoid organs via afferent lymph. *J Immunol* **192**, 3805–3815 (2014).
103. Caruso, R. A. *et al.* Prognostic value of intratumoral neutrophils in advanced gastric carcinoma in a high-risk area in Northern Italy. *Modern Pathology* **15**, 831–837 (2002).
104. Villegas, F. R. *et al.* Prognostic significance of tumor infiltrating natural killer cells subset CD57 in patients with squamous cell lung cancer. *Lung Cancer* **35**, 23–28 (2002).
105. Hsia, J. Y. *et al.* Prognostic significance of intratumoral natural killer cells in primary resected esophageal squamous cell carcinoma. *Chang Gung Med J* **28**, 335–340 (2005).
106. Takanami, I., Takeuchi, K. & Giga, M. The prognostic value of natural killer cell infiltration in resected pulmonary adenocarcinoma. *J Thorac Cardiovasc Surg* **121**, 1058–1063 (2001).
107. Ali, T. H. *et al.* Enrichment of CD56(dim)KIR + CD57 + highly cytotoxic NK cells in tumour-infiltrated lymph nodes of melanoma patients. *Nat Commun* **5**, (2014).
108. Böttcher, J. P. *et al.* NK Cells Stimulate Recruitment of cDC1 into the Tumor Microenvironment Promoting Cancer Immune Control. *Cell* **172**, 1022–1037.e14 (2018).
109. Nath, P. R. *et al.* Natural killer cell recruitment and activation are regulated by cd47 expression in the tumor microenvironment. *Cancer Immunol Res* **7**, 1547–1561 (2019).
110. Barry, K. C. *et al.* A natural killer-dendritic cell axis defines checkpoint therapy-responsive tumor microenvironments. *Nat Med* **24**, 1178–1191 (2018).
111. Chiossone, L., Dumas, P. Y., Vienne, M. & Vivier, E. Natural killer cells and other innate lymphoid cells in cancer. *Nature Reviews Immunology* 2018 18:11 **18**, 671–688 (2018).
112. Raulet, D. H. Missing self recognition and self tolerance of natural killer (NK) cells. *Semin Immunol* **18**, 145–150 (2006).
113. Laskowski, T. J., Biederstädt, A. & Rezvani, K. Natural killer cells in antitumour adoptive cell immunotherapy. *Nature Reviews Cancer* 2022 22:10 **22**, 557–575 (2022).
114. Morvan, M. G. & Lanier, L. L. NK cells and cancer: you can teach innate cells new tricks. *Nature Reviews Cancer* 2016 16:1 **16**, 7–19 (2015).
115. Malarkannan, S. The balancing act: inhibitory Ly49 regulate NKG2D-mediated NK cell functions. *Semin Immunol* **18**, 186–192 (2006).
116. Brodin, P., Lakshmikanth, T., Johansson, S., Kä Rre, K. & Hö, P. The strength of inhibitory input during education quantitatively tunes the functional responsiveness of individual natural killer cells. (2009) doi:10.1182/blood-2008-05-156836.
117. Burshtyn, D. N. *et al.* Recruitment of tyrosine phosphatase HCP by the killer cell inhibitory receptor. *Immunity* **4**, 77–85 (1996).
118. Pahl, J. & Cerwenka, A. Tricking the balance: NK cells in anti-cancer immunity. *Immunobiology* **222**, 11–20 (2017).

119. Wang, W., Erbe, A. K., Hank, J. A., Morris, Z. S. & Sondel, P. M. NK Cell-Mediated Antibody-Dependent Cellular Cytotoxicity in Cancer Immunotherapy. *Front Immunol* **6**, 1 (2015).
120. Mittal, D., Gubin, M. M., Schreiber, R. D. & Smyth, M. J. New insights into cancer immunoediting and its three component phases — elimination, equilibrium and escape. *Curr Opin Immunol* **27**, 16 (2014).
121. Schreiber, R. D., Old, L. J. & Smyth, M. J. Cancer immunoediting: Integrating immunity's roles in cancer suppression and promotion. *Science (1979)* **331**, 1565–1570 (2011).
122. O'Donnell, J. S., Teng, M. W. L. & Smyth, M. J. Cancer immunoediting and resistance to T cell-based immunotherapy. *Nat Rev Clin Oncol* **16**, 151–167 (2019).
123. Schumacher, T. N. & Schreiber, R. D. *Neoantigens in cancer immunotherapy*. www.sciencemag.org.
124. Linnemann, C. *et al.* High-throughput epitope discovery reveals frequent recognition of neo-antigens by CD4+ T cells in human melanoma. *Nature Medicine* **2014 21:1 21**, 81–85 (2014).
125. Eroglu, Z. *et al.* High response rate to PD-1 blockade in desmoplastic melanomas. *Nature* **553**, 347–350 (2018).
126. Van Allen, E. M. *et al.* Genomic correlates of response to CTLA-4 blockade in metastatic melanoma. *Science (1979)* **350**, 207–211 (2015).
127. Yarchoan, M., Hopkins, A. & Jaffee, E. M. Tumor Mutational Burden and Response Rate to PD-1 Inhibition. *N Engl J Med* **377**, 2500 (2017).
128. McGranahan, N. *et al.* Clonal neoantigens elicit T cell immunoreactivity and sensitivity to immune checkpoint blockade. *Science* **351**, 1463–1469 (2016).
129. Gao, Y. *et al.* Integration of the Tumor Mutational Burden and Tumor Heterogeneity Identify an Immunological Subtype of Melanoma With Favorable Survival. *Front Oncol* **10**, 571545 (2020).
130. McGranahan, N. & Swanton, C. Clonal Heterogeneity and Tumor Evolution: Past, Present, and the Future. *Cell* **168**, 613–628 (2017).
131. Anagnostou, V. *et al.* Evolution of neoantigen landscape during immune checkpoint blockade in non-small cell lung cancer. *Cancer Discov* **7**, 264–276 (2017).
132. Verdegaal, E. M. E. *et al.* Neoantigen landscape dynamics during human melanoma–T cell interactions. *Nature* **2016 536:7614 536**, 91–95 (2016).
133. Radoja, S., Rao, T. D., Hillman, D. & Frey, A. B. Mice bearing late-stage tumors have normal functional systemic T cell responses in vitro and in vivo. *J Immunol* **164**, 2619–2628 (2000).
134. LV, B. *et al.* Immunotherapy: Reshape the Tumor Immune Microenvironment. *Front Immunol* **13**, (2022).
135. Maimela, N. R., Liu, S. & Zhang, Y. Fates of CD8+ T cells in Tumor Microenvironment. *Comput Struct Biotechnol J* **17**, 1–13 (2019).
136. Baharom, F. *et al.* Systemic vaccination induces CD8+ T cells and remodels the tumor microenvironment. *Cell* **185**, 4317–4332.e15 (2022).
137. Zhang, J., Huang, D., Saw, P. E. & Song, E. Turning cold tumors hot: from molecular mechanisms to clinical applications. *Trends Immunol* **43**, 523–545 (2022).
138. Cable, J. *et al.* Frontiers in cancer immunotherapy—a symposium report. *Ann N Y Acad Sci* **1489**, 30–47 (2021).

References

139. Hoteit, M. *et al.* Cancer immunotherapy: A comprehensive appraisal of its modes of application (Review). *Oncology Letters* vol. 22 Preprint at <https://doi.org/10.3892/ol.2021.12916> (2021).
140. Binnewies, M. *et al.* Understanding the tumor immune microenvironment (TIME) for effective therapy. *Nature Medicine* 2018 24:5 **24**, 541–550 (2018).
141. Mlecnik, B. *et al.* Multicenter international society for immunotherapy of cancer study of the consensus immunoscore for the prediction of survival and response to chemotherapy in stage III colon cancer. *Journal of Clinical Oncology* **38**, 3638–3651 (2020).
142. Tumeh, P. C. *et al.* PD-1 blockade induces responses by inhibiting adaptive immune resistance. *Nature* 2014 515:7528 **515**, 568–571 (2014).
143. Hodgins, J. J., Khan, S. T., Park, M. M., Auer, R. C. & Ardolino, M. Killers 2.0: NK cell therapies at the forefront of cancer control. *J Clin Invest* **129**, 3499 (2019).
144. Yang, L. & Zhang, Y. Tumor-associated macrophages: from basic research to clinical application. *J Hematol Oncol* **10**, 58 (2017).
145. Li, X. *et al.* Harnessing tumor-associated macrophages as aids for cancer immunotherapy. *Mol Cancer* **18**, (2019).
146. Liu, J., Geng, X., Hou, J. & Wu, G. New insights into M1/M2 macrophages: key modulators in cancer progression. *Cancer Cell Int* **21**, 1–7 (2021).
147. Boutilier, A. J. & ElSawa, S. F. Macrophage Polarization States in the Tumor Microenvironment. *Int J Mol Sci* **22**, (2021).
148. Bruns, H. *et al.* Vitamin D-dependent induction of cathelicidin in human macrophages results in cytotoxicity against high-grade B cell lymphoma. *Sci Transl Med* **7**, (2015).
149. Marin-Acevedo, J. A. *et al.* Next generation of immune checkpoint therapy in cancer: New developments and challenges. *J Hematol Oncol* **11**, 1–20 (2018).
150. Ribas, A. & Wolchok, J. D. Cancer immunotherapy using checkpoint blockade. *Science* **359**, 1350–1355 (2018).
151. Chambers, C. A., Kuhns, M. S., Egen, J. G. & Allison, J. P. CTLA-4-MEDIATED INHIBITION IN REGULATION OF T CELL RESPONSES: Mechanisms and Manipulation in Tumor Immunotherapy. (2001).
152. Leach, D. R., Krummel, M. F. & Allison, J. P. Enhancement of antitumor immunity by CTLA-4 blockade. *Science* **271**, 1734–1736 (1996).
153. Walunas, T. L. *et al.* CTLA-4 can function as a negative regulator of T cell activation. *Immunity* **1**, 405–413 (1994).
154. Pardoll, D. M. The blockade of immune checkpoints in cancer immunotherapy. (2012) doi:10.1038/nrc3239.
155. Baumeister, S. H., Freeman, G. J., Dranoff, G. & Sharpe, A. H. Coinhibitory Pathways in Immunotherapy for Cancer. <https://doi.org/10.1146/annurev-immunol-032414-112049> **34**, 539–573 (2016).
156. Harjunpää, H. & Guillerey, C. TIGIT as an emerging immune checkpoint. *Clin Exp Immunol* **200**, 108 (2020).
157. Kandel, S., Adhikary, P., Li, G. & Cheng, K. The TIM3/Gal9 signaling pathway: An emerging target for cancer immunotherapy. *Cancer Lett* **510**, 67–78 (2021).
158. Roychoudhuri, R., Eil, R. L. & Restifo, N. P. The interplay of effector and regulatory T cells in cancer. *Current Opinion in Immunology* vol. 33 101–111 Preprint at <https://doi.org/10.1016/j.coi.2015.02.003> (2015).

159. Rahemtulla, A. *et al.* Normal development and function of CD8+ cells but markedly decreased helper cell activity in mice lacking CD4. *Nature* 1991 353:6340 **353**, 180–184 (1991).
160. Gabrilovich, D. I. *et al.* The Terminology Issue for Myeloid-Derived Suppressor Cells. *Cancer Res* **67**, 425–425 (2007).
161. Yang, Y., Li, C., Liu, T., Dai, X. & Bazhin, A. V. Myeloid-Derived Suppressor Cells in Tumors: From Mechanisms to Antigen Specificity and Microenvironmental Regulation. *Front Immunol* **11**, 1371 (2020).
162. Hanson, E. M., Clements, V. K., Sinha, P., Ilkovitch, D. & Ostrand-Rosenberg, S. Myeloid-Derived Suppressor Cells Down-Regulate L-Selectin Expression on CD4+ and CD8+ T Cells. *The Journal of Immunology* **183**, 937–944 (2009).
163. Youn, J.-I., Nagaraj, S., Collazo, M. & Gabrilovich, D. I. Subsets of Myeloid-Derived Suppressor Cells in Tumor-Bearing Mice. *The Journal of Immunology* **181**, 5791–5802 (2008).
164. Markowitz, J. *et al.* Nitric oxide mediated inhibition of antigen presentation from DCs to CD4+ T cells in cancer and measurement of STAT1 nitration. *Sci Rep* **7**, (2017).
165. Rodríguez, P. C. & Ochoa, A. C. Arginine regulation by myeloid derived suppressor cells and tolerance in cancer: mechanisms and therapeutic perspectives. *Immunol Rev* **222**, 180–191 (2008).
166. Dysthe, M. & Parihar, R. Myeloid-Derived Suppressor Cells in the Tumor Microenvironment. *Adv Exp Med Biol* **1224**, 117–140 (2020).
167. Hart, K. M., Byrne, K. T., Molloy, M. J., Usherwood, E. M. & Berwin, B. IL-10 immunomodulation of myeloid cells regulates a murine model of ovarian cancer. *Front Immunol* **2**, 29 (2011).
168. Azzaoui, I. *et al.* T-cell defect in diffuse large B-cell lymphomas involves expansion of myeloid-derived suppressor cells. *Blood* **128**, 1081–1092 (2016).
169. Flavell, R. A., Sanjabi, S., Wrzesinski, S. H. & Licona-Limón, P. The polarization of immune cells in the tumour environment by TGFbeta. *Nat Rev Immunol* **10**, 554–567 (2010).
170. Shrivastava, R. *et al.* M2 polarization of macrophages by Oncostatin M in hypoxic tumor microenvironment is mediated by mTORC2 and promotes tumor growth and metastasis. *Cytokine* **118**, 130–143 (2019).
171. Zhang, F. *et al.* TGF-β induces M2-like macrophage polarization via SNAIL-mediated suppression of a pro-inflammatory phenotype. **7**, (2016).
172. Zhang, H. *et al.* Critical role of myeloid-derived suppressor cells in tumor-induced liver immune suppression through inhibition of NKT cell function. *Front Immunol* **8**, 129 (2017).
173. Li, H., Han, Y., Guo, Q., Zhang, M. & Cao, X. Cancer-Expanded Myeloid-Derived Suppressor Cells Induce Anergy of NK Cells through Membrane-Bound TGF-β1. *The Journal of Immunology* **182**, 240–249 (2009).
174. Waigel, S. *et al.* MIF inhibition reverts the gene expression profile of human melanoma cell line-induced MDSCs to normal monocytes. *Genom Data* **7**, 240–242 (2016).
175. Blidner, A. G. *et al.* Differential Response of Myeloid-Derived Suppressor Cells to the Nonsteroidal Anti-Inflammatory Agent Indomethacin in Tumor-Associated and Tumor-Free Microenvironments. *The Journal of Immunology* **194**, 3452–3462 (2015).

References

176. Chen, X. & Song, E. Turning foes to friends: targeting cancer-associated fibroblasts. *Nat Rev Drug Discov* **18**, 99–115 (2019).
177. Bu, L. *et al.* Biological heterogeneity and versatility of cancer-associated fibroblasts in the tumor microenvironment. *Oncogene* **2019** *38:25* **38**, 4887–4901 (2019).
178. De Wever, O., Demetter, P., Mareel, M. & Bracke, M. Stromal myofibroblasts are drivers of invasive cancer growth. *Int J Cancer* **123**, 2229–2238 (2008).
179. Petersen, O. W. *et al.* Epithelial to Mesenchymal Transition in Human Breast Cancer Can Provide a Nonmalignant Stroma. *Am J Pathol* **162**, 391 (2003).
180. Yin, C., Evason, K. J., Asahina, K. & Stainier, D. Y. R. Hepatic stellate cells in liver development, regeneration, and cancer. *J Clin Invest* **123**, 1902–1910 (2013).
181. Omary, M. B., Lugea, A., Lowe, A. W. & Pandol, S. J. The pancreatic stellate cell: a star on the rise in pancreatic diseases. *Journal of Clinical Investigation* **117**, 50 (2007).
182. Kalluri, R. The biology and function of fibroblasts in cancer. *Nat Rev Cancer* **16**, 582–598 (2016).
183. Baeriswyl, V. & Christofori, G. The angiogenic switch in carcinogenesis. *Semin Cancer Biol* **19**, 329–337 (2009).
184. Yang, X. *et al.* FAP Promotes Immunosuppression by Cancer-Associated Fibroblasts in the Tumor Microenvironment via STAT3-CCL2 Signaling. *Cancer Res* **76**, 4124–4135 (2016).
185. Orimo, A. *et al.* Stromal Fibroblasts Present in Invasive Human Breast Carcinomas Promote Tumor Growth and Angiogenesis through Elevated SDF-1/CXCL12 Secretion. *Cell* **121**, 335–348 (2005).
186. Galluzzi, L., Humeau, J., Buqué, A., Zitvogel, L. & Kroemer, G. Immunostimulation with chemotherapy in the era of immune checkpoint inhibitors. *Nature Reviews Clinical Oncology* **2020** *17:12* **17**, 725–741 (2020).
187. Moorthi, C., Manavalan, R. & Kathiresan, K. Nanotherapeutics to overcome conventional cancer chemotherapy limitations. *J Pharm Pharm Sci* **14**, 67–77 (2011).
188. Pan, S. T., Li, Z. L., He, Z. X., Qiu, J. X. & Zhou, S. F. Molecular mechanisms for tumour resistance to chemotherapy. *Clin Exp Pharmacol Physiol* **43**, 723–737 (2016).
189. Szakács, G., Paterson, J. K., Ludwig, J. A., Booth-Genthe, C. & Gottesman, M. M. Targeting multidrug resistance in cancer. *Nat Rev Drug Discov* **5**, 219–234 (2006).
190. Hegde, P. S. & Chen, D. S. Perspective Top 10 Challenges in Cancer Immunotherapy. *Immunity* **52**, 17–35 (2020).
191. Wang, S., Xie, K. & Liu, T. Cancer Immunotherapies: From Efficacy to Resistance Mechanisms – Not Only Checkpoint Matters. *Frontiers in Immunology* vol. 12 2904 Preprint at <https://doi.org/10.3389/fimmu.2021.690112> (2021).
192. Conlon, K. C., Miljkovic, M. D. & Waldmann, T. A. Cytokines in the Treatment of Cancer. *Journal of Interferon & Cytokine Research* **39**, 6 (2019).
193. Berraondo, P. *et al.* Cytokines in clinical cancer immunotherapy. *British Journal of Cancer* **2018** *120:1* **120**, 6–15 (2018).
194. Qiu, Y. *et al.* Clinical Application of Cytokines in Cancer Immunotherapy. *Drug Des Devel Ther* **15**, 2269 (2021).
195. Kirkwood, J. Cancer immunotherapy: The interferon- α experience. *Semin Oncol* **29**, 18–26 (2002).

196. Fyfe, G. *et al.* Results of treatment of 255 patients with metastatic renal cell carcinoma who received high-dose recombinant interleukin-2 therapy. *J Clin Oncol* **13**, 688–696 (1995).
197. Belardelli, F., Ferrantini, M., Proietti, E. & Kirkwood, J. M. Interferon-alpha in tumor immunity and immunotherapy. *Cytokine Growth Factor Rev* **13**, 119–134 (2002).
198. Borden, E. C. Interferons α and β in cancer: therapeutic opportunities from new insights. *Nature Reviews Drug Discovery* **2018 18:3** **18**, 219–234 (2019).
199. Hervas-Stubbs, S. *et al.* Direct effects of type I interferons on cells of the immune system. *Clinical Cancer Research* **17**, 2619–2627 (2011).
200. Herndon, T. M. *et al.* U.S. Food and Drug Administration Approval: peginterferon- α -2b for the adjuvant treatment of patients with melanoma. *Oncologist* **17**, 1323–1328 (2012).
201. Lenardo, M. J. Fas and the art of lymphocyte maintenance. *J Exp Med* **183**, 721–724 (1996).
202. Shevach, E. M. The Resurrection of T Cell-Mediated Suppression. *The Journal of Immunology* **186**, 3805–3807 (2011).
203. Atkins, M. B. *et al.* High-dose recombinant interleukin 2 therapy for patients with metastatic melanoma: analysis of 270 patients treated between 1985 and 1993. *J Clin Oncol* **17**, 2105–2116 (1999).
204. Rosenberg, S. A. *et al.* Experience with the use of high-dose interleukin-2 in the treatment of 652 cancer patients. *Ann Surg* **210**, 474–485 (1989).
205. Lu, Y. C. *et al.* Treatment of Patients With Metastatic Cancer Using a Major Histocompatibility Complex Class II-Restricted T-Cell Receptor Targeting the Cancer Germline Antigen MAGE-A3. *J Clin Oncol* **35**, 3322–3329 (2017).
206. Andersen, R. *et al.* Tumor infiltrating lymphocyte therapy for ovarian cancer and renal cell carcinoma. *Hum Vaccin Immunother* **11**, 2790–2795 (2015).
207. Conlon, K. C. *et al.* Redistribution, hyperproliferation, activation of natural killer cells and CD8 T cells, and cytokine production during first-in-human clinical trial of recombinant human interleukin-15 in patients with cancer. *J Clin Oncol* **33**, 74–82 (2015).
208. Ma, H.-L. *et al.* IL-21 activates both innate and adaptive immunity to generate potent antitumor responses that require perforin but are independent of IFN- γ . *J Immunol* **171**, 608–615 (2003).
209. Skak, K., Kragh, M., Hausman, D., Smyth, M. J. & Sivakumar, P. V. Interleukin 21: combination strategies for cancer therapy. *Nat Rev Drug Discov* **7**, 231–240 (2008).
210. Thompson, J. A. *et al.* Phase I study of recombinant interleukin-21 in patients with metastatic melanoma and renal cell carcinoma. *Journal of Clinical Oncology* **26**, 2034–2039 (2008).
211. Darvin, P., Toor, S. M., Sasidharan Nair, V. & Elkord, E. Immune checkpoint inhibitors: recent progress and potential biomarkers. *Exp Mol Med* **50**, 165 (2018).
212. Cameron, F., Whiteside, G. & Perry, C. Ipilimumab: First global approval. *Drugs* **71**, 1093–1104 (2011).
213. Van Elsas, A., Hurwitz, A. A. & Allison, J. P. Combination Immunotherapy of B16 Melanoma Using Anti-Cytotoxic T Lymphocyte-Associated Antigen 4 (Ctla-4) and Granulocyte/Macrophage Colony-Stimulating Factor (Gm-Csf)-Producing Vaccines Induces Rejection of Subcutaneous and Metastatic Tumors Accompanied by Autoimmune Depigmentation. *J Exp Med* **190**, 355 (1999).

References

214. Small, E. J. *et al.* A Pilot Trial of CTLA-4 Blockade with Human Anti-CTLA-4 in Patients with Hormone-Refractory Prostate Cancer. *Clinical Cancer Research* **13**, 1810–1815 (2007).
215. Hodi, F. S. *et al.* Improved Survival with Ipilimumab in Patients with Metastatic Melanoma. *New England Journal of Medicine* **363**, 711–723 (2010).
216. Pardoll, D. M. The blockade of immune checkpoints in cancer immunotherapy. *Nature Reviews Cancer* **12**, 252–264 (2012).
217. Blank, C. *et al.* PD-L1/B7H-1 inhibits the effector phase of tumor rejection by T cell receptor (TCR) transgenic CD8+ T cells. *Cancer Res* **64**, 1140–1145 (2004).
218. Dong, H. *et al.* Tumor-associated B7-H1 promotes T-cell apoptosis: A potential mechanism of immune evasion. *Nature Medicine* **8**, 793–800 (2002).
219. Okazaki, T. & Honjo, T. PD-1 and PD-1 ligands: from discovery to clinical application. *Int Immunol* **19**, 813–824 (2007).
220. Ishida, Y., Agata, Y., Shibahara, K. & Honjo, T. Induced expression of PD-1, a novel member of the immunoglobulin gene superfamily, upon programmed cell death. *EMBO J* **11**, 3887–3895 (1992).
221. Freeman, G. J. *et al.* Engagement of the PD-1 immunoinhibitory receptor by a novel B7 family member leads to negative regulation of lymphocyte activation. *J Exp Med* **192**, 1027–1034 (2000).
222. Iwai, Y. *et al.* Involvement of PD-L1 on tumor cells in the escape from host immune system and tumor immunotherapy by PD-L1 blockade. *Proc Natl Acad Sci U S A* **99**, 12293–12297 (2002).
223. Topalian, S. L. *et al.* Safety, activity, and immune correlates of anti-PD-1 antibody in cancer. *N Engl J Med* **366**, 2443–2454 (2012).
224. Zhao, B., Zhao, H. & Zhao, J. Efficacy of PD-1/PD-L1 blockade monotherapy in clinical trials. *Ther Adv Med Oncol* **12**, (2020).
225. June, C. H. & Sadelain, M. Chimeric Antigen Receptor Therapy. *N Engl J Med* **379**, 64 (2018).
226. Kumar, A., Watkins, R. & Vilgelm, A. E. Cell Therapy With TILs: Training and Taming T Cells to Fight Cancer. *Front Immunol* **12**, (2021).
227. Sadelain, M., Brentjens, R. & Rivière, I. The promise and potential pitfalls of chimeric antigen receptors. *Curr Opin Immunol* **21**, 215–223 (2009).
228. Davenport, A. J. *et al.* CAR-T Cells Inflict Sequential Killing of Multiple Tumor Target Cells. *Cancer Immunol Res* **3**, 483–494 (2015).
229. Brocker, T. & Karjalainen, K. Signals through T cell receptor-zeta chain alone are insufficient to prime resting T lymphocytes. *J Exp Med* **181**, 1653–1659 (1995).
230. Gong, M. C. *et al.* Cancer patient T cells genetically targeted to prostate-specific membrane antigen specifically lyse prostate cancer cells and release cytokines in response to prostate-specific membrane antigen. *Neoplasia* **1**, 123–127 (1999).
231. Maher, J., Brentjens, R. J., Gunset, G., Rivière, I. & Sadelain, M. Human T-lymphocyte cytotoxicity and proliferation directed by a single chimeric TCRzeta/CD28 receptor. *Nat Biotechnol* **20**, 70–75 (2002).
232. Newick, K., O'Brien, S., Moon, E. & Albelda, S. M. CAR T Cell Therapy for Solid Tumors. <https://doi.org/10.1146/annurev-med-062315-120245> **68**, 139–152 (2017).
233. Knochelmann, H. M. *et al.* CAR T Cells in Solid Tumors: Blueprints for Building Effective Therapies. *Front Immunol* **9**, (2018).

234. Wagner, J., Wickman, E., DeRenzo, C. & Gottschalk, S. CAR T Cell Therapy for Solid Tumors: Bright Future or Dark Reality? *Molecular Therapy* **28**, 2320 (2020).
235. Brown, C. E. *et al.* Bioactivity and safety of IL13R α 2-redirected chimeric antigen receptor CD8⁺ T cells in patients with recurrent glioblastoma. *Clinical Cancer Research* **21**, 4062–4072 (2015).
236. Ahmed, N. *et al.* HER2-Specific Chimeric Antigen Receptor-Modified Virus-Specific T Cells for Progressive Glioblastoma: A Phase 1 Dose-Escalation Trial. *JAMA Oncol* **3**, 1094–1101 (2017).
237. Thistlethwaite, F. C. *et al.* The clinical efficacy of first-generation carcinoembryonic antigen (CEACAM5)-specific CAR T cells is limited by poor persistence and transient pre-conditioning-dependent respiratory toxicity. *Cancer Immunol Immunother* **66**, 1425–1436 (2017).
238. Ahmed, N. *et al.* Human Epidermal Growth Factor Receptor 2 (HER2) -Specific Chimeric Antigen Receptor-Modified T Cells for the Immunotherapy of HER2-Positive Sarcoma. *J Clin Oncol* **33**, 1688–1696 (2015).
239. Zhao, Y. *et al.* Tumor Infiltrating Lymphocyte (TIL) Therapy for Solid Tumor Treatment: Progressions and Challenges. *Cancers (Basel)* **14**, (2022).
240. Rosenberg, S. A., Spiess, P. & Lafreniere, R. A New Approach to the Adoptive Immunotherapy of Cancer with Tumor-Infiltrating Lymphocytes. *Science (1979)* **233**, 1318–1321 (1986).
241. Rosenberg, S. A. *et al.* Treatment of Patients With Metastatic Melanoma With Autologous Tumor-Infiltrating Lymphocytes and Interleukin 2. *JNCI: Journal of the National Cancer Institute* **86**, 1159–1166 (1994).
242. Inozume, T. *et al.* Selection of CD8⁺PD-1⁺ lymphocytes in fresh human melanomas enriches for tumor-reactive T cells. *Journal of Immunotherapy* **33**, 956–964 (2010).
243. Lu, Y.-C. *et al.* Mutated PPP1R3B Is Recognized by T Cells Used To Treat a Melanoma Patient Who Experienced a Durable Complete Tumor Regression. *The Journal of Immunology* **190**, 6034–6042 (2013).
244. Lu, Y. C. *et al.* Efficient Identification of Mutated Cancer Antigens Recognized by T Cells Associated with Durable Tumor Regressions. *Clinical Cancer Research* **20**, 3401–3410 (2014).
245. Gros, A. *et al.* Prospective identification of neoantigen-specific lymphocytes in the peripheral blood of melanoma patients. *Nature Medicine* 2016 22:4 **22**, 433–438 (2016).
246. Tran, E. *et al.* T-Cell Transfer Therapy Targeting Mutant KRAS in Cancer. *New England Journal of Medicine* **375**, 2255–2262 (2016).
247. Tran, E. *et al.* Cancer immunotherapy based on mutation-specific CD4⁺ T cells in a patient with epithelial cancer. *Science (1979)* **344**, 641–645 (2014).
248. Zacharakis, N. *et al.* Immune recognition of somatic mutations leading to complete durable regression in metastatic breast cancer. *Nature Medicine* 2018 24:6 **24**, 724–730 (2018).
249. Rath, J. A. & Arber, C. Engineering Strategies to Enhance TCR-Based Adoptive T Cell Therapy. *Cells* 2020, Vol. 9, Page 1485 **9**, 1485 (2020).
250. Gasteiger, G. & Rudensky, A. Y. Interactions between innate and adaptive lymphocytes. *Nat Rev Immunol* **14**, 631–639 (2014).
251. Olson, J. A. *et al.* NK cells mediate reduction of GVHD by inhibiting activated, alloreactive T cells while retaining GVT effects. *Blood* **115**, 4293–4301 (2010).

References

252. Patel, S. *et al.* Beyond CAR T cells: Other cell-based immunotherapeutic strategies against cancer. *Front Oncol* **9**, 196 (2019).
253. Pollard, A. J. & Bijker, E. M. A guide to vaccinology: from basic principles to new developments. *Nature Reviews Immunology* **2020** *21:2* **21**, 83–100 (2020).
254. Doria-Rose, N. *et al.* Antibody Persistence through 6 Months after the Second Dose of mRNA-1273 Vaccine for Covid-19. *New England Journal of Medicine* **384**, 2259–2261 (2021).
255. Polack, F. P. *et al.* Safety and Efficacy of the BNT162b2 mRNA Covid-19 Vaccine. *New England Journal of Medicine* **383**, 2603–2615 (2020).
256. Barreiro, A. *et al.* Preclinical evaluation of a COVID-19 vaccine candidate based on a recombinant RBD fusion heterodimer of SARS-CoV-2. *iScience* **26**, 106126 (2023).
257. Falsey, A. R. *et al.* Phase 3 Safety and Efficacy of AZD1222 (ChAdOx1 nCoV-19) Covid-19 Vaccine. *N Engl J Med* **385**, 2348–2360 (2021).
258. Corominas, J. *et al.* Safety and immunogenicity of the protein-based PHH-1V compared to BNT162b2 as a heterologous SARS-CoV-2 booster vaccine in adults vaccinated against COVID-19: a multicentre, randomised, double-blind, non-inferiority phase IIb trial. *The Lancet Regional Health – Europe* **0**, 100613 (2023).
259. Hammerich, L. *et al.* Systemic clinical tumor regressions and potentiation of PD1 blockade with in situ vaccination. *Nat Med* **25**, 814–824 (2019).
260. Brody, J. D. *et al.* In situ vaccination with a TLR9 agonist induces systemic lymphoma regression: a phase I/II study. *J Clin Oncol* **28**, 4324–4332 (2010).
261. Higano, C. S. *et al.* Sipuleucel-T. *Nat Rev Drug Discov* **9**, 513–514 (2010).
262. Kantoff, P. W. *et al.* Sipuleucel-T Immunotherapy for Castration-Resistant Prostate Cancer. *New England Journal of Medicine* **363**, 411–422 (2010).
263. Lin, M. J. *et al.* Cancer vaccines: the next immunotherapy frontier. doi:10.1038/s43018-022-00418-6.
264. Gopanenko, A. V., Kosobokova, E. N. & Kosorukov, V. S. Main Strategies for the Identification of Neoantigens. *Cancers (Basel)* **12**, 1–28 (2020).
265. Tacken, P. J., De Vries, I. J. M., Torensma, R. & Figdor, C. G. Dendritic-cell immunotherapy: from ex vivo loading to in vivo targeting. *Nature Reviews Immunology* **2007** *7:10* **7**, 790–802 (2007).
266. Bonifaz, L. C. *et al.* In Vivo Targeting of Antigens to Maturing Dendritic Cells via the DEC-205 Receptor Improves T Cell Vaccination. *Journal of Experimental Medicine* **199**, 815–824 (2004).
267. Zhao, W., Wu, J., Chen, S. & Zhou, Z. Shared neoantigens: ideal targets for off-the-shelf cancer immunotherapy. <https://doi.org/10.2217/pgs-2019-0184> **21**, 637–645 (2020).
268. Hamilton, E., Shastry, M., Shiller, S. M. & Ren, R. Targeting HER2 heterogeneity in breast cancer. *Cancer Treat Rev* **100**, (2021).
269. Goldenberg, M. M. Trastuzumab, a recombinant DNA-derived humanized monoclonal antibody, a novel agent for the treatment of metastatic breast cancer. *Clin Ther* **21**, 309–18 (1999).
270. Baselga, J. *et al.* Phase II study of weekly intravenous recombinant humanized anti-p185HER2 monoclonal antibody in patients with HER2/neu-overexpressing metastatic breast cancer. *J Clin Oncol* **14**, 737–744 (1996).
271. Cobleigh, M. A. *et al.* Multinational study of the efficacy and safety of humanized anti-HER2 monoclonal antibody in women who have HER2-overexpressing

- metastatic breast cancer that has progressed after chemotherapy for metastatic disease. *J Clin Oncol* **17**, 2639–2648 (1999).
272. Mittendorf, E. A. *et al.* Primary analysis of a prospective, randomized, single-blinded phase II trial evaluating the HER2 peptide AE37 vaccine in breast cancer patients to prevent recurrence. *Ann Oncol* **27**, 1241–1248 (2016).
273. Mittendorf, E. A. *et al.* Efficacy and Safety Analysis of Nelipepimut-S Vaccine to Prevent Breast Cancer Recurrence: A Randomized, Multicenter, Phase III Clinical Trial. *Clin Cancer Res* **25**, 4248–4254 (2019).
274. Knutson, K. L., Schiffman, K. & Disis, M. L. Immunization with a HER-2/neu helper peptide vaccine generates HER-2/neu CD8 T-cell immunity in cancer patients. *J Clin Invest* **107**, 477–484 (2001).
275. Scanlan, M. J., Gure, A. O., Jungbluth, A. A., Old, L. J. & Chen, Y. T. Cancer/testis antigens: an expanding family of targets for cancer immunotherapy. *Immunol Rev* **188**, 22–32 (2002).
276. Esfandiary, A. & Ghafouri-Fard, S. New York esophageal squamous cell carcinoma-1 and cancer immunotherapy. <http://dx.doi.org/10.2217/imt.15.3> **7**, 411–439 (2015).
277. Wang, R. F. & Wang, H. Y. Immune targets and neoantigens for cancer immunotherapy and precision medicine. *Cell Res* **27**, 11 (2017).
278. Pearlman, A. H. *et al.* Targeting public neoantigens for cancer immunotherapy. *Nat Cancer* **2**, 487 (2021).
279. Vogelstein, B. *et al.* Cancer genome landscapes. *Science* **339**, 1546–1558 (2013).
280. Fossum, B. *et al.* Overlapping epitopes encompassing a point mutation (12 Gly → Arg) in p21 ras can be recognized by HLA-DR, -DP and -DQ restricted T cells. *Eur J Immunol* **23**, 2687–2691 (1993).
281. Bamford, S. *et al.* The COSMIC (Catalogue of Somatic Mutations in Cancer) database and website. *Br J Cancer* **91**, 355–358 (2004).
282. Petitjean, A. *et al.* Impact of mutant p53 functional properties on TP53 mutation patterns and tumor phenotype: lessons from recent developments in the IARC TP53 database. *Hum Mutat* **28**, 622–629 (2007).
283. Davies, H. *et al.* Mutations of the BRAF gene in human cancer. *Nature* **417**:6892 **417**, 949–954 (2002).
284. Harrison, P. T., Vyse, S. & Huang, P. H. Rare epidermal growth factor receptor (EGFR) mutations in non-small cell lung cancer. *Semin Cancer Biol* **61**, 167–179 (2020).
285. Yang, W. *et al.* Immunogenic neoantigens derived from gene fusions stimulate T cell responses. *Nat Med* **25**, 767–775 (2019).
286. Turajlic, S. *et al.* Insertion-and-deletion-derived tumour-specific neoantigens and the immunogenic phenotype: a pan-cancer analysis. *Lancet Oncol* **18**, 1009–1021 (2017).
287. Blass, E. & Ott, P. A. Advances in the development of personalized neoantigen-based therapeutic cancer vaccines. *Nature Reviews Clinical Oncology* **2021** **18**:4 **18**, 215–229 (2021).
288. Roudko, V., Greenbaum, B. & Bhardwaj, N. Computational Prediction and Validation of Tumor-Associated Neoantigens. *Frontiers in Immunology* vol. 11 Preprint at <https://doi.org/10.3389/fimmu.2020.00027> (2020).

References

289. Andreatta, M. & Nielsen, M. Gapped sequence alignment using artificial neural networks: application to the MHC class I system. *Bioinformatics* **32**, 511–517 (2016).
290. Nielsen, M. & Andreatta, M. NetMHCpan-3.0; improved prediction of binding to MHC class I molecules integrating information from multiple receptor and peptide length datasets. *Genome Med* **8**, 1–9 (2016).
291. Hoof, I. *et al.* NetMHCpan, a method for MHC class I binding prediction beyond humans. *Immunogenetics* **61**, 1 (2009).
292. Nielsen, M. *et al.* NetMHCpan, a method for quantitative predictions of peptide binding to any HLA-A and -B locus protein of known sequence. *PLoS One* **2**, (2007).
293. Gomez-Perosanz, M., Ras-Carmona, A., Lafuente, E. M. & Reche, P. A. Identification of CD8+ T cell epitopes through proteasome cleavage site predictions. *BMC Bioinformatics* **21**, (2020).
294. Amengual-Rigo, P. & Guallar, V. NetCleave: an open-source algorithm for predicting C-terminal antigen processing for MHC-I and MHC-II. *Scientific Reports* **2021 11:1 11**, 1–8 (2021).
295. Bjerregaard, A. M. *et al.* An Analysis of Natural T Cell Responses to Predicted Tumor Neoepitopes. *Front Immunol* **8**, (2017).
296. Vitiello, A. *et al.* Comparison of cytotoxic T lymphocyte responses induced by peptide or DNA immunization: Implications on immunogenicity and immunodominance. *Eur J Immunol* **27**, 671–678 (1997).
297. Hu, Z., Ott, P. A. & Wu, C. J. Towards personalized, tumour-specific, therapeutic vaccines for cancer. *Nature Reviews Immunology* vol. 18 168–182 Preprint at <https://doi.org/10.1038/nri.2017.131> (2018).
298. Lang, F., Schrörs, B., Löwer, M., Türeci, Ö. & Sahin, U. Identification of neoantigens for individualized therapeutic cancer vaccines. *Nature Reviews Drug Discovery* vol. 21 261–282 Preprint at <https://doi.org/10.1038/s41573-021-00387-y> (2022).
299. Skwarczynski, M. & Toth, I. Peptide-based synthetic vaccines. *Chemical Science* vol. 7 842–854 Preprint at <https://doi.org/10.1039/c5sc03892h> (2016).
300. Bijker, M. S. *et al.* CD8+ CTL priming by exact peptide epitopes in incomplete Freund's adjuvant induces a vanishing CTL response, whereas long peptides induce sustained CTL reactivity. *J Immunol* **179**, 5033–5040 (2007).
301. Ott, P. A. *et al.* An Immunogenic Personal Neoantigen Vaccine for Melanoma Patients. *Nature* **547**, 217 (2017).
302. Keskin, D. B. *et al.* Neoantigen vaccine generates intratumoral T cell responses in phase Ib glioblastoma trial. *Nature* **2018 565:7738 565**, 234–239 (2018).
303. Sahin, U. *et al.* Personalized RNA mutanome vaccines mobilize poly-specific therapeutic immunity against cancer. *Nature* **547**, 222–226 (2017).
304. Gubin, M. M. *et al.* Checkpoint Blockade Cancer Immunotherapy Targets Tumour-Specific Mutant Antigens. *Nature* **515**, 577 (2014).
305. Hemmi, H. *et al.* A Toll-like receptor recognizes bacterial DNA. *Nature* **408**, 740–745 (2000).
306. Zahm, C. D., Colluru, V. T. & McNeel, D. G. DNA vaccines for prostate cancer. *Pharmacol Ther* **174**, 27–42 (2017).
307. Vishweshwaraiah, Y. L. & Dokholyan, N. V. mRNA vaccines for cancer immunotherapy. *Front Immunol* **13**, 7468 (2022).
308. Rojas, L. A. *et al.* Personalized RNA neoantigen vaccines stimulate T cells in pancreatic cancer. *Nature* **2023 1–7** (2023) doi:10.1038/s41586-023-06063-y.

309. Roldão, A., Mellado, M. C. M., Castilho, L. R., Carrondo, M. J. T. & Alves, P. M. Virus-like particles in vaccine development. <http://dx.doi.org/10.1586/erv.10.1159>, 1149–1176 (2014).
310. Noad, R. & Roy, P. Virus-like particles as immunogens. *Trends Microbiol* **11**, 438–444 (2003).
311. Caldeira, J. C., Perrine, M., Pericle, F. & Cavallo, F. Virus-Like Particles as an Immunogenic Platform for Cancer Vaccines. *Viruses* 2020, Vol. 12, Page 488 **12**, 488 (2020).
312. Manolova, V. *et al.* Nanoparticles target distinct dendritic cell populations according to their size. *Eur J Immunol* **38**, 1404–1413 (2008).
313. Yan, D., Wei, Y. Q., Guo, H. C. & Sun, S. Q. The application of virus-like particles as vaccines and biological vehicles. *Applied Microbiology and Biotechnology* 2015 **99**:24 **99**, 10415–10432 (2015).
314. Nooraei, S. *et al.* Virus-like particles: preparation, immunogenicity and their roles as nanovaccines and drug nanocarriers. *Journal of Nanobiotechnology* 2021 **19**:1 **19**, 1–27 (2021).
315. Welsch, S., Müller, B. & Kräusslich, H. G. More than one door – Budding of enveloped viruses through cellular membranes. *FEBS Lett* **581**, 2089 (2007).
316. Kramer, K. *et al.* Functionalisation of virus-like particles enhances antitumour immune responses. *J Immunol Res* **2019**, (2019).
317. Cervera, L. *et al.* Production of HIV-1-based virus-like particles for vaccination: achievements and limits. *Applied Microbiology and Biotechnology* vol. 103 7367–7384 Preprint at <https://doi.org/10.1007/s00253-019-10038-3> (2019).
318. Briggs, J. A. G. & Kräusslich, H. G. The molecular architecture of HIV. *J Mol Biol* **410**, 491–500 (2011).
319. Paliard, X. *et al.* Priming of strong, broad, and long-lived HIV type 1 p55gag-specific CD8+ cytotoxic T cells after administration of a virus-like particle vaccine in rhesus macaques. *AIDS Res Hum Retroviruses* **16**, 273–282 (2000).
320. Klein, J. S. & Bjorkman, P. J. Few and far between: how HIV may be evading antibody avidity. *PLoS Pathog* **6**, 1–6 (2010).
321. Tarrés-Freixas, F. *et al.* An engineered HIV-1 Gag-based VLP displaying high antigen density induces strong antibody-dependent functional immune responses. *NPJ Vaccines* **8**, 51 (2023).
322. Ortiz, R. *et al.* Exploring FeLV-Gag-Based VLPs as a New Vaccine Platform—Analysis of Production and Immunogenicity. *International Journal of Molecular Sciences* 2023, Vol. 24, Page 9025 **24**, 9025 (2023).
323. Cafri, G. *et al.* mRNA vaccine-induced neoantigen-specific T cell immunity in patients with gastrointestinal cancer. *Journal of Clinical Investigation* **130**, 5976–5988 (2020).
324. Reynisson, B., Alvarez, B., Paul, S., Peters, B. & Nielsen, M. NetMHCpan-4.1 and NetMHCIIpan-4.0: improved predictions of MHC antigen presentation by concurrent motif deconvolution and integration of MS MHC eluted ligand data. *Nucleic Acids Res* **48**, W449–W454 (2020).
325. O’Donnell, T. J. *et al.* MHCflurry: Open-Source Class I MHC Binding Affinity Prediction. *Cell Syst* **7**, 129–132.e4 (2018).
326. Kee, G. S. *et al.* Exploiting the intracellular compartmentalization characteristics of the *S. cerevisiae* host cell for enhancing primary purification of lipid-envelope virus-like particles. *Biotechnol Prog* **26**, 26–33 (2010).

References

327. Gaik, S. K., Pujar, N. S. & Titchener-Hooker, N. J. Study of Detergent-Mediated Liberation of Hepatitis B Virus-like Particles from *S. cerevisiae* Homogenate: Identifying a Framework for the Design of Future-Generation Lipoprotein Vaccine Processes. *Biotechnol Prog* **24**, 623–631 (2008).
328. Kamala, T. Hock immunization: a humane alternative to mouse footpad injections. *J Immunol Methods* **328**, 204–214 (2007).
329. Mo, A. X. Y., van Lelyveld, S. F. L., Craiu, A. & Rock, K. L. Sequences That Flank Subdominant and Cryptic Epitopes Influence the Proteolytic Generation of MHC Class I-Presented Peptides. *The Journal of Immunology* **164**, 4003–4010 (2000).
330. Li, L. *et al.* Optimized polyepitope neoantigen DNA vaccines elicit neoantigen-specific immune responses in preclinical models and in clinical translation. *Genome Med* **13**, 1–13 (2021).
331. Levy, A. *et al.* A melanoma multiepitope polypeptide induces specific CD8+ T-cell response. *Cell Immunol* **250**, 24–30 (2007).
332. Duperret, E. K. *et al.* A synthetic DNA, multi-neoantigen vaccine drives predominately MHC class I CD8 β T-cell responses, impacting tumor challenge. *Cancer Immunol Res* **7**, 174–182 (2019).
333. Velders, M. P. *et al.* Defined Flanking Spacers and Enhanced Proteolysis Is Essential for Eradication of Established Tumors by an Epitope String DNA Vaccine. *The Journal of Immunology* **166**, 5366–5373 (2001).
334. Nezafat, N. *et al.* Production of a novel multi-epitope peptide vaccine for cancer immunotherapy in TC-1 tumor-bearing mice. *Biologicals* **43**, 11–17 (2015).
335. Zhang, Y. *et al.* The Immunogenicity and Anti-tumor Efficacy of a Rationally Designed Neoantigen Vaccine for B16F10 Mouse Melanoma. *Front Immunol* **10**, 1–16 (2019).
336. Wei, J. chao *et al.* Design and evaluation of a multi-epitope peptide against Japanese encephalitis virus infection in BALB/c mice. *Biochem Biophys Res Commun* **396**, 787–792 (2010).
337. Mothe, B. *et al.* A human immune data-informed vaccine concept elicits strong and broad T-cell specificities associated with HIV-1 control in mice and macaques. *J Transl Med* **13**, 1–23 (2015).
338. Li, X. *et al.* Design and Evaluation of a Multi-Epitope Peptide of Human Metapneumovirus. *Intervirology* **58**, 403–412 (2016).
339. Yano, A. *et al.* An ingenious design for peptide vaccines. *Vaccine* **23**, 2322–2326 (2005).
340. Sabet, L. P. *et al.* Immunogenicity of multi-epitope DNA and peptide vaccine candidates based on core, E2, NS3 and NS5B HCV epitopes in BALB/c mice. *Hepat Mon* **14**, (2014).
341. Seliger, B., Wollscheid, U., Momburg, F., Blankenstein, T. & Huber, C. Characterization of the major histocompatibility complex class I deficiencies in B16 melanoma cells. *Cancer Res* **61**, 1095–1099 (2001).
342. Merritt, R. E. *et al.* Augmenting major histocompatibility complex class I expression by murine tumors in vivo enhances antitumor immunity induced by an active immunotherapy strategy. *Journal of Thoracic and Cardiovascular Surgery* **127**, 355–364 (2004).
343. Blum, J. S., Wearsch, P. A. & Cresswell, P. *Pathways of antigen processing. Annual Review of Immunology* vol. 31 (2013).

344. Didierlaurent, A. M. *et al.* Enhancement of Adaptive Immunity by the Human Vaccine Adjuvant AS01 Depends on Activated Dendritic Cells. *The Journal of Immunology* **193**, 1920–1930 (2014).
345. Sharma, P. & Allison, J. P. The future of immune checkpoint therapy. *Science* **348**, 56–61 (2015).
346. Hilf, N. *et al.* Actively personalized vaccination trial for newly diagnosed glioblastoma. *Nature* **2018** 565:7738 **565**, 240–245 (2018).
347. Ott, P. A. *et al.* A Phase Ib Trial of Personalized Neoantigen Therapy Plus Anti-PD-1 in Patients with Advanced Melanoma, Non-small Cell Lung Cancer, or Bladder Cancer. *Cell* **183**, 347–362.e24 (2020).
348. Kang, K., Xie, F., Mao, J., Bai, Y. & Wang, X. Significance of Tumor Mutation Burden in Immune Infiltration and Prognosis in Cutaneous Melanoma. *Front Oncol* **10**, 1801 (2020).
349. Zhang, Y. *et al.* The Immunogenicity and Anti-tumor Efficacy of a Rationally Designed Neoantigen Vaccine for B16F10 Mouse Melanoma. *Front Immunol* **10**, 473325 (2019).
350. Kleffel, S. *et al.* Melanoma cell-intrinsic PD-1 receptor functions promote tumor growth. *Cell* **162**, 1242 (2015).
351. Hu, Z. *et al.* Personal neoantigen vaccines induce persistent memory T cell responses and epitope spreading in patients with melanoma. *Nat Med* **27**, 515–525 (2021).
352. Lavado-García, J. *et al.* Characterization of HIV-1 virus-like particles and determination of Gag stoichiometry for different production platforms. *Biotechnol Bioeng* **118**, 2660–2675 (2021).
353. Aguilar-Gurrieri, C. *et al.* Alanine-based spacers promote an efficient antigen processing and presentation in neoantigen polypeptide vaccines. *Cancer Immunology, Immunotherapy* **2023** 1–13 (2023) doi:10.1007/S00262-023-03409-3.
354. Fransen, F., Boog, C. J., Van Putten, J. P. & Van Der Ley, P. Agonists of Toll-Like Receptors 3, 4, 7, and 9 Are Candidates for Use as Adjuvants in an Outer Membrane Vaccine against *Neisseria meningitidis* Serogroup B. *Infect Immun* **75**, 5939 (2007).
355. Rhee, E. G. *et al.* TLR4 Ligands Augment Antigen-Specific CD8+ T Lymphocyte Responses Elicited by a Viral Vaccine Vector. *J Virol* **84**, 10413 (2010).
356. Thompson, C. M. *et al.* Critical assessment of influenza VLP production in Sf9 and HEK293 expression systems. *BMC Biotechnol* **15**, 1–12 (2015).
357. Peyret, H. A protocol for the gentle purification of virus-like particles produced in plants. *J Virol Methods* **225**, 59–63 (2015).
358. Moon, K. B. *et al.* Construction of SARS-CoV-2 virus-like particles in plant. *Scientific Reports* **2022** 12:1 **12**, 1–7 (2022).
359. Venereo-Sanchez, A. *et al.* Hemagglutinin and neuraminidase containing virus-like particles produced in HEK-293 suspension culture: An effective influenza vaccine candidate. *Vaccine* **34**, 3371–3380 (2016).
360. McCune, J. S. Rapid Advances in Immunotherapy to Treat Cancer. *Clin Pharmacol Ther* **103**, 540–544 (2018).
361. Lin, M. J. *et al.* Cancer vaccines: the next immunotherapy frontier. *Nature Cancer* **2022** 3:8 **3**, 911–926 (2022).

References

362. Van Den Berg, J. H. *et al.* Tumor infiltrating lymphocytes (TIL) therapy in metastatic melanoma: boosting of neoantigen-specific T cell reactivity and long-term follow-up. *J Immunother Cancer* **8**, (2020).
363. Cohen, C. J. *et al.* Isolation of neoantigen-specific T cells from tumor and peripheral lymphocytes. *J Clin Invest* **125**, 3981 (2015).
364. Ribas, A. *et al.* SD-101 in Combination with Pembrolizumab in Advanced Melanoma: Results of a Phase Ib, Multicenter Study. *Cancer Discov* **8**, (2018).
365. Kreiter, S., Castle, J. C., Türeci, Ö. & Sahin, U. Targeting the tumor mutanome for personalized vaccination therapy. <https://doi.org/10.4161/onci.19727> **1**, 768–769 (2012).
366. Castle, J. C. *et al.* Exploiting the mutanome for tumor vaccination. *Cancer Res* **72**, 1081–1091 (2012).
367. Szarewski, A. Cervarix®: a bivalent vaccine against HPV types 16 and 18, with cross-protection against other high-risk HPV types. *Expert Rev Vaccines* **11**, 645–657 (2012).
368. Laurens, M. B. RTS,S/AS01 vaccine (Mosquirix™): an overview. *Hum Vaccin Immunother* **16**, (2020).
369. Villa, L. L. Overview of the clinical development and results of a quadrivalent HPV (types 6, 11, 16, 18) vaccine. *Int J Infect Dis* **11 Suppl 2**, (2007).
370. Keech, C. *et al.* Phase 1-2 Trial of a SARS-CoV-2 Recombinant Spike Protein Nanoparticle Vaccine. *N Engl J Med* **383**, 2320–2332 (2020).
371. O'Donnell, K. & Marzi, A. The Ebola virus glycoprotein and its immune responses across multiple vaccine platforms. *Expert Rev Vaccines* **19**, 267–277 (2020).
372. Tregoning, J. S. First human efficacy study of a plant-derived influenza vaccine. *The Lancet* **396**, 1464–1465 (2020).
373. Rockman, S., Laurie, K. L., Parkes, S., Wheatley, A. & Barr, I. G. New Technologies for Influenza Vaccines. *Microorganisms* **8**, 1–20 (2020).
374. D'Aoust, M. A. *et al.* The production of hemagglutinin-based virus-like particles in plants: a rapid, efficient and safe response to pandemic influenza. *Plant Biotechnol J* **8**, 607–619 (2010).
375. Caldeira, J. C., Perrine, M., Pericle, F. & Cavallo, F. Virus-Like Particles as an Immunogenic Platform for Cancer Vaccines. *Viruses* **12**, (2020).
376. Tornesello, A. L., Tagliamonte, M., Buonaguro, F. M., Tornesello, M. L. & Buonaguro, L. Virus-like Particles as Preventive and Therapeutic Cancer Vaccines. *Vaccines (Basel)* **10**, (2022).
377. Ma, X., Serna, A., Xu, R.-H. & Sigal, L. J. The amino acids sequences flanking an antigenic determinant can strongly affect MHC class I cross-presentation without altering direct-presentation. *J Immunol* **182**, 4601 (2009).
378. Le Gall, S., Stamegna, P. & Walker, B. D. Portable flanking sequences modulate CTL epitope processing. *J Clin Invest* **117**, 3563–3575 (2007).
379. Velders, M. P. *et al.* Defined Flanking Spacers and Enhanced Proteolysis Is Essential for Eradication of Established Tumors by an Epitope String DNA Vaccine. *The Journal of Immunology* **166**, 5366–5373 (2001).
380. Del Val, M., Schlicht, H. J., Ruppert, T., Reddehase, M. J. & Koszinowski, U. H. Efficient processing of an antigenic sequence for presentation by MHC class I molecules depends on its neighboring residues in the protein. *Cell* **66**, 1145–1153 (1991).

381. Eggers, M., Boes-Fabian, B., Ruppert, T., Kloetzel, P. M. & Koszinowski, U. H. The cleavage preference of the proteasome governs the yield of antigenic peptides. *J Exp Med* **182**, 1865 (1995).
382. Cascio, P., Hilton, C., Kisselev, A. F., Rock, K. L. & Goldberg, A. L. 26S proteasomes and immunoproteasomes produce mainly N-extended versions of an antigenic peptide. *EMBO J* **20**, 2357 (2001).
383. Steppert, P. *et al.* Purification of HIV-1 gag virus-like particles and separation of other extracellular particles. *J Chromatogr A* **1455**, 93–101 (2016).
384. Jorritsma, S. H. T., Gowans, E. J., Grubor-Bauk, B. & Wijesundara, D. K. Delivery methods to increase cellular uptake and immunogenicity of DNA vaccines. *Vaccine* **34**, 5488–5494 (2016).
385. Pardi, N., Hogan, M. J., Porter, F. W. & Weissman, D. mRNA vaccines — a new era in vaccinology. *Nature Reviews Drug Discovery* **2018** *17*:4 **17**, 261–279 (2018).
386. Wang, B.-Z. *et al.* Incorporation of high levels of chimeric human immunodeficiency virus envelope glycoproteins into virus-like particles. *J Virol* **81**, 10869–10878 (2007).
387. Benen, T. D. *et al.* Development and immunological assessment of VLP-based immunogens exposing the membrane-proximal region of the HIV-1 gp41 protein. *J Biomed Sci* **21**, 1–13 (2014).
388. Excler, J. L. & Kim, J. H. Novel prime-boost vaccine strategies against HIV-1. *Expert Rev Vaccines* **18**, 765–779 (2019).
389. Yadav, M. *et al.* Predicting immunogenic tumour mutations by combining mass spectrometry and exome sequencing. *Nature* **2014** *515*:7528 **515**, 572–576 (2014).
390. Wells, D. K. *et al.* Key Parameters of Tumor Epitope Immunogenicity Revealed Through a Consortium Approach Improve Neoantigen Prediction. *Cell* **183**, 818-834.e13 (2020).
391. Robbins, P. F. *et al.* Mining exomic sequencing data to identify mutated antigens recognized by adoptively transferred tumor-reactive T cells. *Nat Med* **19**, 747–752 (2013).
392. Bobisse, S. *et al.* Sensitive and frequent identification of high avidity neo-epitope specific CD8 + T cells in immunotherapy-naïve ovarian cancer. *Nat Commun* **9**, (2018).
393. McGranahan, N. *et al.* Clonal neoantigens elicit T cell immunoreactivity and sensitivity to immune checkpoint blockade. *Science* **351**, 1463–1469 (2016).
394. Schmidt, J. *et al.* Prediction of neo-epitope immunogenicity reveals TCR recognition determinants and provides insight into immunoediting. *Cell Rep Med* **2**, (2021).
395. Sette, A. *et al.* The relationship between class I binding affinity and immunogenicity of potential cytotoxic T cell epitopes. *The Journal of Immunology* **153**, 5586–5592 (1994).
396. Montemurro, A. *et al.* NetTCR-2.0 enables accurate prediction of TCR-peptide binding by using paired TCR α and β sequence data. *Communications Biology* **2021** *4*:1 **4**, 1–13 (2021).
397. Gielis, S. *et al.* Detection of Enriched T Cell Epitope Specificity in Full T Cell Receptor Sequence Repertoires. *Front Immunol* **10**, 489238 (2019).
398. Ogishi, M. & Yotsuyanagi, H. Quantitative prediction of the landscape of T cell epitope immunogenicity in sequence space. *Front Immunol* **10**, 442802 (2019).

References

399. Slingluff, C. L. *et al.* Randomized multicenter trial of the effects of melanoma-associated helper peptides and cyclophosphamide on the immunogenicity of a multipeptide melanoma vaccine. *J Clin Oncol* **29**, 2924–2932 (2011).
400. Hamid, O. *et al.* Alum with interleukin-12 augments immunity to a melanoma peptide vaccine: correlation with time to relapse in patients with resected high-risk disease. *Clin Cancer Res* **13**, 215–222 (2007).
401. Slingluff, C. L. *et al.* EFFECT OF GM-CSF ON CIRCULATING CD8+ AND CD4+ T CELL RESPONSES TO A MULTYPEPTIDE MELANOMA VACCINE: OUTCOME OF A MULTICENTER RANDOMIZED TRIAL. *Clin Cancer Res* **15**, 7036 (2009).
402. Slingluff, C. L. *et al.* Immunologic and clinical outcomes of a randomized phase II trial of two multipeptide vaccines for melanoma in the adjuvant setting. *Clin Cancer Res* **13**, 6386–6395 (2007).
403. Baumgaertner, P. *et al.* Ex vivo detectable human CD8 T-cell responses to cancer-testis antigens. *Cancer Res* **66**, 1912–1916 (2006).
404. Bijker, M. S. *et al.* Superior induction of anti-tumor CTL immunity by extended peptide vaccines involves prolonged, DC-focused antigen presentation. *Eur J Immunol* **38**, 1033–1042 (2008).
405. Stephens, A. J., Burgess-Brown, N. A. & Jiang, S. Beyond Just Peptide Antigens: The Complex World of Peptide-Based Cancer Vaccines. *Front Immunol* **12**, 2629 (2021).
406. Rabu, C. *et al.* Cancer vaccines: designing artificial synthetic long peptides to improve presentation of class I and class II T cell epitopes by dendritic cells. *Oncoimmunology* **8**, (2019).
407. Garcia-Garijo, A., Fajardo, C. A. & Gros, A. Determinants for neoantigen identification. *Front Immunol* **10**, 1392 (2019).
408. Yu, J. W. *et al.* Tumor-immune profiling of murine syngeneic tumor models as a framework to guide mechanistic studies and predict therapy response in distinct tumor microenvironments. *PLoS One* **13**, e0206223 (2018).
409. Spranger, S., Bao, R. & Gajewski, T. F. Melanoma-intrinsic β -catenin signalling prevents anti-tumour immunity. *Nature* **523**, 231–235 (2015).
410. Overwijk, W. W. & Restifo, N. P. B16 as a Mouse Model for Human Melanoma. *Current protocols in immunology / edited by John E. Coligan ... [et al.]* **CHAPTER, Unit** (2001).
411. Pereira, S. P. *et al.* Early detection of pancreatic cancer. *Lancet Gastroenterol Hepatol* **5**, 698 (2020).
412. Fitzkee, N. C. & Rose, G. D. Steric restrictions in protein folding: An α -helix cannot be followed by a contiguous β -strand. *Protein Sci* **13**, 633 (2004).
413. Charlton Hume, H. K. *et al.* Synthetic biology for bioengineering virus-like particle vaccines. *Biotechnol Bioeng* **116**, 919–935 (2019).
414. Rist, M. J. *et al.* HLA peptide length preferences control CD8+ T cell responses. *Journal of Immunology* **191**, 561–571 (2013).


ACKNOWLEDGMENTS



ACKNOWLEDGMENTS

CAST

(In order of appearance)

“hombre barroco”	Sin vosotrxs esto hubiera sido muy aburrido
Raquel Ortiz	Amigaaaaaaaaaaaa 
Amaya Blanco	Gracias por ser una persona desequilibrada y hacerme reír mucho!!
Miguel Marin	Insoportable, pero te has hecho querer
Carlos Ávila	Gracias por siempre poner un punto de vista critico a las cosas

VIC group

PhD team “Los discípulos del Boss”

Ferran Tarrés · Edwards Pradenas · Anna Pons
Tetyana Pidkova · Ferran Abancó · Júlia Albons

Silvia Marfil · Benjamin Trinité · Victor Urrea · Carla Rovirosa

With the special collaboration of

Julià Blanco · Carmen Aguilar
As thesis supervisors

A special thanks to

“Albajunos”
Ester Aparicio
Francesc Cunyat
Cris del Val
Victor C

NeoVaCan & IgG

With the support of

“Old predocs”

Dani, Edurne, Oscar B, Luis R, Ify, Clara, Lucía, Eudald, Silvia B, Ángel

“Predocs que fuman”

Para los que estáis y para los que no han podido estar

And thank you to everyone else!!

Specially,

Itziar · M^a Carmen · Maria S · Mariona · Eli · Roger · Eva · Ruth · Alex O · Samandhy ·
Tuixent · Cris P · Susana E. & muestras team · Rita & Elena

To all the PIs,

Specially

Nuria de la I., Jorge, Ceci, Ester B, Julia GP, and Nuria I.

An immense thank you to

Penélope

Cris

Arnau

Special mention for

Lourdes G

Bonaventura C

And an even more special mention for

Lidia R

